TARGETING CELLULAR SIGNALING PATHWAYS IN ESTROGEN RECEPTOR POSITIVE BREAST CANCER

By

Sonia Kumar Gentile

A DISSERTATION

Submitted to
Michigan State University
in partial fulfillment of the requirements
for the degree of

Physiology – Doctor of Philosophy

2018

ABSTRACT

TARGETING CELLULAR SIGNALING PATHWAYS IN ESTROGEN RECEPTOR POSITIVE BREAST CANCER

By

Sonia Kumar Gentile

Estrogen receptor positive (ER+) breast cancer is the most common type of breast cancer diagnosed in women. While usually initially responsive to combinations of chemotherapy with hormonal therapies, resistance to current clinically used treatments is becoming more and more frequent. It is vital to continue to study the mechanisms of resistance to endocrine therapies and discover methods for combating this drug resistance to improve patient survival.

The mixed lineage kinase (MLK) inhibitor, CEP-1347, was studied in culture and in pre-clinical models to evaluate its efficacy, alone and in combination with the clinically available selective estrogen receptor downregulator ICI 182,780, in treating endocrine sensitive and resistant ER+ breast cancers. Using cell lines models, its effects on cell viability, cell death, and cell cycle progression were analyzed, and nuclear and cellular morphology throughout mitosis were examined. Studies were expanded to animals to determine the efficacy of CEP-1347 against tumor growth in a pre-clinical setting. Tumor cell growth and death were studied, as well as the potential for tumor regrowth after the cessation of treatment. Investigation into drug efficacy were expanded into patient derived xenograft (PDX) lines and effects on cell cycle progression were analyzed.

The data demonstrate that CEP-1347, especially in combination with ICI 182,780 has the potential to treat endocrine resistant disease through causing a cell cycle arrest which leads to a combination of decreasing proliferation and inducing apoptosis of tumor cells. Furthermore, inhibition of regrowth after cessation of treatment in endocrine sensitive cells suggests that perhaps if used as an earlier line therapy, CEP-1347 in combination with ICI 182,780 may slow or prevent the development of resistance.

To the two strongest men in my life
who raised me to be curious and inspired my love for science
who continually pushed me to reach my fullest potential
who are my role models in every way.

ACKNOWLEDGEMENTS

The completion of this work would not have been possible without the assistance and support of a number of people. First, to my mentor, Dr. Susan Conrad, whose guidance and reassurance throughout the course of this work was remarkable. To my technician, Eva Miller, whose assistance with the little details was limitless. To the undergraduate students who have assisted in their own way, especially Hiba Saifuddin, who continued to work diligently while I left the lab for one year to complete the first portion of medical school. A special thanks to my committee members: Dr. Kathy Gallo, Dr. Karen Liby, Dr. Eran Andrechek, and Dr. Janet Osuch, who have provided assistance and direction when it was most needed, and a special thanks to Dr. Kathy Gallo who acted more as a co-mentor than a committee member over the last several years. To other students past and present, with limitless gratitude to Dr. Chotirat Rattanasinchai and Sean Misek who were available at all hours to answer my endless questions. To the many cores on campus, without whom this work would not have been possible. To Amy Porter, Kathy Joseph, and Bill Lienhart in the Histopathology Core, thank you for the hours of troubleshooting and the endless rush jobs that you accepted and completed with ease. To Sandra O'Reilly, thank you for your continual assistance and education with all of the animals studies, from teaching me how to hold a mouse, to completing all euthanasia until I was ready. An extra special thank you for the emotional support over the years. To Louis King for patiently assisting with flow cytometry experiments and explaining the intricacies of data analysis. To Dr. Dan Jones and Lijun Chen of the Mass Spectrometry Core for their endless direction and assistance with education on foundations and

applications. To the Physiology Department and College of Human Medicine, as well as the MD/PhD Program, thank you for your financial support and flexibility with scheduling overlapping requirements. Finally, thank you to my parents, Dr. Rajesh Kumar and Meena Kumar who have supported me in everything I have endeavored to accomplish since the day I was born. Thank you to my sisters Ruby and Monica Kumar for listening to my rambles day in and day out. Thank you to all of my friends and extended family who have supported me always. And a very special thank you to my husband, Dr. Jeremy Gentile, for constantly being my rock and my cheerleader every step of the way.

TABLE OF CONTENTS

LIST OF TABLES

LIST OF FIGURES

KEY TO ABBREVIATIONS

ACA	anti-centromere antibody
ACJJ	American Joint Commission of Cancer
ACOG	American College of Obstetricians and Gynecologists
ACS	American Cancer Society
AI	aromatase inhibitor
Akt	protein kinase B
AMPK	adenosine monophosphate-activated protein kinase
ANG	angiogenesis
ANOVA	analysis of variance
AP-1	activator protein 1
APCI	atmospheric pressure chemical ionization
AR	androgen receptor
ATP	adenosine triphosphate
BRCA	breast cancer susceptibility gene
BrdU	bromodeoxyuridine
BSA	bovine serum albumin
CaMKKβ	calmodulin-dependent kinase kinase beta
CCK-8	cell counting kit-8
CCND1	cyclin D 1 gene
CDK	cyclin dependent kinase
CK	cytokeratin
CRIB	Cdc42-/Rac1-interactive binding

DAPI	4',6-diamidino-2-phenylindole
DCIS	ductal carcinoma *in situ*
DMSO	dimethyl sulfoxide
DNA	deoxyribonucleic acid
EDTA	ethylene diaminotetraacetic acid
EI	estrogen independent
ER	estrogen receptor
ERBB2	erythroblastic leukemia viral oncogene homolog 2
ERK	extracellular-signal regulated kinase
ESI	electrospray ionization
FACS	fluorescence-activated cell sorting
GTP	guanine triphosphate
H&E	hematoxylin and eosin
HER2	human epidermal growth factor receptor 2
HMGCR	3-hydroxy-3methylglutaryl-CoA reductase
i.p.	intraperiteonal
i.v.	intravenous
IDC	invasive ductal carcinoma
IHC	immunohistochemistry
IKKα	IκB kinase α
IKKβ	IκB kinase β
ILC	invasive lobular carcinoma
JNK/SAPK	c-Jun N-terminal kinase/stress-activated protein kinase

LCIS	lobular carcinoma *in situ*
LHRH	luteinizing hormone releasing hormone
LKB1	liver kinase B1
Luc	luciferase
MAP2K	mitogen activated protein kinase kinase
MAP3K	mitogen activated protein kinase kinase kinase
MAPK	mitogen activated protein kinase
MEK	mitogen activated protein kinase kinase
MLK	mixed lineage kinase
MRI	magnetic resonance imaging
MS	mass spectrometry
mTOR	mammalian target of rapamycin
NF-κB	nuclear factor kappa-light-chain enhancer of activated B cells
NIMA	never in mitosis gene-A
NOD/SCID	non-obese diabetic/severe combined immunodeficient
OS	overall survival
p.o.	per os (oral)
p70s6k	p70 S6 kinase
PARP	poly-adenosine diphosphate ribose polymerase
PBS	phosphate buffered saline
PD	Parkinson's disease
PDX	patient derived xenograft
PFS	progression free survival

PI	propidium iodide
PI3K	phosphoinositol 3-kinase
PLK1	Polo-like kinase 1
PR	progesterone receptor
Rb	retinoblastoma
RFP	red fluorescent protein
RNA	ribonucleic acid
RNaseA	ribonuclease A
RPPA	reverse phase protein phosphorylation array
s.c.	subcutaneous
SAC	spindle assembly checkpoint
SD	standard deviation
SDS	sodium dodecyl sulfate
SEM	standard error of the mean
SERD	selective estrogen receptor downregulator
SERM	selective estrogen receptor modulator
STR	short tandem repeat
TNM	tumor, lymph node, metastasis
TUNEL	terminal deoxynucleotidyl transferase dUTP nick end labeling
USPSTF	United States Preventive Services Task Force

Chapter 1: Introduction/Literature Review

Epidemiology of breast cancer

Breast cancer is the leading cause of cancer in women in the US. With more than 250,000 new cases of invasive disease and more than 63,000 new cases of in-situ disease diagnosed in 2017, it represents almost 30% of all female cancer diagnoses. In 2017, breast cancer led to more than 40,000 deaths in women, making it the second leading cause of cancer-related deaths [1]. The incidence of breast cancer in women peaks between 50 and 70 years of age, with the median age falling between 60 and 65 years old, depending on race. A decrease in incidence is seen in patients above 85 years of age, and is believed to be due to a reduction in screening of women in this age group. The incidence of breast cancer is highest in non-Hispanic white women, followed by non-Hispanic black women; however, cancer-related mortality is greatest in non-Hispanic black women [1, 2]. This discrepancy can be attributed to variations in access to healthcare, patient co-morbidities, and genetics, as well as to a higher rate of the most aggressive subtype of breast cancer being diagnosed in non-Hispanic black women. Asian/Pacific Islanders have the lowest incidence of breast cancer and disease-related mortality among all races studied [1, 2]. The 5-year survival rate of patients diagnosed with localized or regional disease varies between 78-98% depending on race, and drops to 26-40% when patients present with distant metastatic disease [1-3]. The different forms of breast cancer can be classified using multiple methods, including histopathological subtype, molecular subtype, and by gene expression profiling.

Histopathological subtypes of breast cancer

Breast cancer can be characterized as four different histopathological subtypes based on the location and invasiveness of tumor cells within the mammary gland. The majority of breast tissue consists of adipocytes, with epithelial lobules that differentiate into milk-producing glands and ducts that transport milk to the nipple, as illustrated in Figure 1-1. Lobular carcinoma in situ (LCIS) makes up approximately 20% of non-invasive breast cancers, and can be divided into multiple histological variants including pleomorphic, classic, histiocytoid, and tubulolobular [4]. It is classified as abnormal growth of cells within the milk-producing lobules of the breast, and may or may not progress to an invasive disease. Ductal carcinoma in situ (DCIS) makes up 80% of non-invasive disease, is defined by abnormal growth of epithelial cells within the milk-delivery passageways of the breast, and includes multiple architectural subtypes, including papillary, micropapillary, cribiform, and solid [4].. Invasive lobular carcinoma (ILC) makes up 10% of all invasive disease and is made up of cancer cells within a lobule invading into surrounding tissue. Invasive ductal carcinoma (IDC) makes up approximately 80% of invasive breast cancer. This pathology is cancer cells within a mammary duct invading beyond the basement membrane of the duct into extra-ductal tissue. An additional subtype is inflammatory breast cancer, which presents with diffuse inflammation of the whole breast with or without lymphatic infiltration of tumor emboli, making it more ductal than lobular [5]. The remaining 10% of invasive disease is a mixed ductal-lobular pathology [3, 6, 7].

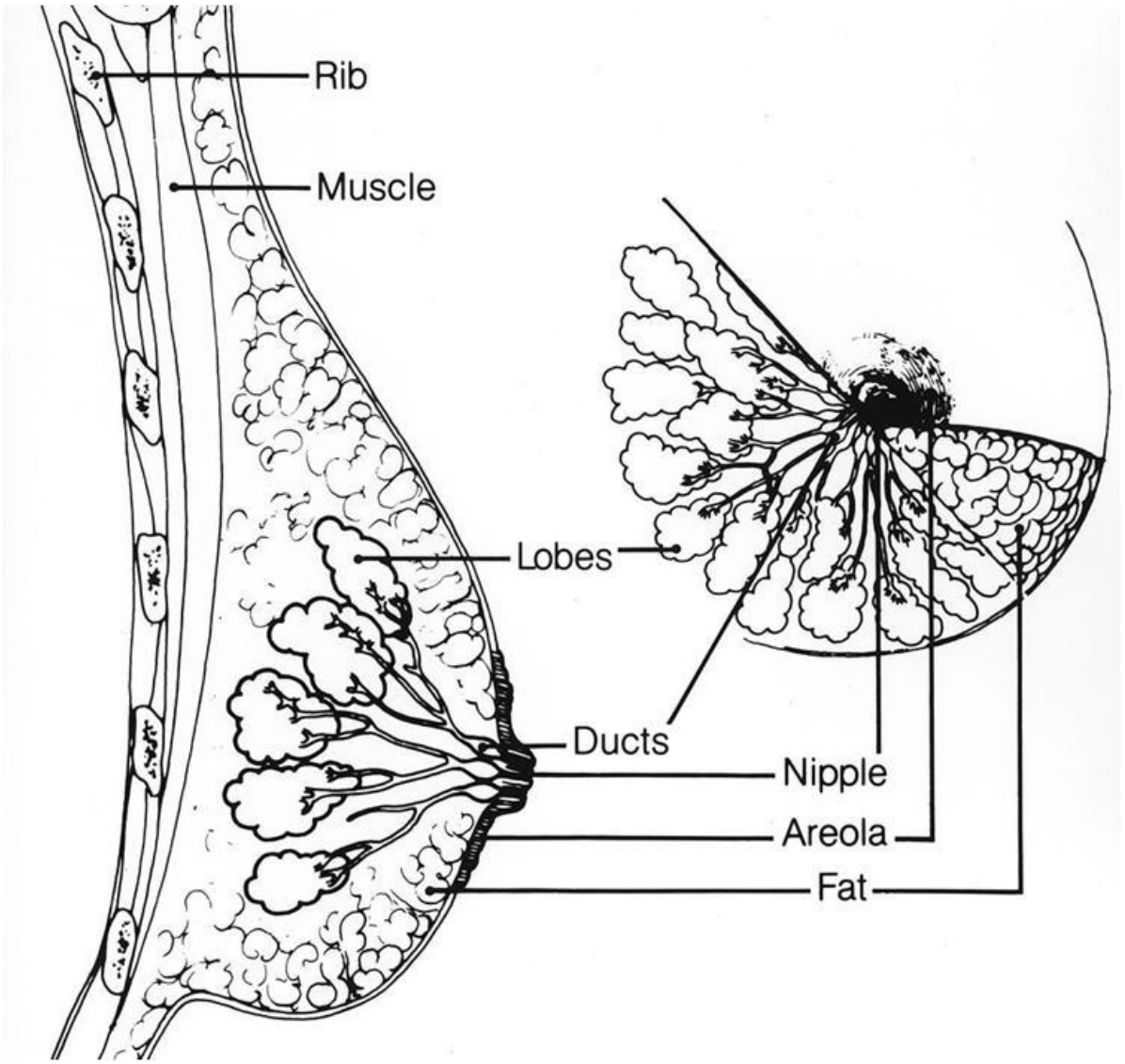

Figure 1-1: Anatomical structure of the breast. Structure of the female breast indicating lobes and ducts from which breast cancers can arise. Image is open source and provided by the National Cancer Institute.

Molecular subtypes of breast cancer

Molecular classification of breast cancer is based on the presence or absence of receptors, identified by immunohistochemical staining, and four histological subtypes of breast cancer have been identified as illustrated in Figure 1-2 [8, 9]. Luminal A breast

cancers are usually estrogen receptor (ER) positive, progesterone receptor (PR) positive, and human epidermal growth factor receptor 2 (HER2) negative. These cancers are well differentiated and usually respond well to hormonal therapies that inhibit the production of estrogen or the activity of the estrogen receptor [8, 9]. Luminal B breast cancer tends to be ER+, PR+, and HER2+, and sometimes express androgen receptor (AR). These cancers are more aggressive and less differentiated than luminal A tumors, but can be treated with anti-HER2 agents, anti-androgens, or anti-estrogens [8, 9]. The third molecular classification of breast cancer is based on the expression of HER3/neu exclusively. This type tends to be clinically more aggressive and histologically less well differentiated than the luminal subtypes. Because ER and PR are not expressed in this subtype, treatment is limited to anti-HER2/neu agents and chemotherapy. Finally, triple-negative breast cancer lacks expression of all three receptors and is difficult to treat with targeted agents. This is the most aggressive and poorly differentiated subtype of breast cancer, and is characterized by expression of cytokeratins 5, 14, and/or 17. It can respond to conventional cytotoxic chemotherapeutics, poly-ADP-ribose polymerase (PARP) inhibitors, and angiogenesis inhibitors [8, 9], but exhibits the highest incidence of cancer-related mortality [3]. Of these molecular subtypes, luminal-type cancers typically arise from cells lining the lumen of lobules and ducts, while triple-negative cancers arise from the myoepithelial or basal cells that are medial to basement membranes, and form the periphery of lobules and ducts [8]. Among these different subtypes, the two luminal subtypes together make up more than 70% of all breast cancers [3, 8, 9].

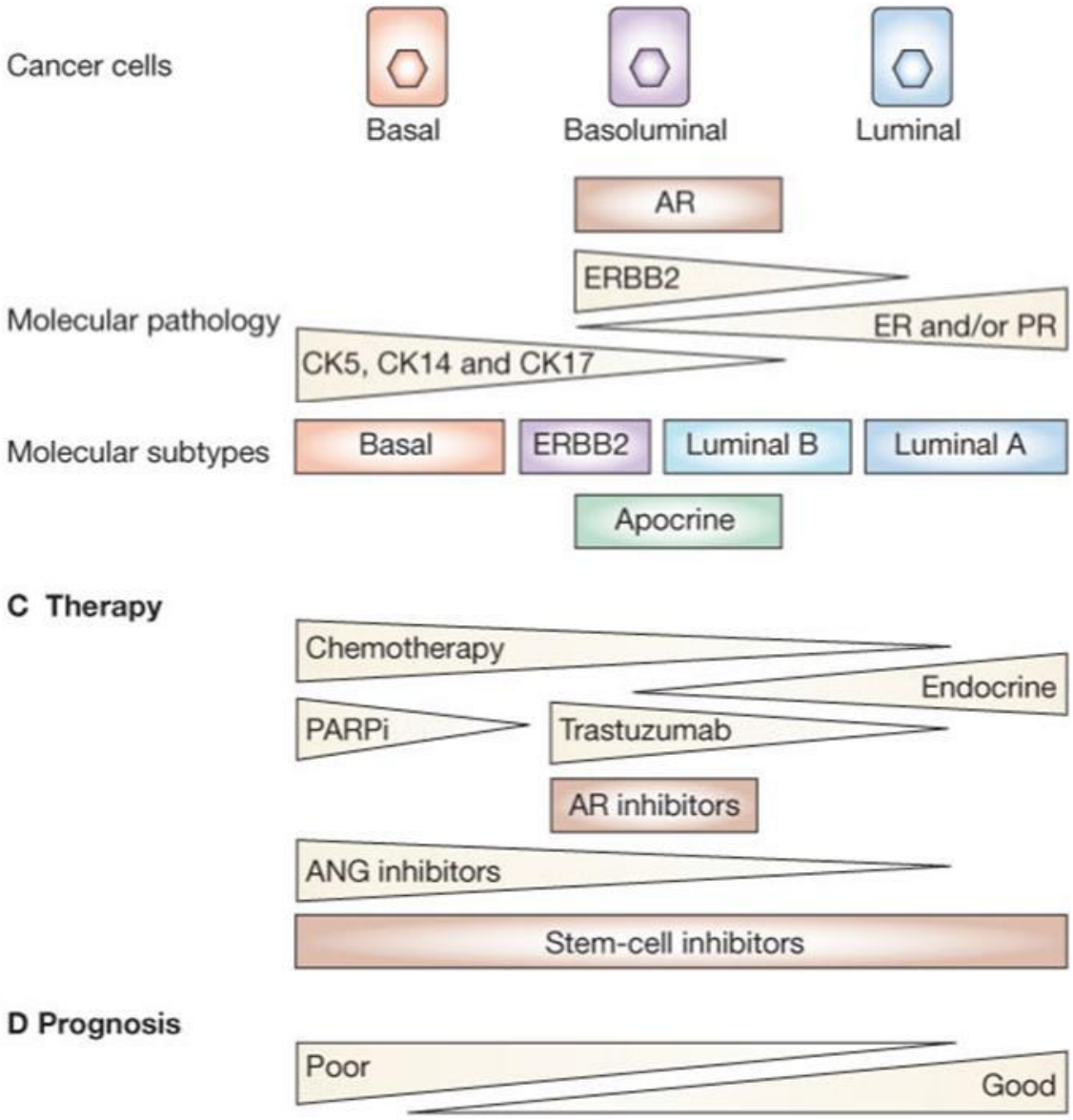

Figure 1-2: A model of how stem-cell hierarchy may account for the origins of different subtypes of breast cancer. Abbreviations: ANG, angiogenesis; AR, androgen receptor; CK, cytokeratin; ER, estrogen receptor; ERBB2 (HER2), erythroblastic leukemia viral oncogene homolog 2; PARPi, poly (ADP-ribose) polymerase inhibitors; PR, progesterone receptor. Adapted from [9].

Gene expression profiling of breast cancer

In the early 2000s, gene expression profiling was explored in an attempt to identify and perhaps predict patient outcome based on the genetic profile of individual tumors [10]. Excitingly, these experiments identified several unique molecular breast cancer subtypes: luminal A, luminal B, luminal C, normal breast-like, ERBB2 overexpressing, and basal-like [10, 11]. Because widespread gene expression profiling of all patient tumors was not feasible at the time, methods of distinguishing subtypes with immunohistochemical analysis of receptor expression became standard in diagnosing and guiding treatment [12]. Advances in gene expression profiling have allowed for more detailed characterization of breast tumors [11, 13], and have exposed further divisions of known subtypes [10, 11]. Furthermore, gene expression analysis has been used to predict metastatic potential of tumors [11, 14, 15] and is being studied to predict response to therapies [16, 17]. With the advent of widespread availability, gene expression analysis panels, such as OncotypeDX, PAM50, and EndoPredict, have become vital in making decisions for therapy, and allow for a more individualized approach to treatment [18].

Role of estrogen and ER in luminal breast cancer

The majority of all breast cancers are luminal A/B and ER+. Thus, it is important to study the structure and function of ER and the role of estrogen signaling in breast cancer pathogenesis. The ER is made up 6 distinct domains, including a DNA binding domain and C-terminal ligand-binding domain [19]. Canonically, estrogen molecules cross cell membranes and bind to ER at the ligand-binding domain. In the nucleus, the

estrogen-ER complex binds to promotors and recruits co-activators or co-repressors to regulate the transcription of genes involved in growth, survival, and proliferation [20, 21]. Estrogen receptor may also function as a transcription factor independent of bound estrogen. In this case, ligand binding to receptor tyrosine kinases on the cell surface activates signaling cascades that lead to direct phosphorylation and activation of ER in the absence of estrogen [21, 22]. ER also has non-transcriptional cytoplasmic functions involved in regulating growth and survival pathways [23].

Importance of ER in cell cycle progression and regulation

Estrogen acts as a potent mitogen and plays a role activating a number of genes that are involved in cell cycle progression. The earliest gene for which transcription is increased upon exposure to estrogen is c-myc [24]. The multifunctional c-Myc protein functions in cell cycle progression and plays roles in apoptosis and oncogenesis. Cyclin D1 is also induced in response to estrogen, and the increase in cyclin D1 protein leads to formation of complexes with cyclin dependent kinase 4 (Cdk4). Both c-myc and cyclin D1 are involved in the early stages of G1, and they both play a role in activating downstream cyclin E/Cdk2 complexes. Activated cyclin D1/Cdk4 and cyclin E/Cdk2 complexes both phosphorylate the retinoblastoma protein (Rb), allowing its release from the transcription factor E2F, a step which is vital for cell cycle progression from G1 into S [25-28] as illustrated in Figure 1-3. Estrogens and ER also exert further control of progression through G1 via regulation of Cdk inhibitors and the cell cycle phosphatase, Cdc25A [29, 30]. Furthermore, ER has been shown to play a role DNA remodeling and

regulation of histone methylation and acetylation via recruitment of numerous cofactors to mediate gene transcription [31].

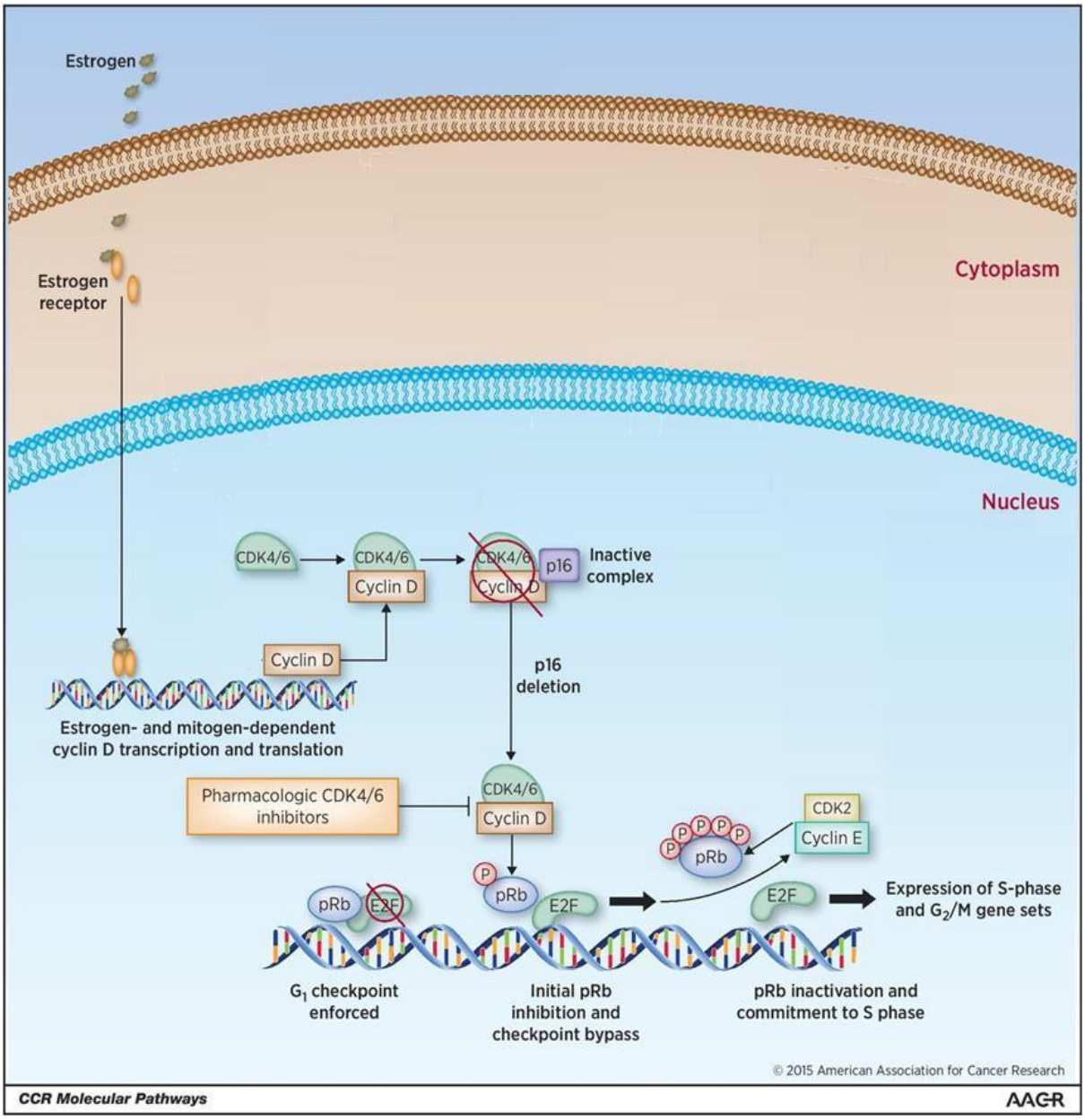

Figure 1-3: Regulation and functions of cyclin D-CDK4/6 kinases. Mitogenic signals stimulate the accumulation of D-type cyclins in early G1 phase. In breast cancer cells, cyclin D expression is enhanced by ligand-or mutationally activated estrogen receptors, which bind directly to the CCND1 promoter. The activated cyclin D-CDK4/6 complexes

Figure 1-3 (cont'd)

initiate the phosphorylation of pRb and collaborate with cyclin E-CDK2 complexes (which begin to accumulate in mid/late G1 phase) to provoke full hyperphosphorylation and functional inactivation of pRb. The subsequent release of E2F transcription factors drives the expression of genes required for cellular commitment to enter S-phase, and ultimately mitotic cell division. p16 binding to cyclin D-CDK4/6 complexes inhibits their activation, but loss of p16 allows dysregulated cell cycle progression. Image and legend adapted from [28].

Current guidelines and options for treatment of ER+ breast cancer

Guidelines for treatment of breast cancer have changed significantly throughout the last century, especially upon the discovery that hormone receptor status strongly correlated with prognostic and diagnostic outcomes. There are a number of hormonal therapies that target either the production of estrogen or the activity of estrogen receptor. While specific guidelines exist for which of these drugs can be used in pre-menopausal versus post-menopausal women, there is disagreement about the appropriate sequence in which to use them. A single “perfect” order of treatment may not exist for all ER+ breast cancers; rather, guidelines for the appropriate sequence should be based on a number of factors including patient history, past drug exposures, extent of disease upon presentation, genetic profile of the tumor, and patient wishes, among several other considerations, and are summarized at the end of this section [32-36]. Screening is utilized in high risk populations in order to identify cancerous lesions as early as possible. After diagnosis with biopsy, patients receive the stage and grade of their

tumor, and are provided with options for surgery, radiation, and hormonal and chemotherapeutics. The available options for patients with ER+ breast cancer will be discussed.

Staging and Grading

The American Joint Commission of Cancer (AJCC) uses the tumor, lymph node, metastasis (TNM) model for staging of breast cancer. This system takes into account the size and invasiveness of the primary tumor (T), involvement and location of regional and distant lymph nodes (N), and evidence of metastasis in distant organs. Taking into account all three of these criteria, patients are given a cancer stage, ranging from stage 0 to stage IV [3]. The grading of breast cancer is based on the extent of differentiation of tumor tissue, mitotic activity, abnormal nuclear morphology, and presence of normal breast architecture. In 2017, the AJCC called for modifications to the TNM staging system, requiring inclusion of additional prognostic information including biomarker expression, histological subtype, tumor grade, and results from genetic panels such as Oncotype DX and PAM50, in order to more accurately convey disease severity and enhance predicted response to therapy [41].

Surgery and radiation

Surgical options after diagnosis include total mastectomy or breast-conserving lumpectomy depending on patient wishes as well as extent of disease. Both of these options require removal of lymph nodes for staging and updated guidelines state that sentinal lymph node dissection may replace the more traditional axillary lymph node

dissection in certain cases [35]. After surgery, radiation to the whole breast is recommended for all lumpectomy patients. For mastectomy patients, radiation to the chest wall is recommended for patients with greater than 3 positive lymph nodes and strongly considered for patients with 1-3 positive lymph nodes, primary tumors greater than 5 cm, or post surgical excision that exhibits positive margins [35].

Endocrine therapies

Hormonal therapies are the primary treatment for ER+ breast cancers and have shown extraordinary efficacy. First developed in 1958 in England as a potential contraceptive, the first anti-estrogen, tamoxifen (described below), was found to induce ovulation rather than inhibit it [42]. In the 1970s, it was studied as a potential therapeutic for women with breast cancer and found to be extremely beneficial in a subset of cases. It was approved for use in the United States in 1977, and multiple classes of endocrine therapies have been developed since [43].

Selective estrogen receptor modulators (SERMs)

SERMs such as tamoxifen function by binding to the ligand binding domain of ER and blocking binding of estrogen. The SERM/ER complex then binds to promotors in the nucleus and inhibits transcription to induce a G0/G1 cell cycle arrest [44-46]. The only clinically available SERMs to treat breast cancer is tamoxifen, with a number of others in clinical trials [47, 48]. Tamoxifen also has non-genomic targets and is a partial agonistic for ER-alpha, including in the uterus. This drug has agonist activity in bones, preventing the development of osteoporosis [49, 50]. A serious side effect of SERM

therapy is the development of venous thrombosis, including deep vein thrombosis, pulmonary embolism, and retinal vein thrombosis, which occur in approximately 1% of all patients. Other more common side effects include hot flashes and vaginal atrophy, which can occur in 50-60% of all patients [47].

Selective estrogen receptor downregulators (SERDs)

Another class of anti-estrogens, SERDs, are similar to SERMs. They function by binding to the ligand binding domain of ER and inhibiting binding of estrogen. However, unlike SERMs, SERDS target the drug:ER complex for proteosomal degradation. The only SERD clinically available is fulvestrant, a.k.a. faslodex, ICI 182,780, although others are being studied pre-clinically [48]. These compounds are often called "pure anti-estrogens" as they do not exhibit any agonist activity [48]. Like SERMs, SERDs lead to a G0/G1 cell cycle arrest [51]. This class of drugs is usually reserved for later line therapy, especially in patients who become refractory to alternate endocrine agents. This is because tumors that become resistant to SERMs are often still sensitive to SERDs, while the opposite is not true [35]. The most commonly reported side effect from SERD use is gastrointestinal disruption [48].

Aromatase inhibitors (AIs)

AIs bind and inhibit the enzyme aromatase, which is responsible for converting testosterone to estrogen, thus targeting the major route for estrogen production. This class of drugs is divided into two groups: steroidal and non-steroidal. Steroidal AIs include exemestane, and bind covalently and irreversibly to aromatase, while non-

steroidal AIs include anastrazole and letrozole and can only reversibly bind to the enzyme [52]. Regardless of type, all AIs lead to a G0/G1 cell cycle arrest of breast cancer cells [51]. This class of drugs is usually selected as first line therapy for post-menopausal patients, and is only used in pre-menopausal patients after ovarian ablation [34].

Other targeted and untargeted treatment options

While endocrine agents are important in the treatment of patients with ER+ breast cancer, resistance to these therapies is common, especially in metastatic disease, and alternate options are necessary. Recent investigations have found that combination of endocrine agents with other targeted therapies are superior to endocrine agents alone, especially in advanced or metastatic settings. Some of these alternate therapies are described below.

CDK 4/6 inhibitors

Cell cycle checkpoints regulate progression through the cell cycle. Cyclin dependent kinases (CDKs) 4 and 6 function in G1 of the cell cycle. They bind to D-type cyclins and together form a complex that phosphorylates the retinoblastoma protein (Rb). E2F is a family of seven transcription factors involved in the expression of genes required for cell cycle progression and need to form heterodimers with one of two DP proteins to be active [53, 54]. Hypophosphorylated Rb binds E2F and recruits co-repressors to inhibit gene transcription. Upon phosphorylation, Rb is released from E2F, which then activates genes required for the G1 to S transition [55]. Dysregulation of CDK4/6 activity

allows progression through G1 and into S without fulfilling appropriate checkpoint criteria. CDK4/6 inhibitors prevent proliferation by arresting cells in G1. Palbociclib, abemaciclib, and ribociclib are three CDK 4/6 inhibitors that have recently been studied in the context of endocrine resistant ER+ breast cancer [56]. Clinical evidence indicates that the combination of CDK 4/6 inhibitors with letrozole or fulvestrant provides an advantage over endocrine therapies alone in increasing progression-free survival (PFS), while not changing overall survival (OS), especially in patients with endocrine resistant and/or metastatic breast cancer [57-60].

PI3K/Akt/mTOR inhibitors

Phospho-inositol-3-kinase (PI3K) is activated at the cell membrane downstream of cell surface receptors, and once active, it indirectly participates in downstream activation of Akt. Three isoforms of Akt exist (Akt 1, 2, and 3), and are all expressed in most cell types. Akt amplifications have been described in multiple tumor types, with Akt2 amplification being specific to breast cancer [61]. Akt is able to relay activation signals to mammalian target of rapamycin (mTOR), which is involved in numerous cell processes, including progression through G1 into the S phase [61]. Everolimus is an mTOR inhibitor that has been studied as a breast cancer therapeutic, specifically in patients with endocrine resistant or advanced disease. It has been shown to increase PFS when combined with exemestane, tamoxifen, or fulvestrant [62-64] by inhibiting phosphorylation of the S6 kinase, preventing phosphorylation of the ribosomal S6 protein, and subsequently blocking protein synthesis and leading to a G1 cell cycle arrest [65], but again, overall survival was not different between treatment arms.

Cytotoxic chemotherapeutics

An untargeted approach to cancer treatment involves use of conventional chemotherapeutics. These drugs non-specifically target all rapidly dividing cells, causing cytotoxicity and cell death. The list of chemotherapeutics used in breast cancer is expansive and includes several classes of drugs. The two major classes of cytotoxic chemotherapies used in the context of breast cancer include anthracyclines (i.e. doxorubicin) which inhibit topoisomerase II and intercalate into double stranded DNA, inhibiting RNA synthesis, and taxanes (i.e.paclitaxel) which stabilize microtubule assembly and cause a mitotic arrest [66].

Summary

As illustrated in Figure 1-4, general post-surgical/post-radiation adjuvant hormonal therapy guidelines for pre-menopausal women with localized or metastatic disease includes use of the SERM tamoxifen, or an AI with ovarian suppression using luteinizing hormone releasing hormone (LHRH) agonist, or ovarian ablation with oophorectomy. Addition of other agents is considered with increased disease severity, such as large tumor size, many positive nodes, or metastatic disease [35]. The majority of clinical studies that examine patient prognosis and survival after endocrine therapies exist for post-menopausal women; thus, upon ovarian suppression or ablation, pre-menopausal patients are treated as post-menopausal and progress through treatment based on post-menopausal guidelines. For post-menopausal women, post-surgical/post-radiation adjuvant hormonal therapy for localized disease includes AI or SERM, with SERDs reserved for later line treatments [35]. For metastatic disease, an AI, SERM, or SERD is

combined with everolimus or palbociclib, and these combinations have been shown to provide greater overall survival and progression free survival when compared to SERM or AI alone; however these data also reveal that enhanced patient survival is limited to patients who have not been exposed to prior hormonal therapy. For pre- and post-menopausal women with extensive metastatic disease or endocrine resistance, hormonal therapies, especially in combination with CDK4/6 inhibitors or mTOR inhibtors are first line [34]. In all cases, if a patient has stage III disease, addition of cytotoxic chemotherapy is recommended as it shows a high benefit compared to risk. However, in patients with less than stage III disease, genetic testing is recommended using screens such as OncotypeDX or PAM50. In these patients, treatment recommendations are on a case-by-case basis after taking into consideration both the clinical and genetic risk of relapse [18]. Finally, if patients have failed on all targeted therapeutics, cytotoxic chemotherapeutics are considered [32-36].

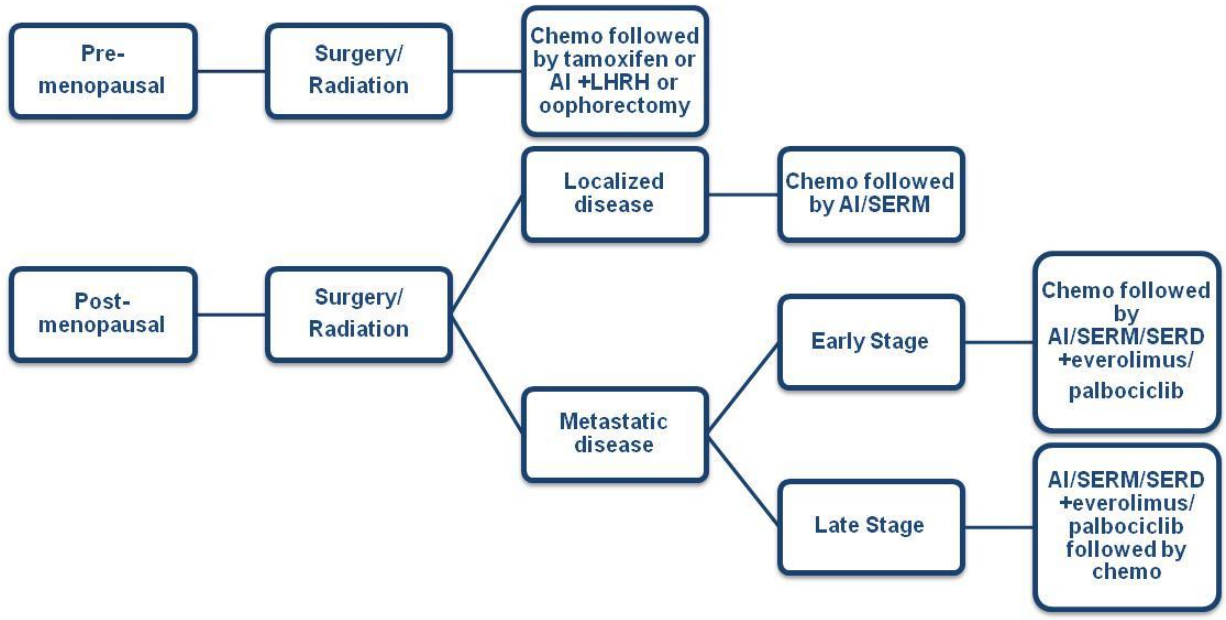

Figure 1-4: Guidelines for use of hormonal therapies in ER+ breast cancer. After surgery and radiation, pre-menopausal women are treated with chemotherapy followed by tamoxifen or an aromatase inhibitor with ovarian suppresion or ablation. Post-menopausal women are treated with an chemotherapy followed by an AI or SERM for localized disease, or with chemotherapy followed by an endocrine agent combined with another targeted therapy for metastatic disease. For very late stage disease, patients are treated with endocrine therapy first to minimize side effects and maximize quality of life.

Mechanisms of resistance to current ER+ breast cancer therapeutics

Resistance to therapies used to treat ER+ breast cancer accounts for many cases of relapse or recurrence. In fact, in women who have taken tamoxifen for 5 years, nearly 30% will relapse within 15 years [67]. Mechanisms of resistance are diverse and may be

specific to the class of therapy or individual drugs used in treatment, related to the genetics of each individual tumor, or be due to some combination of the two. Some of the mechanisms that have been characterized either in cell culture or from analysis of human tumors are outlined below.

Resistance to endocrine therapies

ER mutations

Multiple ER mutations exist and provide one route of resistance to hormonal therapies. A missense mutation on tyrosine 537 within the ligand-binding domain renders ER ligand independent [68], truncated forms of ER-alpha have been identified in human tumors and correlated with resistance to tamoxifen [67], and point mutations that lead to constitutive activation of ER, especially after use of AIs, have also been characterized [69].

Drug modification

Altered metabolism or efflux of endocrine agents can change patient responsiveness. For example, cells may metabolize active substrates to inactive forms, initiate efflux drugs from estrogen-dependent cells [67], or modify compounds in a way that inhibits binding of drugs to their targets [70].

Activation of alternate signaling pathways

The number of signaling pathways implicated in endocrine resistance are vast. Mitogen activated protein kinase (MAPK), PI3K/Akt/mTOR, insulin growth factor (IGF), human

epidermal growth factor receptor (HER2/neu) signaling, among others, have been reported to be activated in ER+ tumors that are resistant to endocrine therapies [67, 68, 70-72]. Phosphorylation of ER by activation of these pathways can render it ligand independent. For example, ER can be phosphorylated at serine 167 by Akt, at serine 118 by MAPKs, or at serine 305 by protein kinase A, and phosphorylation at serine 305 is associated with poor patient outcome [50, 68, 73]. Co-regulators of ER can either be overexpressed or activated by phosphorylation to render cells endocrine resistant [21, 67, 68], and aberrant expression of cell cycle associated proteins like cyclin D and c-myc have also been shown to be involved in conferring resistance to endocrine therapies [50, 67, 68].

microRNA regulation

Overexpression of microRNAs 221 and 222 have been shown to be involved in activation of signaling pathways that confer resistance to fulvestrant [67, 74].

Summary

Multiple pathways of resistance to endocrine therapies exist and treatment with different endocrine therapies can lead to resistance via similar or distinct mechanisms. Importantly, resistance to an AI does not confer resistance to SERMs or SERDs, and resistance to SERMs does not confer resistance to SERDs. Thus, the sequence of treatment begins with AIs, followed by SERMs, with SERDs reserved for a later line endocrine option.

Resistance to CDK4/6 inhibitors

Although clinical use of combining endocrine agents with targeted treatments such as CDK4/6 inhibitors has only recently become widespread, resistance to these combinations have been reported. Upregulation of cyclin E or loss of Rb can render cells resistant to palbociclib [59]. Cyclin-dependent kinase 2 (CDK2) has been shown to complex directly with cyclin E or cyclin D to promote progression into S phase despite CDK4/6 inhibition [59, 75]. Dysregulation of E2F and increased activity of the PI3K signaling pathway have also been implicated [59].

Resistance to mTOR inhibitors

Resistance to mTOR inhibitors used in conjunction with endocrine therapies has also been reported. Upregulation of c-myc mRNA and protein, and activation of autophagy have been implicated in resistance to everolimus [76, 77].

Combating drug resistance in ER+ breast cancer

With the emergence of resistance to even the most novel of combination therapies currently used clinically, there is an urgent need to uncover novel compounds and study their efficacy against resistant cancers. It is also vital to identify new therapeutic targets that prevent or decrease the development of resistance. One potential pathway of interest lies within the mitogen activated protein kinase (MAPK) signaling pathway.

MAPK signaling

Mitogen activated protein kinase kinase kinases (MAPKKKs, MAP3Ks) are serine/threonine kinases which act as central signaling nodes that receive inputs from cell surface receptors and relay activation signals to multiple downstream pathways involved in cell proliferation, survival, differentiation, and migration. Mixed-lineage kinases (MLKs) are a family of seven MAP3Ks that can be divided into 3 sub-families based on protein structure, of which MLK3 is the best studied. They act as central signaling nodes that phosphorylate and activate mitogen-activated protein kinase kinases (MAP2Ks), which in turn phosphorylate and activate mitogen-activated protein kinases (MAPKs). MAPKs phosphorylate and activate transcription factors, leading to transcription of genes involved in growth and survival, and have been implicated in direct phosphorylation and activation of ER independent of the presence of estrogen. They can also phosphorylate cytoplasmic substrates that affect cell migration, among other cellular activities [78, 79]. Overexpression and over activation of MAPK pathway members have been implicated in a number of cancers, making them ideal targets for chemotherapeutics [79]. Identification of compounds that are able to inhibit signaling through the MAPK pathway may be useful in combating endocrine sensitive and resistant ER+ breast cancers.

Development of CEP-1347

CEP-1347 is an indolocarbazole derivative that competitively binds to the ATP binding site on MLKs and inhibits kinase activity. CEP-1347 was isolated as a neurotrophic agent targeted to protect neurons in the substantia nigra from degradation and

apoptosis and inhibit progression of Parkinson's disease (PD) [80, 81]. The in vitro and in vivo work completed with CEP-1347 in the context of Parkinson's disease identified this compound as a pan-MLK inhibitor, with selectivity for MLK3 (MAP3K11) that caused downstream inhibition of the MAPKs extracellular signaling regulated kinase (ERK), c-Jun N-terminal kinase/stress-activated protein kinase (JNK/SAPK), and p38. The focus of the PD-based studies was on CEP-1347-induced inhibition of JNK activation after treatment, leading to a decrease in apoptosis in dopaminergic neurons [80, 81]. CEP-1347 showed promising results in pre-clinical studies leading to its advancement into early phase clinical trials.

PRECEPT clinical trial for Parkinson's disease

CEP-1347 progressed through Phase I safety trials and was well-tolerated and non-toxic in healthy adults [82]. Thus, a Phase II/III trial, Parkinson Research Examination of CEP-1347 Trial, PRECEPT, was initiated. More than 800 consenting adults were recruited to participate in the 48 month study, and the primary endpoint of progression requiring dopaminergic therapy was established. CEP-1347 ultimately failed to be efficacious in patients, and the trial was prematurely ended at 24.1 months [83]. Although the PRECEPT trial was not successful, safety of CEP-1347 was established, and evidence of inhibition of the MLK pathways was provided in pre-clinical trials [84].

Post-PRECEPT studies of CEP-1347 and CEP-11004

Since the early termination of the PRECEPT study, CEP-1347 has been studied in the context of other neurological disorders, including Huntington's disease [85, 86],

Alzheimer's disease [81], and auditory disorders [87], primarily for its role in preventing JNK activation. It has also been studied for its effect as an anti-inflammatory agent in the brain [88, 89] and pancreas [90]. Our lab investigated CEP-1347 as an inhibitor of ER+ breast cancer cell proliferation and found that it decreased cell viability, caused early mitotic cell cycle arrest, led to polyploidy, and induced apoptosis in ER+ cell lines. In addition, it was selective for transformed versus non-transformed cell lines at the concentrations used [91], supporting its possible use as a breast cancer therapeutic. Most recently, CEP-1347 was investigated as an agent to inhibit tumor-initiating stem cell proliferation and differentiation [92].

CEP-11004 is closely related to CEP-1347. It is also an MLK inhibitor and has been shown to inhibit ERK, JNK, and p38 MAPKs downstream of MLK3 [93, 94]. Like CEP-1347, treatment with CEP-11004 is selective for transformed versus non-transformed cell lines [93]. Phenotypes exhibited by treatment include aberrant DNA condensation and abnormal mitotic spindle formation [93]. This compound has also been studied in the context of inflammation [88, 95, 96], and neuroprotection in neurological diseases [85, 97-99]. No clinical evidence of safety or tolerability in humans yet exists for CEP-11004, and in neuronal cells, CEP-1347 is a more potent inhibitor of JNK activation [100], making CEP-1347 a more desirable compound to evaluate further.

Overarching goal

The goal of this thesis was to evaluate the efficacy of CEP-1347, alone and in combination with the clinically available anti-estrogen fulvestrant, on proliferation and

apoptosis of endocrine sensitive and resistant ER+ breast cancer cells in vitro and in vivo. I also further investigated the mechanism of action by which CEP-1347 acts to alter cell growth and death and studied the kinase targets of this compound. I hypothesize that combination therapy will be more effective in preventing proliferation and enhancing apoptosis compared to either compound alone, and that novel kinase targets of CEP-1347 exist and play a role in generating the phenotype observed after treatment.

Proposed targets and mechanism of action

The in vitro and in vivo work using CEP-1347 showed inhibition of MLK activity, with specificity for MLK3, and downstream inhibition of JNK phosphorylation. JNK phosphorylates and activates a number of different proteins involved in transcription, cytoskeletal regulation, vesicle transport, and apoptosis and autophagy, including Myc, Bim, Bcl-2, among others [101, 102]. One important target of JNK is c-Jun, a protein that is a subunit of the AP-1 transcription factor [81]. Our own studies have confirmed inhibition of multiple members of the MAPK pathway, including c-Jun, JNK, p38, ERK, and MEK1/2, and have identified a novel direct or indirect target of CEP-1347. AMP-activated protein kinase (AMPK) phosphorylation was significantly inhibited by treatment with CEP-1347, and its roles in ER+ breast cancer proliferation are further investigated in this thesis. Both MLK3 and AMPK are discussed in greater detail below.

MLK3

Function

MLK3 is the most well studied MAP3K that is overexpressed or mutated in multiple cancer types. It transmits signals from cell surface receptors including receptor tyrosine kinases (RTKs), G-protein-coupled receptors (GPCRs), and tumor necrosis factor receptors (TNFRs) downstream to activate transcription factors that are involved in cell proliferation, survival, and invasion [79, 103-105]. MLK3 can activate the three major MAPKs [106-108]: JNK/SAPK via the MAP2K MKK4/7 [109, 110], p38 MAPK via the MAP2K MKK3/6 [111, 112], and ERK either via the MAP2K MKK1/2 or by acting as a scaffold to allow activation of MKK1/2 in a kinase-independent manner [108] (illustrated in Figure 1-5). MLK3 can also regulate the NF-kappaB (NF-κB) transcription factor via phosphorylation and activation of IκB kinase α (IKKα) and IκB kinase β (IKKβ) [113]. All of these downstream proteins have been widely linked to cancer proliferation, survival, and migration [114-116].

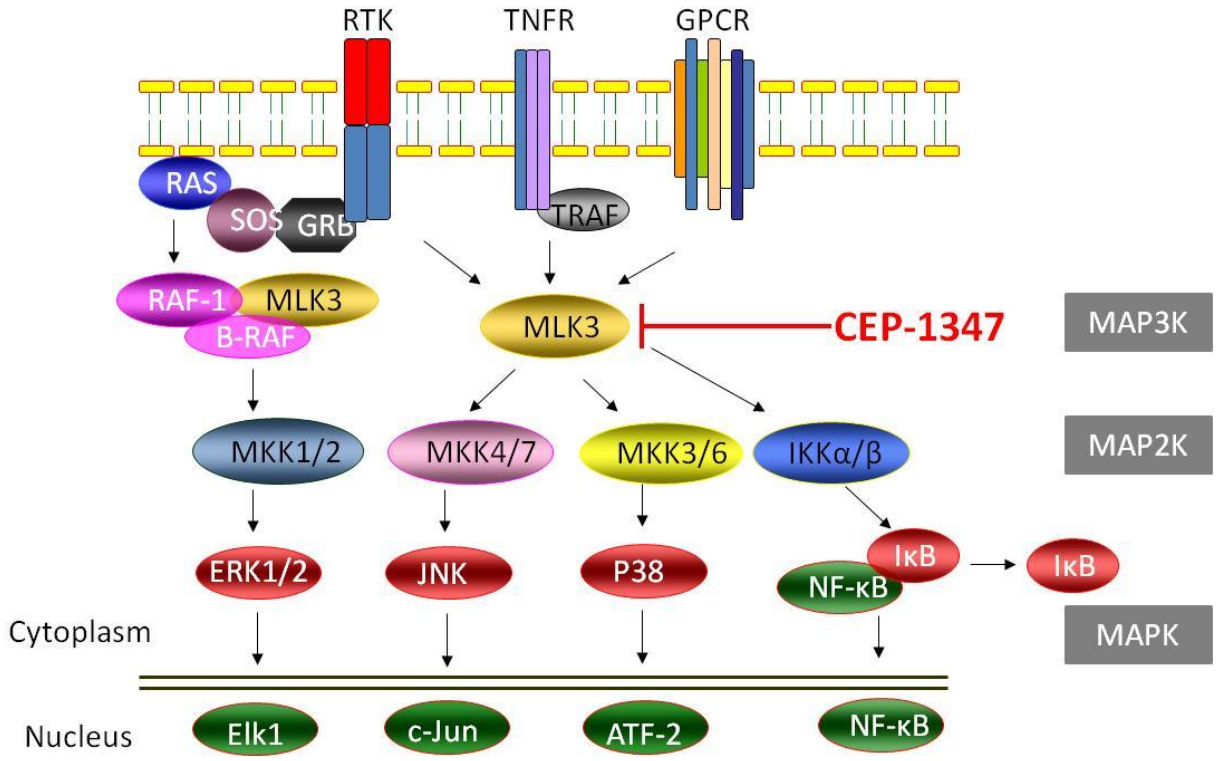

Figure 1-5: MLK3 in the MAPK signaling pathway. MLK3 is a MAP3K that receives signals from cell surface receptors and transduces them downstream to MAP2Ks which phosphorylate and activate MAPKs. MLK3 can also act as a scaffold for other proteins to create a complex that is also able to activate downstream MAP2Ks. Figure adapted from Jian Chen.

Regulation

MLK3 contains autoinhibitory and autophosphorylation domains. To prevent activation, the N-terminal domain maintains MLK3 in a folded configuration [117, 118]. Binding of a guanine triphosphatase (GTPase) to the Cdc42-/Rac1-interactive binding (CRIB) motif near the C-terminus is required to unfold MLK3 and allow activation [119-121]. When unfolded, MLK3 is able to homodimerize and autophosphorylate threonine 277 and

serine 281 on both monomers [122]. MLK3 activity is negatively regulated by the tumor suppressor Merlin [108, 123]. Binding of Merlin to the C-terminus of MLK3 blocks access of a GTPase to the CRIB motif, and prevents subsequent activation [79].

Significance in cancer

Studies have shown that MLK3 plays a role in the cell cycle. The structure of MLK3 is homologous to the non-catalytic region of never in mitosis A (NIMA) kinase, which regulates its function [94]. NIMA kinases are involved in progression through G2/M, and they share more sequence homology to MLK3 than any other member of the MLK family, suggesting that MLK3 may also play an important role in mitotic progression [124]. Treatment with CEP-1347 led to G2/M arrest [91, 93], which could be reversed by MLK3 overexpression [93], and overexpression of MLK3 has been linked to inhibition of astral microtubule formation [94]. MLK3 has also been implicated in phosphorylation and activation of Pin1, a protein that plays a major role in progression through mitosis [125].

Treatment with CEP-1347 was reported to prevent nuclear translocation of NF-κB subunit p65 and inhibit phosphorylation of the transcription factor c-Jun in ER+ breast cancer cells, suggesting that the target of CEP-1347 plays a role in cancer cell transcriptional regulation [91]. Expression and regulation of the three MAPKs downstream of MLK3 are dysregulated in breast cancer and contribute to endocrine and chemotherapy resistance [126]. In addition to involvement in transcription, MLK3 has also been shown to play an important role in breast cancer migration and invasion.

Overexpression of MLK3 has been shown to transform non-tumorigenic mammary epithelial cells into an invasive and malignant phenotype and promoting focal adhesion turnover [79, 103, 127, 128]. Furthermore, knockdown of MLK3 was sufficient to inhibit metastasis in the highly metastatic cell line MDA-MB-231[129], and has been shown to decrease expression of a number of matrix-metalloproteases [104]. MLK3 has also been implicated in promoting apoptosis [130, 131]. While MLK3 has been studied to be the preferred target of CEP-1347, it is important to explore other potential targets of the drug to fully understand its mechanism of action.

AMP-activated protein kinase (AMPK) Signaling

Function

A novel potential target of CEP-1347 that was identified in this thesis is AMPK, a serine/threonine kinase that is canonically known to play a major role in cellular energy homeostatis and metabolism [132, 133]. The exact role of AMPK in cancer development and persistence has been difficult to elucidate and it is now posited to play both tumor suppressor and tumor promoter roles depending on cancer cell type and stage of cancer development [132-134]. AMPK levels have been shown to be both up- and downregulated in various cancer types, and correlated with both good and poor prognosis [134]. AMPK inhibits fatty acid biosynthesis by phosphorylating and inhibiting acetyl-CoA carboxylase, inhibits steroid biosynthesis by phosphorylating and inactivating 3-hydroxy-3methylglutaryl-CoA reductase (HMGCR), and protein synthesis by inhibiting the mTOR complex 1 (mTORC1). AMPK is also able to cause a cell cycle arrest by modulating p53 function [132-134]. However, AMPK activation can also

promote tumor cell persistence via protection from metabolic stress and survival in hypoxic and nutrient-deplete conditions [132-134]. AMPK expression is induced during mitosis and active AMPK plays a role in and mitotic spindle orientation [135] and in regulating cellular polarity [136].

Regulation

Liver kinase B1 (LKB1), a known tumor suppressor, was the first identified regulator of AMPK. Calmodulin-dependent kinase kinase beta (CaMKKβ) was later identified as an upstream activator in cases of high levels of intracellular calcium. Adenosine monophosphate (AMP) or adenosine diphosphate (ADP) binding to AMPK leads to a change in conformation allowing the phosphorylation site to be accessed by LKB1 or CaMKKβ [132]. Because LKB1 is a known tumor suppressor, it was hypothesized that AMPK may also play a role in tumor suppression [132]. In fact, a number of studies suggest that treatment with metformin, an indirect AMPK activator, in diabetic patients leads to reduced risk and incidence of cancer [137]. Furthermore, AMPK can also be phosphorylated by MLK3 [138] or PLK1 [139], and multiple autophosphorylation sites have been identified [140].

Significance in cancer

The major role of AMPK in cancer is hypothesized to be via preventing a switch of cancer cells from oxidative metabolism to a Warburg glycolytic energy state [132, 134, 137]. Furthermore, AMPK inhibition increases apoptosis [141], activation has been shown to promote angiogenesis [142], and both inhibition [143, 144] and activation [145]

decreases proliferation. AMPK also plays a role in mitotic progression. As AMPK activation inhibits fatty acid synthesis, insufficient fatty acids synthesis for two cell membranes for cytokinesis to progress, leading to a cell cycle arrest [146]. AMPK is also involved in mitotic spindle assembly [135, 147, 148]. Both constitutive activation and inhibition of AMPK have been shown to dysregulate mitotic spindle formation and alignment, and cause abnormal chromosomal separation and polyploidy [135, 143, 149].

Models for study

To study the efficacy of CEP-1347 against endocrine sensitive and resistant breast cancer, a number of models were utilized.

Cell lines

MCF-7

Immortalized cell lines are commonly used as a starting point for characterizing the mechanisms of drug action in vitro and in vivo. Stable cultures of MCF-7 cells were first established by Herbert D. Soule in 1970 after isolation from the pleural effusion of Sister Catherine Frances (Helen Marion) Mallon at the Michigan Cancer Foundation. Since then, MCF-7 cells have been the mainstay in the study of ER+ breast cancer, and has been vital in the development of novel therapeutics [150, 151]. MCF-7 cells form an epithelial-like monolayer in cell culture, require estrogen for growth, and experience a G1 cell cycle arrest when exposed to any endocrine therapy [152]. They form spheroids with lumens in 3-dimensional culture, express the wild-type form of the tumor

suppressor p53, and are non-metastatic in animals [152]. Thus, MCF-7 cells were elected to be used as a model of estrogen dependent ER+ breast cancer.

LCC9

LCC9 cells were derived from MCF-7 cells and were selected for estrogen independence and anti-estrogen resistance. MCF-7 cells were passaged in vivo in ovariectomized Nu/Nu mice to create MCF-7/LCC1, which exhibited estrogen independence. MCF-7/LCC1 cells were then passaged in vitro under stepwise selection with tamoxifen or fulvestrant to create MCF-7/LCC2 or MCF-7/LCC9 cells, respectively. MCF-7/LCC9 cells (herein called LCC9) exhibited cross-resistance to tamoxifen [153] and are used as a model of endocrine resistant ER+ breast cancer. LCC9 cells retain wild-type ER expression [153], and resistance to fulvestrant is posited to occur via upregulation of the NFκB subunit p65 [154].

Patient derived xenograft (PDX) lines

Cell lines have been adapted for enhanced growth in cell culture and may have lost many characteristics unique to their original tumors. Thus, another model to study drug efficacy that more closely recapitulates patient scenarios uses patient derived xenografts (PDXs). These lines are harvested from patients, and amplified through immunocompromised mice for use in in vitro and in vivo studies. PDXs encompass the heterogeneity and drug sensitivity or resistance of patient tumors that have undergone multiple cycles of chemotherapy, and have exhibited continued growth in response to many treatments.

HCI-011

HCI-011 is an ER+, PR+, and HER2 negative PDX line that was originally derived from a pleural effusion. It is estrogen responsive, and exhibits ductal pathology on histological examination. The patient from which this line was derived was exposed to doxorubicin, cyclophosphamide, paclitaxel, and fulvestrant, and continued to progress despite therapy. In mice, this line has been shown to metastasize to lungs and lymph nodes [155].

HCI-013

HCI-013 is an ER+, PR+ and HER2 negative line that was originally derived from a pleural effusion. It is estrogen responsive, and exhibits lobular pathology on histological examination. The patient from which this line was derived was exposed to leuprolide, letrozole, exemestane, tamoxifen, cyclophosphamide, methotrexate, 5-fluorouracil, paclitaxel, doxorubicin, carboplatin, and gemcitabine, and continued to progress despite therapy. Metastases in mice have not been characterized [155].

1006909 (HCI-013 EI)

HCI-013 EI is an ER+, PR+ and HER2 negative line that was originally derived after long term passage of HCI-013 in ovariectomized immune compromised mice without estrogen supplementation. It is estrogen independent and thus does not require estrogen for growth, and exhibits lobular pathology on histological examination. Metastases in mice have not been characterized [156].

Using these models, the potential efficacy of CEP-1347 as a therapeutic for ER+ breast cancer was evaluated, and its mechanism of action during mitosis was further characterized.

REFERENCES

REFERENCES

1. Siegel, R.L., K.D. Miller, and A. Jemal, Cancer Statistics, 2017. CA Cancer J Clin, 2017. 67(1): p. 7-30.

2. DeSantis, C.E., et al., Breast cancer statistics, 2017, racial disparity in mortality by state. CA Cancer J Clin, 2017. 67(6): p. 439-448.

3. Society, A.C., Breast Cancer Facts & Figures 2017-2018, 2017, American Cancer Society, Inc: Atlanta.

4. Makki, J., Diversity of Breast Carcinoma: Histological Subtypes and Clinical Relevance. Clin Med Insights Pathol, 2015. 8: p. 23-31.

5. Raghav, K., et al., Inflammatory Breast Cancer: A Distinct Clinicopathological Entity Transcending Histological Distinction. PLoS ONE, 2016. 11(1): p. e0145534.

6. Henry-Tillman, R.S. and V.S. Klimberg, In situ breast cancer. Curr Treat Options Oncol, 2000. 1(3): p. 199-209.

7. Kinne, D.W., et al., Breast carcinoma in situ. Arch Surg, 1989. 124(1): p. 33-6.

8. Hergueta-Redondo, M., et al., "New" molecular taxonomy in breast cancer. Clin Transl Oncol, 2008. 10(12): p. 777-85.

9. Sims, A.H., et al., Origins of breast cancer subtypes and therapeutic implications. Nat Clin Pract Oncol, 2007. 4(9): p. 516-25.

10. Perou, C.M., et al., Molecular portraits of human breast tumours. Nature, 2000. 406(6797): p. 747-52.

11. Sorlie, T., et al., Gene expression patterns of breast carcinomas distinguish tumor subclasses with clinical implications. Proc Natl Acad Sci U S A, 2001. 98(19): p. 10869-74.

12. Tang, P. and G.M. Tse, Immunohistochemical Surrogates for Molecular Classification of Breast Carcinoma: A 2015 Update. Arch Pathol Lab Med, 2016. 140(8): p. 806-14.

13. Sorlie, T., et al., Distinct molecular mechanisms underlying clinically relevant subtypes of breast cancer: gene expression analyses across three different platforms. BMC Genomics, 2006. 7: p. 127.

14. van 't Veer, L.J., et al., Gene expression profiling predicts clinical outcome of breast cancer. Nature, 2002. 415(6871): p. 530-6.

15. Sotiriou, C., et al., Breast cancer classification and prognosis based on gene expression profiles from a population-based study. Proc Natl Acad Sci U S A, 2003. 100(18): p. 10393-8.

16. Reis-Filho, J.S. and L. Pusztai, Gene expression profiling in breast cancer: classification, prognostication, and prediction. Lancet, 2011. 378(9805): p. 1812-23.

17. Wesolowski, R. and B. Ramaswamy, Gene expression profiling: changing face of breast cancer classification and management. Gene Expr, 2011. 15(3): p. 105-15.

18. Henry, N.L., et al., Role of Patient and Disease Factors in Adjuvant Systemic Therapy Decision Making for Early-Stage, Operable Breast Cancer: American Society of Clinical Oncology Endorsement of Cancer Care Ontario Guideline Recommendations. J Clin Oncol, 2016. 34(19): p. 2303-11.

19. Levenson, A.S. and V.C. Jordan, MCF-7: the first hormone-responsive breast cancer cell line. Cancer Res, 1997. 57(15): p. 3071-8.

20. Klinge, C.M., Estrogen receptor interaction with estrogen response elements. Nucleic Acids Res, 2001. 29(14): p. 2905-19.

21. Osborne, C.K. and R. Schiff, Mechanisms of endocrine resistance in breast cancer. Annu Rev Med, 2011. 62: p. 233-47.

22. Schiff, R., et al., Cross-talk between estrogen receptor and growth factor pathways as a molecular target for overcoming endocrine resistance. Clin Cancer Res, 2004. 10(1 Pt 2): p. 331S-6S.

23. Levin, E.R. and R.J. Pietras, Estrogen receptors outside the nucleus in breast cancer. Breast Cancer Res Treat, 2008. 108(3): p. 351-61.

24. Mukherjee, S. and S.E. Conrad, c-Myc suppresses p21WAF1/CIP1 expression during estrogen signaling and antiestrogen resistance in human breast cancer cells. J Biol Chem, 2005. 280(18): p. 17617-25.

25. Sutherland, R.L., et al., Estrogen and progestin regulation of cell cycle progression. J Mammary Gland Biol Neoplasia, 1998. 3(1): p. 63-72.

26. Prall, O.W., E.M. Rogan, and R.L. Sutherland, Estrogen regulation of cell cycle progression in breast cancer cells. J Steroid Biochem Mol Biol, 1998. 65(1-6): p. 169-74.

27. Doisneau-Sixou, S.F., et al., Estrogen and antiestrogen regulation of cell cycle progression in breast cancer cells. Endocr Relat Cancer, 2003. 10(2): p. 179-86.

28. VanArsdale, T., et al., Molecular Pathways: Targeting the Cyclin D-CDK4/6 Axis for Cancer Treatment. Clin Cancer Res, 2015. 21(13): p. 2905-10.

29. Foster, J.S., et al., Estrogens and cell-cycle regulation in breast cancer. Trends Endocrinol Metab, 2001. 12(7): p. 320-7.

30. Foster, J.S., et al., Multifaceted regulation of cell cycle progression by estrogen: regulation of Cdk inhibitors and Cdc25A independent of cyclin D1-Cdk4 function. Mol Cell Biol, 2001. 21(3): p. 794-810.

31. Metivier, R., et al., Estrogen receptor-alpha directs ordered, cyclical, and combinatorial recruitment of cofactors on a natural target promoter. Cell, 2003. 115(6): p. 751-63.

32. Senkus, E., et al., Primary breast cancer: ESMO Clinical Practice Guidelines for diagnosis, treatment and follow-up. Ann Oncol, 2015. 26 Suppl 5: p. v8-30.

33. Cardoso, F., et al., 3rd ESO-ESMO International Consensus Guidelines for Advanced Breast Cancer (ABC 3). Ann Oncol, 2017. 28(12): p. 3111.

34. Rugo, H.S., et al., Endocrine Therapy for Hormone Receptor-Positive Metastatic Breast Cancer: American Society of Clinical Oncology Guideline. J Clin Oncol, 2016. 34(25): p. 3069-103.

35. Gradishar, W.J., et al., NCCN Guidelines Insights: Breast Cancer, Version 1.2017. J Natl Compr Canc Netw, 2017. 15(4): p. 433-451.

36. Sledge, G.W., et al., Past, present, and future challenges in breast cancer treatment. J Clin Oncol, 2014. 32(19): p. 1979-86.

37. Oeffinger, K.C., et al., Breast cancer screening for women at average risk: 2015 guideline update from the american cancer society. JAMA, 2015. 314(15): p. 1599-1614.

38. Saslow, D., et al., American Cancer Society guidelines for breast screening with MRI as an adjunct to mammography. CA Cancer J Clin, 2007. 57(2): p. 75-89.

39. Final Recommendation Statement: Breast Cancer: Screening. U.S. Preventive Services Task Force, 2016.

40. Practice Bulletin Number 179: Breast Cancer Risk Assessment and Screening in Average-Risk Women. Obstet Gynecol, 2017. 130(1): p. e1-e16.

41. Giuliano, A.E., et al., Breast Cancer-Major changes in the American Joint Committee on Cancer eighth edition cancer staging manual. CA Cancer J Clin, 2017. 67(4): p. 290-303.

42. Jordan, V.C., The development of tamoxifen for breast cancer therapy: a tribute to the late Arthur L. Walpole. Breast Cancer Res Treat, 1988. 11(3): p. 197-209.

43. Jordan, V.C., Tamoxifen (ICI46,474) as a targeted therapy to treat and prevent breast cancer. Br J Pharmacol, 2006. 147 Suppl 1: p. S269-76.

44. Sutherland, R.L., et al., Tamoxifen induces accumulation of MCF 7 human mammary carcinoma cells in the G0/G1 phase of the cell cycle. Eur J Cancer Clin Oncol, 1983. 19(5): p. 615-21.

45. Taylor, I.W., et al., Effects of tamoxifen on cell cycle progression of synchronous MCF-7 human mammary carcinoma cells. Cancer Res, 1983. 43(9): p. 4007-10.

46. Sutherland, R.L., R.E. Hall, and I.W. Taylor, Cell proliferation kinetics of MCF-7 human mammary carcinoma cells in culture and effects of tamoxifen on exponentially growing and plateau-phase cells. Cancer Res, 1983. 43(9): p. 3998-4006.

47. An, K.C., Selective Estrogen Receptor Modulators. Asian Spine J, 2016. 10(4): p. 787-91.

48. Howell, S.J., S.R. Johnston, and A. Howell, The use of selective estrogen receptor modulators and selective estrogen receptor down-regulators in breast cancer. Best Pract Res Clin Endocrinol Metab, 2004. 18(1): p. 47-66.

49. Mandlekar, S. and A.N. Kong, Mechanisms of tamoxifen-induced apoptosis. Apoptosis, 2001. 6(6): p. 469-77.

50. Zwart, W., V. Theodorou, and J.S. Carroll, Estrogen receptor-positive breast cancer: a multidisciplinary challenge. Wiley Interdiscip Rev Syst Biol Med, 2011. 3(2): p. 216-30.

51. Thiantanawat, A., B.J. Long, and A.M. Brodie, Signaling pathways of apoptosis activated by aromatase inhibitors and antiestrogens. Cancer Res, 2003. 63(22): p. 8037-50.

52. Miller, W.R., et al., Aromatase inhibitors: are there differences between steroidal and nonsteroidal aromatase inhibitors and do they matter? Oncologist, 2008. 13(8): p. 829-37.

53. Bracken, A.P., et al., E2F target genes: unraveling the biology. Trends Biochem Sci, 2004. 29(8): p. 409-17.

54. Attwooll, C., E. Lazzerini Denchi, and K. Helin, The E2F family: specific functions and overlapping interests. EMBO J, 2004. 23(24): p. 4709-16.

55. Akin, S., et al., A novel targeted therapy in breast cancer: cyclin dependent kinase inhibitors. J BUON, 2014. 19(1): p. 42-6.

56. Polk, A., et al., Specific CDK4/6 inhibition in breast cancer: a systematic review of current clinical evidence. ESMO Open, 2016. 1(6): p. e000093.

57. Fasching PA, J.G., Pivot X, Martin M, De Laurentiis M, Blackwell K, Esteva FJ, Paquet-Luzy T, Tang Z, Lorenc KR, Slamon DJ. Phase III study of ribociclib (LEE011) in combination with fulvestrant for the treatment of postmenopausal patients (pts) with hormone receptor-positive (HR+), HER2-negative (HER2–) advanced breast cancer (aBC) who have received no or only one line of prior endocrine treatment: MONALEESA-3. in Proceedings of the Thirty-Eighth Annual CTRC-AACR San Antonio Breast Cancer Symposium. 2016. San Antonio, TX: AACR; Cancer Research.

58. Finn, R.S., et al., Palbociclib and Letrozole in Advanced Breast Cancer. N Engl J Med, 2016. 375(20): p. 1925-1936.

59. Rocca, A., et al., Progress with palbociclib in breast cancer: latest evidence and clinical considerations. Ther Adv Med Oncol, 2017. 9(2): p. 83-105.

60. Turner, N.C., et al., Palbociclib in Hormone-Receptor-Positive Advanced Breast Cancer. N Engl J Med, 2015. 373(3): p. 209-19.

61. Morgensztern, D. and H.L. McLeod, PI3K/Akt/mTOR pathway as a target for cancer therapy. Anticancer Drugs, 2005. 16(8): p. 797-803.

62. Yardley, D.A., et al., Everolimus plus exemestane in postmenopausal patients with HR(+) breast cancer: BOLERO-2 final progression-free survival analysis. Adv Ther, 2013. 30(10): p. 870-84.

63. Kornblum, N., et al., Randomized Phase II Trial of Fulvestrant Plus Everolimus or Placebo in Postmenopausal Women With Hormone Receptor-Positive, Human Epidermal Growth Factor Receptor 2-Negative Metastatic Breast Cancer Resistant to Aromatase Inhibitor Therapy: Results of PrE0102. J Clin Oncol, 2018: p. JCO2017769331.

64. Bachelot, T., et al., Randomized phase II trial of everolimus in combination with tamoxifen in patients with hormone receptor-positive, human epidermal growth factor receptor 2-negative metastatic breast cancer with prior exposure to aromatase inhibitors: a GINECO study. J Clin Oncol, 2012. 30(22): p. 2718-24.

65. Hurvitz, S.A., et al., In vitro activity of the mTOR inhibitor everolimus, in a large panel of breast cancer cell lines and analysis for predictors of response. Breast Cancer Res Treat, 2015. 149(3): p. 669-80.

66. Society, A.C. Chemotherapy for Breast Cancer. 2017 August 1, 2017 [cited 2018 June 6, 2018]; Available from: https://www.cancer.org/cancer/breast-cancer/treatment/chemotherapy-for-breast-cancer.html.

67. Musgrove, E.A. and R.L. Sutherland, Biological determinants of endocrine resistance in breast cancer. Nat Rev Cancer, 2009. 9(9): p. 631-43.

68. Ali, S. and R.C. Coombes, Endocrine-responsive breast cancer and strategies for combating resistance. Nat Rev Cancer, 2002. 2(2): p. 101-12.

69. Robinson, D.R., et al., Activating ESR1 mutations in hormone-resistant metastatic breast cancer. Nat Genet, 2013. 45(12): p. 1446-51.

70. D'Amato, N.C., et al., Cooperative Dynamics of AR and ER Activity in Breast Cancer. Mol Cancer Res, 2016.

71. Zhao, H., et al., Overcoming resistance to fulvestrant (ICI182,780) by downregulating the c-ABL proto-oncogene in breast cancer. Mol Carcinog, 2011. 50(5): p. 383-9.

72. Frogne, T., et al., Activation of ErbB3, EGFR and Erk is essential for growth of human breast cancer cell lines with acquired resistance to fulvestrant. Breast Cancer Res Treat, 2009. 114(2): p. 263-75.

73. Wolf, D.M., et al., Investigation of the mechanism of tamoxifen-stimulated breast tumor growth with nonisomerizable analogues of tamoxifen and metabolites. J Natl Cancer Inst, 1993. 85(10): p. 806-12.

74. Rao, X., et al., MicroRNA-221/222 confers breast cancer fulvestrant resistance by regulating multiple signaling pathways. Oncogene, 2011. 30(9): p. 1082-97.

75. Herrera-Abreu, M.T., et al., Early Adaptation and Acquired Resistance to CDK4/6 Inhibition in Estrogen Receptor-Positive Breast Cancer. Cancer Res, 2016. 76(8): p. 2301-13.

76. Bihani, T., et al., Resistance to everolimus driven by epigenetic regulation of MYC in ER+ breast cancers. Oncotarget, 2015. 6(4): p. 2407-20.

77. Rosich, L., et al., Counteracting autophagy overcomes resistance to everolimus in mantle cell lymphoma. Clin Cancer Res, 2012. 18(19): p. 5278-89.

78. Herynk, M.H. and S.A. Fuqua, Estrogen receptor mutations in human disease. Endocr Rev, 2004. 25(6): p. 869-98.

79. Rattanasinchai, C. and K.A. Gallo, MLK3 Signaling in Cancer Invasion. Cancers (Basel), 2016. 8(5).

80. Sweeney, Z.K. and J.W. Lewcock, ACS chemical neuroscience spotlight on CEP-1347. ACS Chem Neurosci, 2011. 2(1): p. 3-4.

81. Saporito, M.S., R.L. Hudkins, and A.C. Maroney, Discovery of CEP-1347/KT-7515, an inhibitor of the JNK/SAPK pathway for the treatment of neurodegenerative diseases. Prog Med Chem, 2002. 40: p. 23-62.

82. The safety and tolerability of a mixed lineage kinase inhibitor (CEP-1347) in PD. Neurology, 2004. 62(2): p. 330-2.

83. Mixed lineage kinase inhibitor CEP-1347 fails to delay disability in early Parkinson disease. Neurology, 2007. 69(15): p. 1480-90.

84. Wang, L.H. and E.M. Johnson, Jr., Mixed lineage kinase inhibitor CEP-1347 fails to delay disability in early Parkinson disease. Neurology, 2007. 69(15): p. 1480-90.

85. Apostol, B.L., et al., CEP-1347 reduces mutant huntingtin-associated neurotoxicity and restores BDNF levels in R6/2 mice. Mol Cell Neurosci, 2008. 39(1): p. 8-20.

86. Conforti, P., et al., Blood level of brain-derived neurotrophic factor mRNA is progressively reduced in rodent models of Huntington's disease: restoration by the neuroprotective compound CEP-1347. Mol Cell Neurosci, 2008. 39(1): p. 1-7.

87. Pirvola, U., et al., Rescue of hearing, auditory hair cells, and neurons by CEP-1347/KT7515, an inhibitor of c-Jun N-terminal kinase activation. J Neurosci, 2000. 20(1): p. 43-50.

88. Falsig, J., et al., Specific modulation of astrocyte inflammation by inhibition of mixed lineage kinases with CEP-1347. J Immunol, 2004. 173(4): p. 2762-70.

89. Lund, S., et al., Inhibition of microglial inflammation by the MLK inhibitor CEP-1347. J Neurochem, 2005. 92(6): p. 1439-51.

90. Wagner, A.C., et al., CEP-1347 inhibits caerulein-induced rat pancreatic JNK activation and ameliorates caerulein pancreatitis. Am J Physiol Gastrointest Liver Physiol, 2000. 278(1): p. G165-72.

91. Wang, L., K.A. Gallo, and S.E. Conrad, Targeting mixed lineage kinases in ER-positive breast cancer cells leads to G2/M cell cycle arrest and apoptosis. Oncotarget, 2013. 4(8): p. 1158-71.

92. Okada, M., et al., Repositioning CEP-1347, a chemical agent originally developed for the treatment of Parkinson's disease, as an anti-cancer stem cell drug. Oncotarget, 2017. 8(55): p. 94872-94882.

93. Cha, H., et al., Inhibition of mixed-lineage kinase (MLK) activity during G2-phase disrupts microtubule formation and mitotic progression in HeLa cells. Cell Signal, 2006. 18(1): p. 93-104.

94. Swenson, K.I., K.E. Winkler, and A.R. Means, A new identity for MLK3 as an NIMA-related, cell cycle-regulated kinase that is localized near centrosomes and influences microtubule organization. Mol Biol Cell, 2003. 14(1): p. 156-72.

95. Ciallella, J.R., et al., CEP-11004, an inhibitor of the SAPK/JNK pathway, reduces TNF-alpha release from lipopolysaccharide-treated cells and mice. Eur J Pharmacol, 2005. 515(1-3): p. 179-87.

96. Hidding, U., et al., The c-Jun N-terminal kinases in cerebral microglia: immunological functions in the brain. Biochem Pharmacol, 2002. 64(5-6): p. 781-8.

97. Mishra, R., et al., Glycogen synthase kinase-3beta induces neuronal cell death via direct phosphorylation of mixed lineage kinase 3. J Biol Chem, 2007. 282(42): p. 30393-405.

98. Peng, J., et al., The herbicide paraquat induces dopaminergic nigral apoptosis through sustained activation of the JNK pathway. J Biol Chem, 2004. 279(31): p. 32626-32.

99. Boll, J.B., et al., Improvement of embryonic dopaminergic neurone survival in culture and after grafting into the striatum of hemiparkinsonian rats by CEP-1347. J Neurochem, 2004. 88(3): p. 698-707.

100. Wang, L.H., A.J. Paden, and E.M. Johnson, Jr., Mixed-lineage kinase inhibitors require the activation of Trk receptors to maintain long-term neuronal trophism and survival. J Pharmacol Exp Ther, 2005. 312(3): p. 1007-19.

101. Zeke, A., et al., JNK Signaling: Regulation and Functions Based on Complex Protein-Protein Partnerships. Microbiol Mol Biol Rev, 2016. 80(3): p. 793-835.

102. Weston, C.R. and R.J. Davis, The JNK signal transduction pathway. Curr Opin Genet Dev, 2002. 12(1): p. 14-21.

103. Chen, J., E.M. Miller, and K.A. Gallo, MLK3 is critical for breast cancer cell migration and promotes a malignant phenotype in mammary epithelial cells. Oncogene, 2010. 29(31): p. 4399-411.

104. Zhan, Y., et al., Mixed lineage kinase 3 is required for matrix metalloproteinase expression and invasion in ovarian cancer cells. Exp Cell Res, 2012. 318(14): p. 1641-8.

105. Velho, S., et al., Mixed lineage kinase 3 gene mutations in mismatch repair deficient gastrointestinal tumours. Hum Mol Genet, 2010. 19(4): p. 697-706.

106. Gallo, K.A. and G.L. Johnson, Mixed-lineage kinase control of JNK and p38 MAPK pathways. Nat Rev Mol Cell Biol, 2002. 3(9): p. 663-72.

107. Chadee, D.N. and J.M. Kyriakis, A novel role for mixed lineage kinase 3 (MLK3) in B-Raf activation and cell proliferation. Cell Cycle, 2004. 3(10): p. 1227-9.

108. Chadee, D.N., et al., Mixed-lineage kinase 3 regulates B-Raf through maintenance of the B-Raf/Raf-1 complex and inhibition by the NF2 tumor suppressor protein. Proc Natl Acad Sci U S A, 2006. 103(12): p. 4463-8.

109. Zhang, H., et al., Hsp90/p50cdc37 is required for mixed-lineage kinase (MLK) 3 signaling. J Biol Chem, 2004. 279(19): p. 19457-63.

110. Rana, A., et al., The mixed lineage kinase SPRK phosphorylates and activates the stress-activated protein kinase activator, SEK-1. J Biol Chem, 1996. 271(32): p. 19025-8.

111. Tibbles, L.A., et al., MLK-3 activates the SAPK/JNK and p38/RK pathways via SEK1 and MKK3/6. EMBO J, 1996. 15(24): p. 7026-35.

112. Kim, K.Y., et al., Mixed lineage kinase 3 (MLK3)-activated p38 MAP kinase mediates transforming growth factor-beta-induced apoptosis in hepatoma cells. J Biol Chem, 2004. 279(28): p. 29478-84.

113. Hehner, S.P., et al., Mixed-lineage kinase 3 delivers CD3/CD28-derived signals into the IkappaB kinase complex. Mol Cell Biol, 2000. 20(7): p. 2556-68.

114. Sebolt-Leopold, J.S. and R. Herrera, Targeting the mitogen-activated protein kinase cascade to treat cancer. Nat Rev Cancer, 2004. 4(12): p. 937-47.

115. Wagner, E.F. and A.R. Nebreda, Signal integration by JNK and p38 MAPK pathways in cancer development. Nat Rev Cancer, 2009. 9(8): p. 537-49.

116. Dolcet, X., et al., NF-kB in development and progression of human cancer. Virchows Arch, 2005. 446(5): p. 475-82.

117. Pufall, M.A. and B.J. Graves, Autoinhibitory domains: modular effectors of cellular regulation. Annu Rev Cell Dev Biol, 2002. 18: p. 421-62.

118. Zhang, H. and K.A. Gallo, Autoinhibition of mixed lineage kinase 3 through its Src homology 3 domain. J Biol Chem, 2001. 276(49): p. 45598-603.

119. Burbelo, P.D., D. Drechsel, and A. Hall, A conserved binding motif defines numerous candidate target proteins for both Cdc42 and Rac GTPases. J Biol Chem, 1995. 270(49): p. 29071-4.

120. Bock, B.C., et al., Cdc42-induced activation of the mixed-lineage kinase SPRK in vivo. Requirement of the Cdc42/Rac interactive binding motif and changes in phosphorylation. J Biol Chem, 2000. 275(19): p. 14231-41.

121. Teramoto, H., et al., Signaling from the small GTP-binding proteins Rac1 and Cdc42 to the c-Jun N-terminal kinase/stress-activated protein kinase pathway. A role for mixed lineage kinase 3/protein-tyrosine kinase 1, a novel member of the mixed lineage kinase family. J Biol Chem, 1996. 271(44): p. 27225-8.

122. Leung, I.W. and N. Lassam, Dimerization via tandem leucine zippers is essential for the activation of the mitogen-activated protein kinase kinase kinase, MLK-3. J Biol Chem, 1998. 273(49): p. 32408-15.

123. Zhan, Y., et al., Regulation of mixed lineage kinase 3 is required for Neurofibromatosis-2-mediated growth suppression in human cancer. Oncogene, 2011. 30(7): p. 781-9.

124. Osmani, A.H., et al., Activation of the nimA protein kinase plays a unique role during mitosis that cannot be bypassed by absence of the bimE checkpoint. EMBO J, 1991. 10(9): p. 2669-79.

125. Rangasamy, V., et al., Mixed-lineage kinase 3 phosphorylates prolyl-isomerase Pin1 to regulate its nuclear translocation and cellular function. Proc Natl Acad Sci U S A, 2012. 109(21): p. 8149-54.

126. Haagenson, K.K. and G.S. Wu, The role of MAP kinases and MAP kinase phosphatase-1 in resistance to breast cancer treatment. Cancer Metastasis Rev, 2010. 29(1): p. 143-9.

127. Rattanasinchai, C., et al., MLK3 regulates FRA-1 and MMPs to drive invasion and transendothelial migration in triple-negative breast cancer cells. Oncogenesis, 2017. 6(6): p. e345.

128. Chen, J. and K.A. Gallo, MLK3 regulates paxillin phosphorylation in chemokine-mediated breast cancer cell migration and invasion to drive metastasis. Cancer Res, 2012. 72(16): p. 4130-40.

129. Cronan, M.R., et al., Defining MAP3 kinases required for MDA-MB-231 cell tumor growth and metastasis. Oncogene, 2012. 31(34): p. 3889-900.

130. Xu, Z., et al., The MLK family mediates c-Jun N-terminal kinase activation in neuronal apoptosis. Mol Cell Biol, 2001. 21(14): p. 4713-24.

131. Rangasamy, V., et al., Estrogen suppresses MLK3-mediated apoptosis sensitivity in ER+ breast cancer cells. Cancer Res, 2010. 70(4): p. 1731-40.

132. Hardie, D.G. and D.R. Alessi, LKB1 and AMPK and the cancer-metabolism link - ten years after. BMC Biol, 2013. 11: p. 36.

133. Faubert, B., et al., The AMP-activated protein kinase (AMPK) and cancer: many faces of a metabolic regulator. Cancer Lett, 2015. 356(2 Pt A): p. 165-70.

134. Zadra, G., J.L. Batista, and M. Loda, Dissecting the Dual Role of AMPK in Cancer: From Experimental to Human Studies. Mol Cancer Res, 2015. 13(7): p. 1059-72.

135. Thaiparambil, J.T., C.M. Eggers, and A.I. Marcus, AMPK regulates mitotic spindle orientation through phosphorylation of myosin regulatory light chain. Mol Cell Biol, 2012. 32(16): p. 3203-17.

136. Koh, H. and J. Chung, AMPK links energy status to cell structure and mitosis. Biochem Biophys Res Commun, 2007. 362(4): p. 789-92.

137. Li, W., et al., Targeting AMPK for cancer prevention and treatment. Oncotarget, 2015. 6(10): p. 7365-78.

138. Luo, L., et al., MLK3 phophorylates AMPK independently of LKB1. PLoS ONE, 2015. 10(4): p. e0123927.

139. Vazquez-Martin, A., et al., Polo-like kinase 1 regulates activation of AMP-activated protein kinase (AMPK) at the mitotic apparatus. Cell Cycle, 2011. 10(8): p. 1295-302.

140. Steinberg, G.R. and B.E. Kemp, AMPK in Health and Disease. Physiol Rev, 2009. 89(3): p. 1025-78.

141. Fox, M.M., et al., AMP-Activated Protein Kinase alpha 2 Isoform Suppression in Primary Breast Cancer Alters AMPK Growth Control and Apoptotic Signaling. Genes Cancer, 2013. 4(1-2): p. 3-14.

142. Phoenix, K.N., F. Vumbaca, and K.P. Claffey, Therapeutic metformin/AMPK activation promotes the angiogenic phenotype in the ERalpha negative MDA-MB-435 breast cancer model. Breast Cancer Res Treat, 2009. 113(1): p. 101-11.

143. Merlen, G., et al., AMPKalpha1 controls hepatocyte proliferation independently of energy balance by regulating Cyclin A2 expression. J Hepatol, 2014. 60(1): p. 152-9.

144. Laderoute, K.R., et al., 5'-AMP-activated protein kinase (AMPK) supports the growth of aggressive experimental human breast cancer tumors. J Biol Chem, 2014. 289(33): p. 22850-64.

145. Motoshima, H., et al., AMPK and cell proliferation--AMPK as a therapeutic target for atherosclerosis and cancer. J Physiol, 2006. 574(Pt 1): p. 63-71.

146. Scaglia, N., et al., De novo fatty acid synthesis at the mitotic exit is required to complete cellular division. Cell Cycle, 2014. 13(5): p. 859-68.

147. Vazquez-Martin, A., C. Oliveras-Ferraros, and J.A. Menendez, The active form of the metabolic sensor: AMP-activated protein kinase (AMPK) directly binds the

mitotic apparatus and travels from centrosomes to the spindle midzone during mitosis and cytokinesis. Cell Cycle, 2009. 8(15): p. 2385-98.

148. Banko, M.R., et al., Chemical genetic screen for AMPKalpha2 substrates uncovers a network of proteins involved in mitosis. Mol Cell, 2011. 44(6): p. 878-92.

149. Vazquez-Martin, A., et al., AMPK: Evidence for an energy-sensing cytokinetic tumor suppressor. Cell Cycle, 2009. 8(22): p. 3679-83.

150. Lee, A.V., S. Oesterreich, and N.E. Davidson, MCF-7 cells--changing the course of breast cancer research and care for 45 years. J Natl Cancer Inst, 2015. 107(7).

151. Soule, H.D., et al., A human cell line from a pleural effusion derived from a breast carcinoma. J Natl Cancer Inst, 1973. 51(5): p. 1409-16.

152. Comsa, S., A.M. Cimpean, and M. Raica, The Story of MCF-7 Breast Cancer Cell Line: 40 years of Experience in Research. Anticancer Res, 2015. 35(6): p. 3147-54.

153. Brunner, N., et al., MCF7/LCC9: an antiestrogen-resistant MCF-7 variant in which acquired resistance to the steroidal antiestrogen ICI 182,780 confers an early cross-resistance to the nonsteroidal antiestrogen tamoxifen. Cancer Res, 1997. 57(16): p. 3486-93.

154. Riggins, R.B., et al., The nuclear factor kappa B inhibitor parthenolide restores ICI 182,780 (Faslodex; fulvestrant)-induced apoptosis in antiestrogen-resistant breast cancer cells. Mol Cancer Ther, 2005. 4(1): p. 33-41.

155. DeRose, Y.S., et al., Tumor grafts derived from women with breast cancer authentically reflect tumor pathology, growth, metastasis and disease outcomes. Nat Med, 2011. 17(11): p. 1514-20.

156. Sikora, M.J., et al., Invasive lobular carcinoma cell lines are characterized by unique estrogen-mediated gene expression patterns and altered tamoxifen response. Cancer Res, 2014. 74(5): p. 1463-74.

Chapter 2: Combating ER-Positive Breast Cancer Resistance: A Novel Combination with a Repurposed Drug

Abstract

Estrogen receptor positive (ER+) breast cancer makes up the majority of all breast cancers, and while often successfully treated, resistance to current therapies leads to poor patient outcome. In this report, I evaluate the effects of the mixed lineage kinase inhibitor CEP-1347, alone and in combination with the clinically used anti-estrogen ICI 182,780 on proliferation, survival, and drug resistance of endocrine sensitive and resistant ER+ breast cancer cells. Our results indicate that the previously described G2/M arrest and increase in apoptosis induced by CEP-1347 treatment is reduced by combination treatment in endocrine sensitive cell lines, but this effect is not seen in endocrine resistant cells. In pre-clinical xenograft studies, the combination of CEP-1347 and ICI 182,780 inhibited growth of both endocrine sensitive and resistant tumors via a reduction in proliferation, exemplified by decreased BrdU incorporation, and an increase in apoptosis, as determined by TUNEL staining. Together, our data indicate that the combination of CEP-1347 and ICI 182,780 could be effective in treating therapy naïve and resistant ER+ breast cancers and may slow the development of resistance to breast cancer therapeutics.

Introduction

Breast cancer is the leading cause of cancer in women, with more than 250,000 cases diagnosed in the United States in 2017, and the second leading cause of cancer-related deaths [1]. Among the histological subtypes, the luminal subtypes account for more than

70% of all breast cancers. Luminal tumors tend to be estrogen receptor positive (ER+), progesterone receptor positive (PR+), and HER2 receptor negative (HER2-). They are generally treated with surgery, followed by a combination of radio-, chemo-, and endocrine therapies [2]. However, a major clinical dilemma arises when these tumors become resistant to endocrine therapies or are resistant upon initial presentation.

Endocrine therapies include aromatase inhibitors (AIs), selective estrogen receptor modulators (SERMs), and selective estrogen receptor downregulators (SERDs), all of which specifically target cells expressing ER. Resistance to these therapeutics has been posited to occur via numerous mechanisms including efflux or inactivation of drugs, downregulation of ER, upregulation of compensatory cell-surface receptors, and mutation or phosphorylation of ER rendering it ligand independent [3-5]. Several combination therapies have prolonged progression-free survival (PFS) of endocrine-resistant breast cancer patients in recent clinical trials. The PI3K/Akt/mTOR pathway inhibitor everolimus increased PFS when combined with the AI exemestane (BOLERO-2 trial) [6], and with the SERM tamoxifen (TAMRAD trial) [7] in patients who exhibited resistance to other AIs. The PALOMA-2 trial revealed a significant increase in PFS for patients treated with the cyclin dependent kinase (CDK) 4/6 inhibitor palbociclib combined with the AI letrozole compared to letrozole alone [8], and the PALOMA-3 trial showed a moderate effect with palbociclib plus the SERD ICI 182,780 compared to ICI 182,780 alone [9]. The MONALEESA-3 trial using the CDK4/6 inhibitor ribociclib combined with letrozole versus letrozole alone is ongoing [10]. While PFS increased in most of these studies, overall survival was not significantly affected [9, 11], and

resistance is widespread [12-14]. Because all of these therapies induce a G0/G1 cell cycle arrest, evasion of the G1/S cell cycle checkpoint could confer cross resistance to the combinations, and identification of additional targets that act at alternate cell cycle stages may yield novel therapeutic targets for the treatment of ER+ disease.

Mixed-lineage kinases (MLKs) are a family of serine/threonine kinases that act as mitogen-activated protein kinase kinase kinases (MAP3Ks) and receive signals from cell surface receptors and relay them to multiple mitogen-activated protein kinases (MAPKs). A key function of MAPKs is to phosphorylate and activate transcription factors, leading to transcription of genes involved in growth and survival. MAPKs directly phosphorylate and activate ER independent of the presence of estrogen [15], and also phosphorylate cytoplasmic substrates that affect cell migration and invasion, among other cellular phenotypes [16-18]. The indolocarbozole derivatives CEP-1347 and CEP-11004 are kinase inhibitors that show selectivity for MLKs, especially MLK3. After development and characterization [19], CEP-1347 was primarily studied as a neurotrophic agent to inhibit Parkinson's disease (PD) progression [20]. Both in vitro and in vivo experiments demonstrated that CEP-1347 inhibits MLK activity and downstream phosphorylation and activation of c-Jun N-terminal kinase (JNK), and its substrate c-Jun [19, 21, 22]. CEP-1347 progressed through Phase II/III clinical trials, and was well-tolerated and non-toxic in healthy adults, but the trial was prematurely concluded due to lack of efficacy [23]. Although the trial was not successful, the safety and tolerability of CEP-1347 were established.

Previous studies suggest that CEP-1347 may be an effective cancer therapeutic. In vitro experiments with both CEP-11004 and CEP-1347, including some from our lab, indicate that treatment of transformed cell lines, including one ER+ breast cancer cell line that is endocrine resistant, leads to reduced viability and mitotic cell cycle arrest, while not altering viability of non-transformed cell lines [17, 21, 22]. MLK3 plays a role in mitotic progression [24], and CEP-11004 mediated cell cycle arrest can be reversed with MLK3 overexpression [22]. Furthermore, MLK3 overexpression is sufficient to induce migration and invasion in non-transformed mammary epithelial cells [16, 25-27], and MLK3 silencing or CEP-1347 treatment prevent tumor cell migration and invasion [25, 28]. Finally, CEP-1347 is able to inhibit cancer stem cell proliferation in an in vivo model [29].

In the current study, I investigated the impact of CEP-1347, alone and in combination with the clinically used SERD ICI 182,780 on growth of ER+ tumor cell lines in vitro and in vivo, and on patient derived xenograft (PDX) tumor organoids in 3-dimensional culture. MCF-7 cells were utilized as a model for estrogen-dependent and anti-estrogen sensitive breast cancer [30, 31]. LCC9 cells, which are an estrogen-independent, anti-estrogen resistant derivative of MCF-7, were used to model late stage disease with complete endocrine resistance [32]. Our data indicate that CEP-1347, particularly in combination with ICI 182,780, may be an effective therapeutic for ER+ breast cancer, and thus I hypothesized that these two drugs in combination will enhance *in vivo* and *in vitro* effects on cell growth and death compared to the effects observed with either compound alone.

Results

Effects of ICI 182,780 and CEP-1347 treatment on cell viability

Our previous experiments demonstrated that short-term CEP-1347 treatment induced mitotic arrest and apoptosis in ER-positive breast cancer cells [21], but its long-term effects were not examined. To determine the outcomes of long-term treatment, MCF-7 and LCC9 cells were incubated with vehicle, ICI 182,780 alone, CEP-1347 alone, or CEP-1347 plus ICI 182,780. After one week of drug treatment, cell viability was determined using trypan blue exclusion assays (Figure 2-1). The number of viable MCF-7 cells was reduced by all treatments, but CEP-1347 alone and in combination with ICI 182,780 were more effective in reducing viability than ICI 182,780 alone (Figure 2-1A). The number of viable LCC9 cells was also reduced by ICI 182,780, although to a much lesser extent than MCF-7 cells, confirming their estrogen independent but responsive phenotype. In contrast, LCC9 cell number was drastically reduced by CEP-1347, both alone and in combination with ICI 182,780 (Figure 2-1B).

To examine the colony forming ability cells after one week of treatment, an equal number of trypan blue-excluding cells from each treatment group were re-plated and cultured in drug free medium. Resultant colonies were stained with crystal violet (Figure 1-1C). For both MCF-7 and LCC9 cell lines, vehicle treated cells had a plating efficiency of approximately 40%. In MCF-7 cells, all treatments decreased the number of colonies formed; however, CEP-1347 alone and in combination with ICI 182,780 decreased colony formation more than ICI 182,780 alone (Figure 2-1 C-D). In LCC9 cells, ICI 182,780 alone had no effect on colony forming ability, demonstrating their anti-estrogen

resistance. However, CEP-1347 alone and in combination with ICI 182,780 dramatically reduced colony formation (Figure 2-1 C,E).

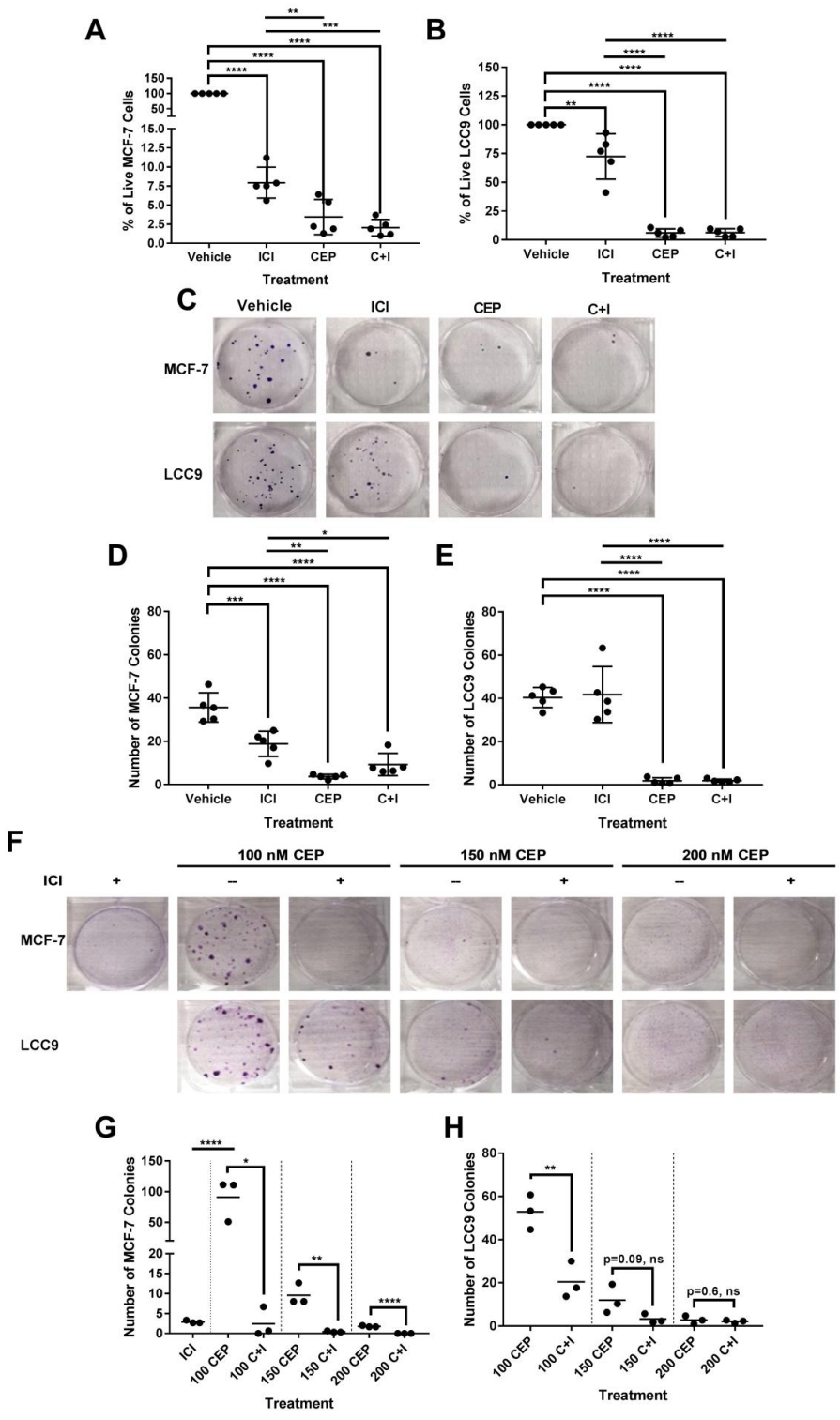

Figure 2-1: CEP-1347 reduces viability and proliferative ability of MCF-7 and LCC9 cells and decreases drug resistance when combined with ICI 182,780. A-E. MCF-7

Figure 2-1 (cont'd)

and LCC9 cells were treated for 7 days with vehicle, 10 nM ICI 182,780, 100 nM CEP-1347, or 10 nM ICI 182,780 + 100 nM CEP-1347. Following treatment, MCF-7 (A) and LCC9 (B) cells were harvested and analyzed for viability using trypan blue exclusion. In each experiment, the number of live cells in vehicle treated cultures was set to 100%, and treatments were normalized to this value. 100 viable cells from each treatment were replated in the absence of drugs, and after 19 days colonies were fixed and stained with crystal violet, and representative plates are shown (C). The number of MCF-7 (D) and LCC9 (E) colonies/plate were quantified. **F-H.** MCF-7 and LCC9 cells were plated and treated continuously for 37-39 days with 100 nM, 150 nM, or 200 nM CEP-1347 alone or in combination with 10 nM ICI 182,780. LCC9 cells treated with ICI 182,780 were confluent and data is not included. Colonies were fixed and stained with crystal violet, and representative plates are shown (F). The number of MCF-7 (G) and LCC9 (H) colonies/plate were quantified. For all graphs, three independent experiments were conducted in triplicate. One-way ANOVA (A-B, D-E) or student's t-test (G-H) were used to complete statistical analyses. Data are shown as mean +/- SD. *$p<0.05$, **$p<0.01$, ***$p<0.001$, ****$p<0.0001$

<u>Combination treatment with CEP-1347 and ICI 182,780 most effectively decreases colony forming ability</u>

A major problem in targeted cancer therapy is the development of drug resistance, and combination treatments can prevent or delay this process [33]. To investigate the effect of combination treatment on resistance, $2.5x10^4$ MCF-7 and LCC9 cells were cultured

long term in ICI 182,780 alone, CEP-1347 alone, or the two drugs in combination, and plates were stained with crystal violet (Figure 2-1F). MCF-7 cells treated with ICI 182,780 alone only developed a few small colonies, indicating that resistance to ICI 182,780 is a rare event. As expected, LCC9 cells treated with ICI 182,780 alone overgrew the plates (data not shown). For both MCF-7 and LCC9 cells, 150 and 200 nM CEP-1347 effectively prevented colony formation. At the lowest concentration (100 nM CEP-1347), approximately 50-100 colonies formed, but the addition of ICI 182,780 reduced this number, even in endocrine resistant LCC9 cells (Figure 2-1F-H). This data suggest that this combination therapy effectively overcomes endocrine resistance, at least in this experimental setting.

Effect of combination treatment on cell cycle and apoptosis

The effect of drug treatments on cell number seen in Figure 2-1A could be due to decreased cell proliferation and/or increased cell death. To compare the effects of treatments on cell cycle and cell death, MCF-7 and LCC9 cells were incubated with vehicle, ICI 182,780, CEP-1347, or both for 3 days. Fixed cells were stained with TUNEL to analyze apoptosis or with propidium iodide (PI) to examine DNA content (Figure 2-2). The majority of MCF-7 cells were TUNEL positive after 3 days of CEP-1347 treatment, indicating that CEP-1347 largely induces apoptosis. The combination treatment also induced apoptosis, but to a lesser extent (Figure 2-2 A, B). In LCC9 cells, CEP-1347 also increased apoptosis, but unlike MCF-7, combination treatment further increased the percentage (Figure 2-2 A, C). ICI 182,780 caused a modest increase in apoptotic MCF-7 cells, and no significant increase in LCC9 cells (Figure 2-2 A-C). Our

lab previously reported that CEP-1347 treatment leads to changes in cellular morphology [21]. This is again evident as CEP-1347 treatment in both cell lines, alone or in combination with ICI 182,780, leads to the formation of cells that have larger nuclei and cytoplasms and appear more vacuolated than control cells (Figure 2-2 A), consistent with a senescent or autophagic phenotype [34]. As previously described, ICI 182,780 treated MCF-7 cells arrest in G1 and CEP-1347 treated cells accumulate in G2/M and display a polyploid population [21]. Analysis of non-apoptotic cell populations revealed that MCF-7 cells treated with both compounds had significantly fewer polyploid cells and a larger population of G1 cells (Figure 2-2 D, E) compared to cells treated with CEP-1347 alone. As expected, ICI 182,780 treatment did not have a significant effect on LCC9 cells. However, treatment with CEP-1347 led to an accumulation of cells in G2/M and the development of a polyploid population, and unlike MCF-7 cells, the LCC9 polyploid population was not altered in the combination treatment (Figure 2-2 D, F).

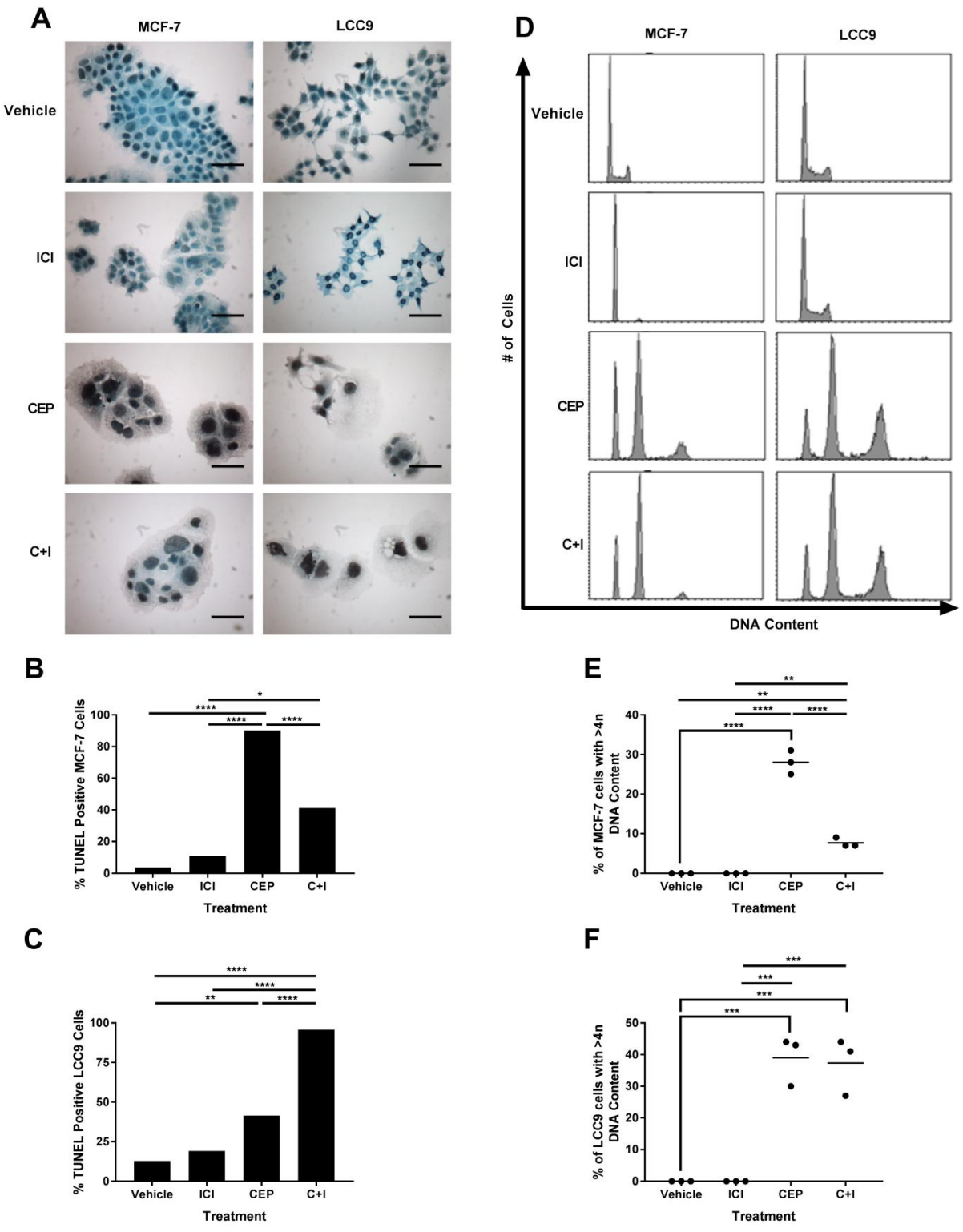

Figure 2-2: Effects of CEP-1347 and ICI 182,780 on cell cycle and apoptosis in cell lines. MCF-7 and LCC9 cells were treated with vehicle, 10 nM ICI 182,780, 100 nM

Figure 2-2 (cont'd)

CEP-1347, or the combination of both. After 3 days, cells were harvested, fixed, and stained with TUNEL and quantified (N>100 cells per treatment) to analyze apoptosis (A-C), or stained with PI to examine cell cycle (D-F). Experiments were completed in triplicate and representative results are shown.

CEP-1347 causes cell cycle arrest in ER+ patient derived xenografts

To confirm the effects of CEP-1347 in a system that more closely reflects human tumors than established cell lines, three ER+, HER2- patient derived xenograft (PDX) lines (HCI-011, HCI-013, and HCI-013 EI) derived from luminal B tumors were examined in three-dimensional cell culture [35]. After implantation and amplification in NOD/SCID mice, tumors were harvested and digested into organoids, embedded in a three-dimensional matrix, and treated with vehicle, ICI 182,780, CEP-1347, or the combination. After one week of treatment, cells were harvested, and analyzed for DNA content by flow cytometry (Figure 2-3, Supplemental Figure 2-1). All three PDX lines revealed slowly cycling populations with vehicle treatment, as indicated by a small S-phase fraction. Treatment with ICI 182,780 slightly increased the G1 population, and G2/M arrest and polyploid (>4n DNA content) cell accumulation were evident after treatment with CEP-1347. The polyploid population was significantly reduced with combination treatment, consistent with data obtained in MCF-7 cells (Figure 2-3A-C), and a similar phenotype was seen with the estrogen independent derivative of HCI-013 (Supplemental Figure 2-1).

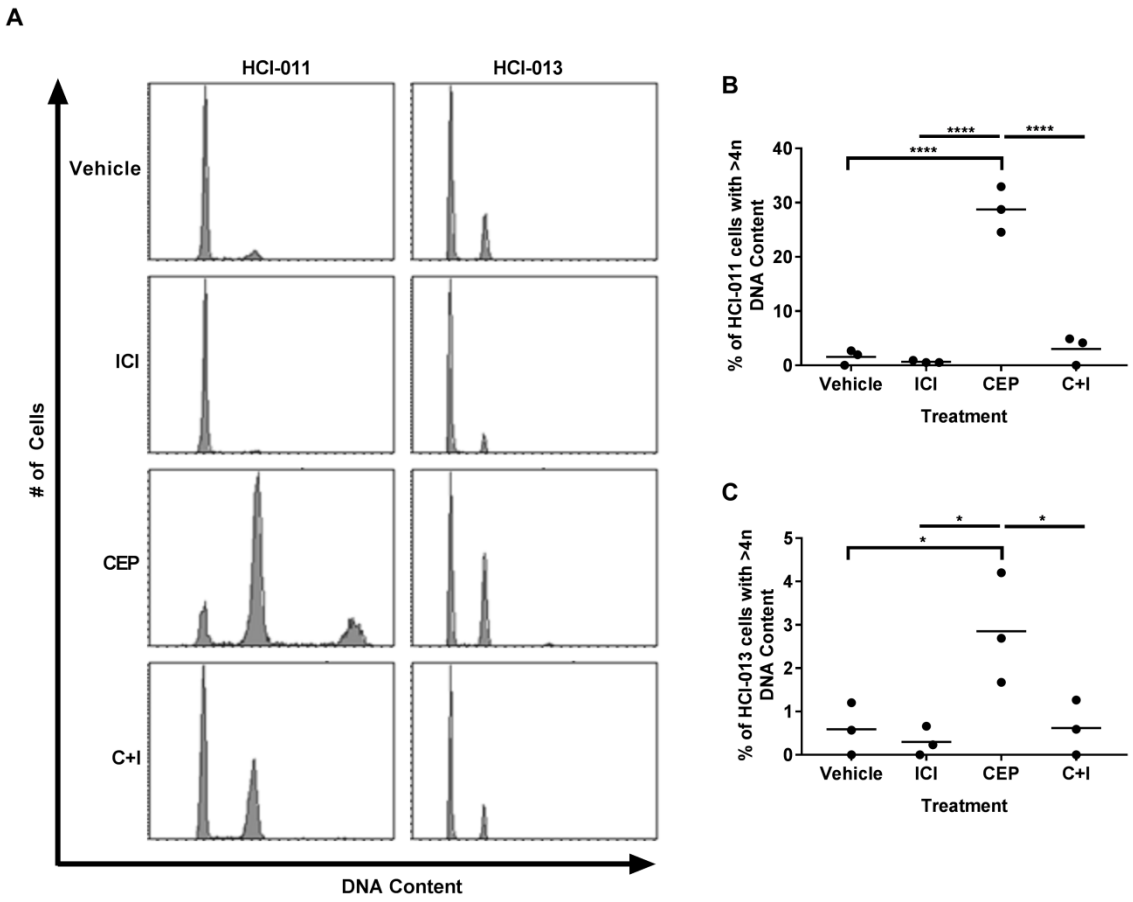

Figure 2-3: Effects of CEP-1347 and ICI 182,780 on cell cycle in ER+ PDX lines.

Organoids prepared from PDX lines were embedded in Matrigel and treated with vehicle, 10 nM ICI 182,780, 400 nM CEP-1347, or the combination of both. After 7 days, organoids were digested into single cells, fixed, and stained with PI to examine cell cycle. Experiments were completed in triplicate and representative histograms are shown (A). To quantify the effects of treatment on the polyploid population, the percentage of cells with >4n DNA content in each experiment were compared to that seen in vehicle treated samples (B,C). One-way ANOVA was used for statistical analyses. Data are shown as mean +/- SD. *p<0.05, **p<0.01, ***p<0.001, ****p<0.0001

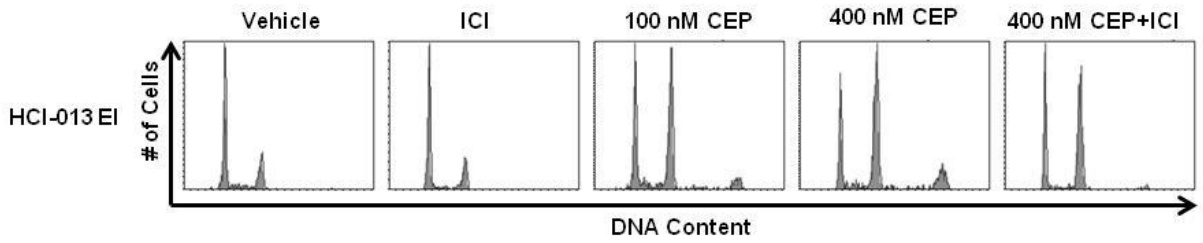

Supplemental Figure 2-1: Effects of CEP-1347 and ICI 182,780 on cell cycle in ER+ estrogen independent PDX line. Organoids prepared from an estrogen independent PDX line were embedded in Matrigel and treated with vehicle, 10 nM ICI 182,780, 100 nM CEP-1347, 400 nM CEP-1347, or 400 nM CEP-1347 in combination with 10 nM ICI 182,780. After 7 days, organoids were digested into single cells, fixed, and stained with PI to examine cell cycle. Experiments were completed in duplicate and representative histograms are shown.

Effects of CEP-1347 and ICI 182,780 on the growth of tumor xenografts

Our in vitro results suggest that CEP-1347, alone or in combination with ICI 182,780, might inhibit the growth of ER+ breast tumors, including ones with acquired anti-estrogen resistance. To test this in a pre-clinical animal model, xenograft studies were carried out with both MCF-7 and LCC9 cells. MCF-7 and LCC9 were engineered to express red fluorescent protein (RFP) and luciferase (Luc), and individual clones were isolated. All MCF-7 subclones were sensitive to ICI 182,780 and CEP-1347, and LCC9 subclones were resistant to ICI 182,780 and sensitive to CEP-1347 (Supplemental Figure 2-2). A single subclone of each cell line was used for tumor studies. For MCF-7 xenografts, all treatments inhibited tumor growth, although ICI 182,780 and the combination were more effective than CEP-1347 alone (Figure 2-4A). For LCC9

xenografts, CEP-1347 alone and ICI 182,780 alone slowed tumor growth somewhat, but the effects were not statistically significant. In contrast, treatment with the combination of CEP-1347 and ICI 182,780 significantly inhibited LCC9 tumor growth (Figure 2-4B). Interestingly, in mice injected with LCC9 cells, micrometastases or single cells were observed in lung parenchyma upon luminescent imaging, and confirmed to be LCC9/Luc cells by immunofluorescence staining of lung sections for luciferin (Supplemental Figure 2-3). Further studies are needed to determine if CEP-1347 or ICI 182,780, alone or in combination, influences their development or progression.

To evaluate if the effects of treatment persist after the cessation of therapy, several animals from each drug-responsive group were maintained and tumor volume was monitored for an additional 6 weeks without drug administration. LCC9 tumors treated with CEP-1347 plus ICI 182,780 resumed growth (Supplemental Figure 2-4), as did MCF-7 tumors treated with CEP-1347 alone. MCF-7 tumors treated with ICI 182,780 alone also grew, although more slowly. However, MCF-7 tumors treated with the combination of both drugs did not regrow, suggesting that combination therapy may prevent relapse upon treatment cessation (Figure 2-4C).

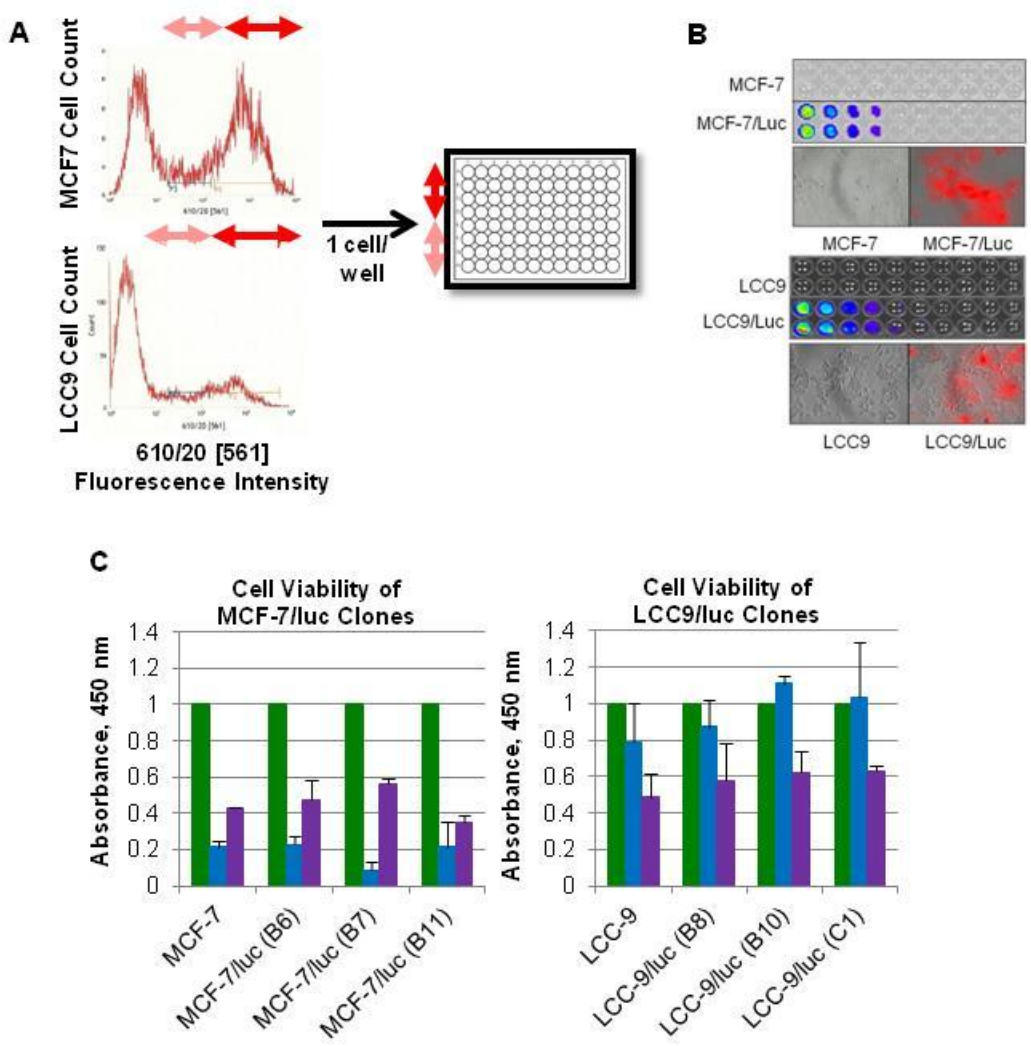

Supplemental Figure 2-2: Establishment and characterization of MCF-7 and LCC9 RFP/Luc derivatives. (A) Cells were sorted based on RFP fluorescence into 96 well plates. (B) Clonal lines were amplified and analyzed for luciferase activity and RFP expression. (C) Parental and clonally derived lines were assayed for sensitivity to ICI 182,780 (blue) and CEP-1347 (purple). Representative examples are shown. A single derivative of MCF-7 (B7) and LCC9 (C1) was selected to use in tumor studies.

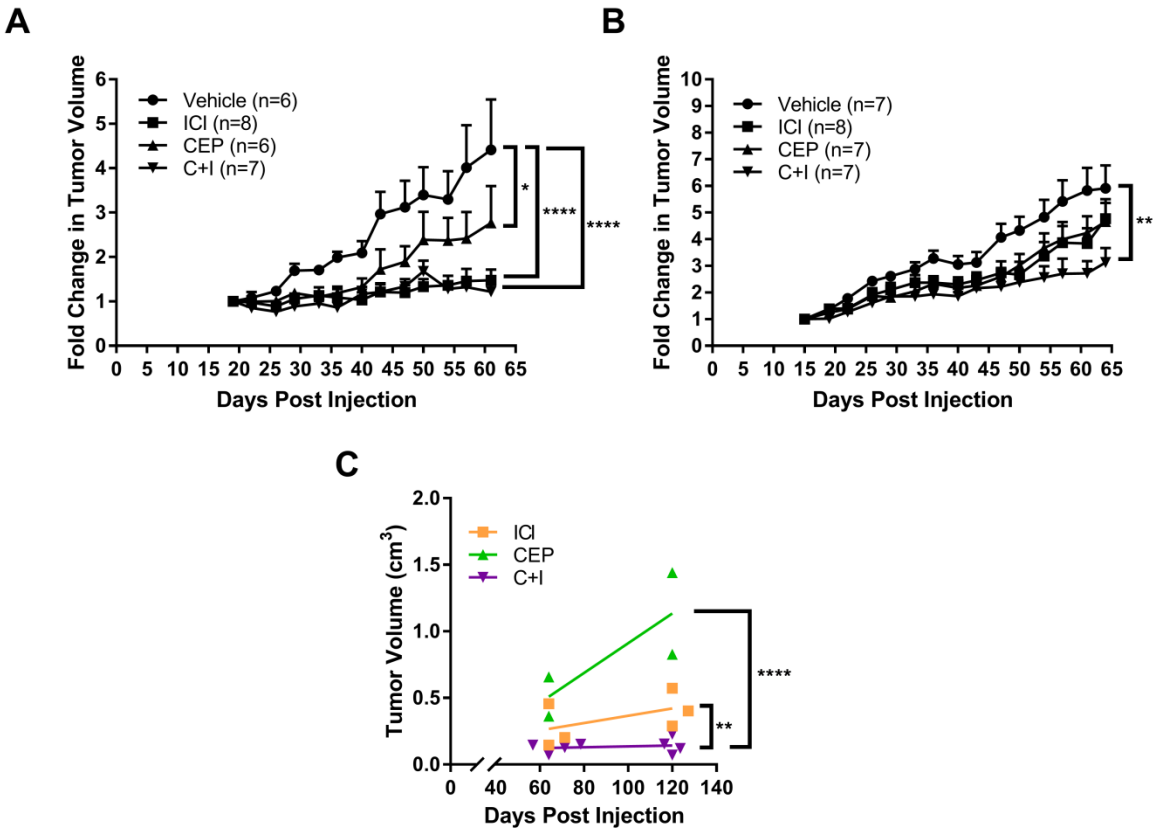

Figure 2-4: Effect of CEP-1347 and ICI 182,780 on tumor growth in vivo. $5x10^6$ MCF-7 or LCC9 cells were injected into the fat pad of Nu/Nu athymic mice and 0.5 mg 17-β estradiol pellets were concurrently implanted subcutaneously. After 2-3 weeks, 10 animals were randomized into each treatment group. Treatments were initiated and continued for 6 weeks. CEP-1347 was dosed at 60 mg/kg orally and ICI 182,780 was dosed at 5 mg/animal subcutaneously. Data are represented as the mean fold change in tumor volume compared to tumor volume at treatment initiation for MCF-7 (A) and LCC9 (B). At the end of treatment, animals were euthanized and tumors harvested for histological analyses. Several (2-3) animals in each drug-responsive group were retained and tumors were allowed to grow for 6 additional weeks in the absence of

Figure 2-4 (cont'd)

treatment (C). Error bars represent SEM. One-way ANOVA was used to complete statistical analyses. *p<0.05, **p<0.01, ***p<0.001, ****p<0.0001.

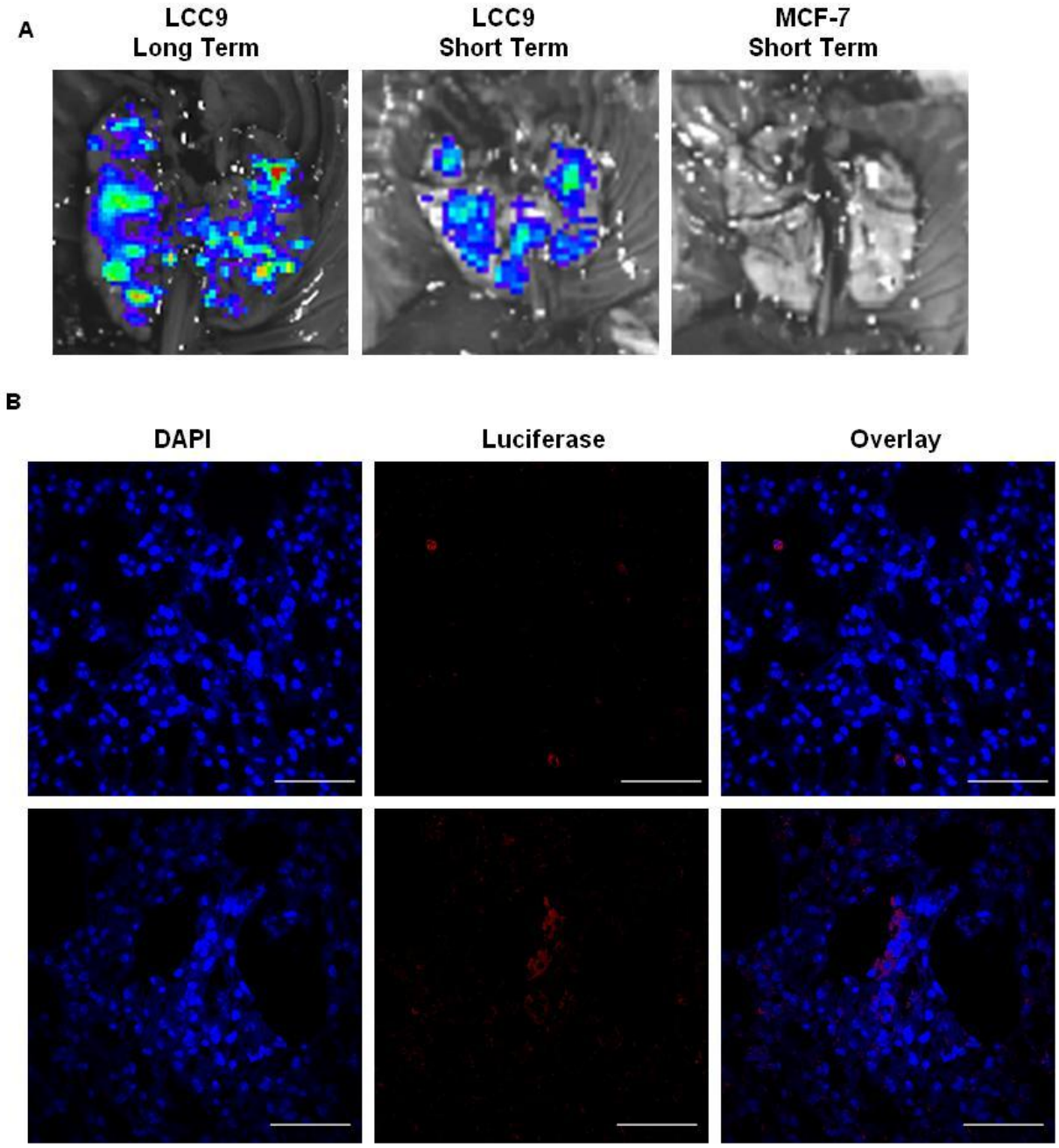

Supplemental Figure 2-3: LCC9 cells metastasize to lungs. (A). At the study endpoint, luciferase imaging was carried out before and after removal of primary

Supplemental Figure 2-3 (cont'd)

tumors, revealing the presence of luciferase expressing cells in the lungs of animals bearing LCC9, but not MCF-7, tumors. (B). Lungs from these animals were re-inflated using 10% formalin, fixed and embedded in paraffin. 5 μm sections were deparaffinized, rehydrated and stained using an anti-luciferase antibody, revealing a both single cells and small clusters within the lung parenchyma. Representative images are shown. Scale bars represent 50 μm.

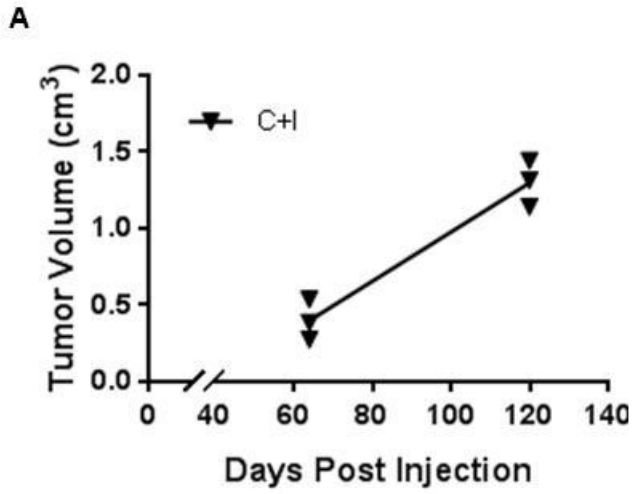

Supplemental Figure 2-4: LCC9 tumors in animals treated with combination therapy grow after cessation of treatment. At the end of treatment, 3 animals treated with a combination of ICI 182,780 and CEP-1347 were retained for 6 additional weeks in the absence of treatment.

<u>Effects on tumor growth include suppression of proliferation and increase in apoptosis</u>

Slowing or stopping tumor growth can be due to decreased proliferation and/or increased cell death, and both ICI 182,780 and CEP-1347 affect both of these

processes [17, 21, 22, 36-38]. To examine acute effects of drug treatments on tumor cells, short-term in vivo studies were completed. MCF-7 and LCC9 cells were injected into the mammary fat pad of athymic nude mice as described above. Once tumors reached an average size of 200 mm^3, a single dose of ICI 182,780 and/or 5 consecutive daily doses of CEP-1347 were administered, and animals were euthanized 24 hours after the final CEP-1347 administration. To assay for cell proliferation, BrdU was injected intraperitoneally into mice two hours prior to sacrifice, and tumor sections were stained and quantified as described in materials and methods (Figure 2-5). In MCF-7 tumors, both ICI 182,780 alone and in combination with CEP-1347 significantly decreased BrdU incorporation (Figure 2-5 A-B). A decrease was also seen with CEP-1347 alone, but the effect was not statistically significant. These results correlate well with the effects on tumor growth where ICI 182,780 alone and in combination with CEP-1347 had a more dramatic effect than CEP-1347 alone. LCC9 tumors trended towards reduced BrdU incorporation with all drug treatments, but none of the effects were statistically significant (Figure 2-5 C-D). This was surprising, since the long-term growth curves showed an effect of combination treatment on tumor growth. When BrdU incorporation was analyzed in tumors from the long-term study, combination therapy was effective in reducing proliferation, while either drug alone was not (Figure 2-5 C, E).

To investigate effects of treatment on apoptosis, TUNEL staining was performed (Figure 2-6). In short term MCF-7 tumors, CEP-1347 alone was the only treatment that displayed a significant increase in apoptotic cells, although the combination treatment had a very similar trend (Figure 2-6 A-B). In the long-term tumor study, CEP-1347 alone

was also the only treatment that caused a significant increase in the percentage of apoptotic cells, and the combination treatment reduced apoptosis, reflecting our in vitro data (Figure 2-6 A, C). In short term LCC9 tumors, there was not a significant difference in apoptosis between any treatment group (Figure 2-6 D-E), but in the long term the combination therapy resulted in a significant increase in apoptosis, corresponding to the growth curve data (Figure 2-6 D, F).

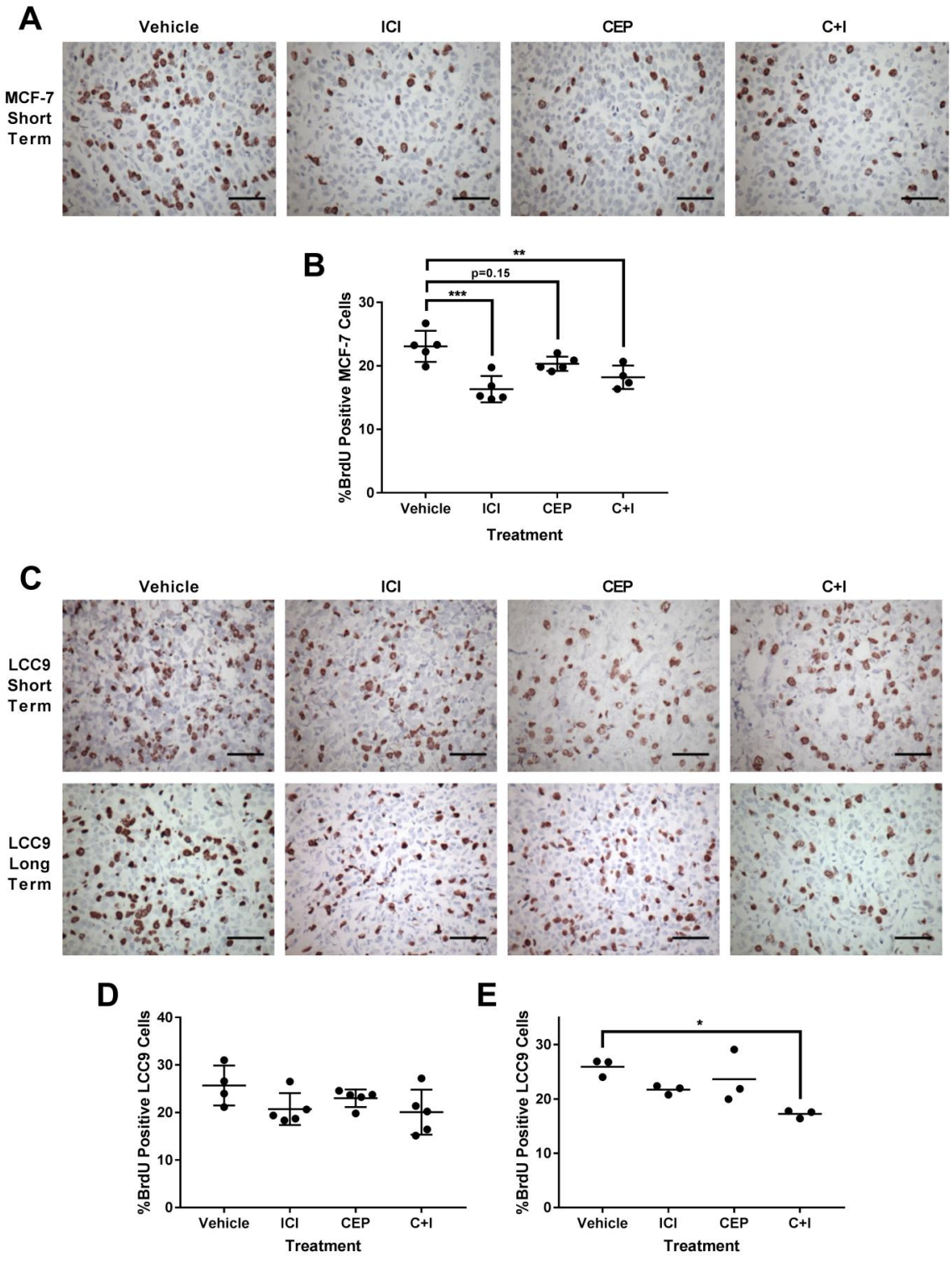

Figure 2-5: Effects of in vivo treatment on BrdU incorporation. BrdU was injected intraperitoneally into animals two hours before euthanasia as described in materials and

Figure 2-5 (cont'd)

methods. Tumor sections were stained with anti-BrdU antibody and quantified to determine effects of drug treatment on proliferation. Data are shown for MCF-7 (A, B) and for LCC9 (C,D) tumors treated for 5 days, as well as LCC9 tumors treated for 6 weeks (C,E). Images are representative and each data point represents an individual animal. Scale bars represent 20 μm. One-way ANOVA was used for statistical analyses. Data are shown as mean +/- SD. *$p<0.05$, **$p<0.01$, ***$p<0.001$

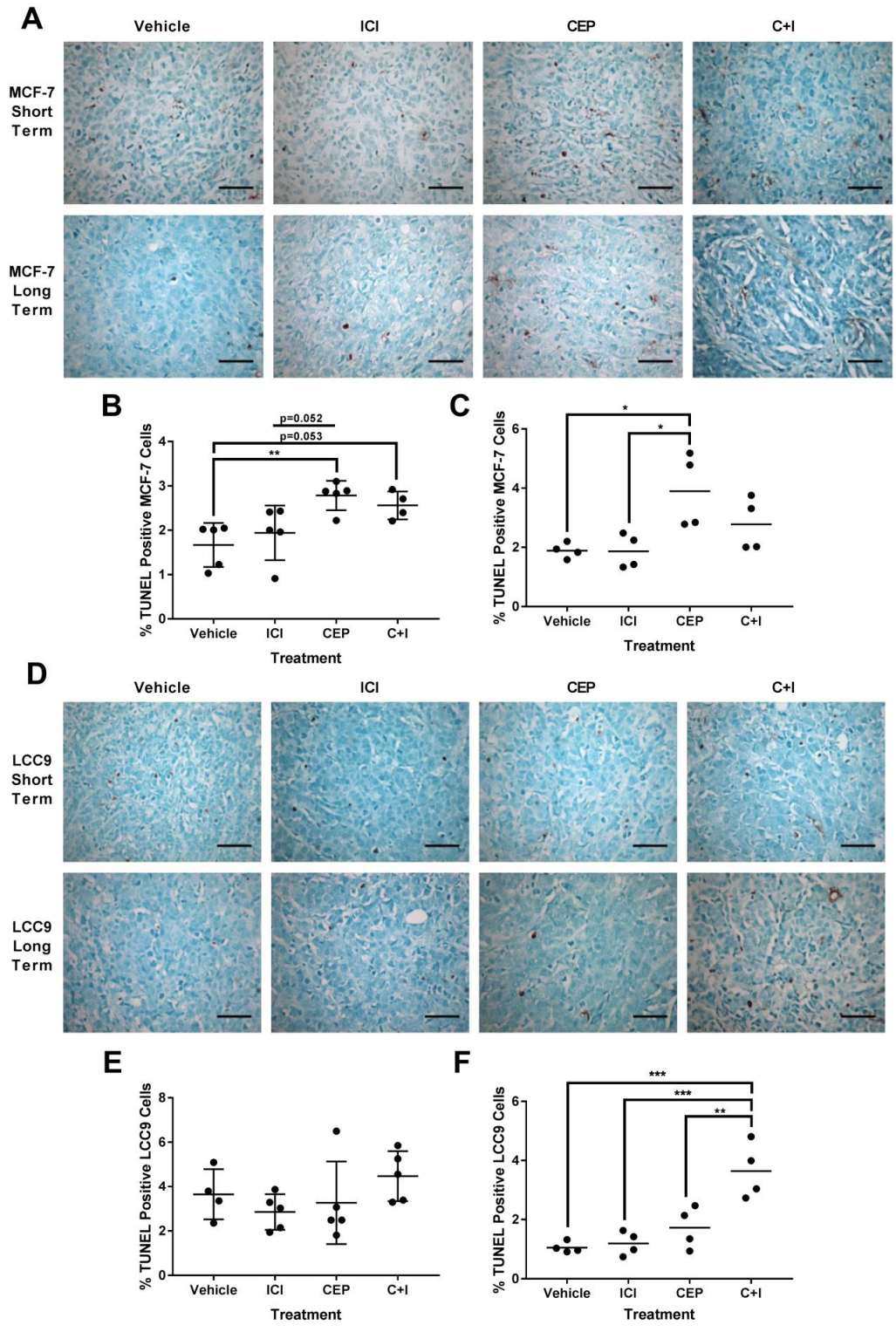

Figure 2-6: Effects of in vivo treatments on TUNEL staining. TUNEL staining was used to determine the effects of drug treatment on apoptosis. Data are shown for MCF-

Figure 2-6 (cont'd)

7 tumors treated for 5 days (A, B) or 6 weeks (A, C), and LCC9 tumors treated for 5 days (D, E) or 6 weeks (D, F). Images are representative and each data point represents an individual animal. Scale bars represent 20 μm. One-way ANOVA was used for statistical analyses. Data are shown as mean +/ SD. *p<0.05, **p<0.01, ***p<0.001

Discussion

Endocrine therapies are a standard treatment for ER+ breast cancer, and while they are very effective, resistance often occurs, particularly in metastatic disease. Combination therapies using CDK 4/6 or other inhibitors together with endocrine agents increase the progression free survival of patients with advanced endocrine resistant disease [6-10, 39], but do not dramatically effect overall survival [9, 11], and mechanisms of resistance to these combinations have already been identified [12-14]. Thus, it is vital to develop additional options to prevent endocrine resistance, and to treat endocrine resistant metastatic disease. In this study, I examined the effects of the small molecule inhibitor CEP-1347, alone and in combination with the clinically used SERD ICI 182,780, on tumor growth, cell proliferation, cell death, and colony formation in ER+ breast cancer models. CEP-1347 is selective for MLKs, a family of MAP3Ks that function in multiple pathways that are important for tumor phenotypes including proliferation and metastasis. CEP-1347 selectively inhibits proliferation and induces cell death in tumorigenic vs. non-tumorigenic cells [21, 22], and was well tolerated in clinical trials [23, 40]. It blocks progression through mitosis while current targeted therapies for ER+

breast cancer cause a G1 arrest. Because different pathways regulate passage through these two cell cycle stages, I reasoned that a combination treatment might more completely block proliferation than either drug alone. Furthermore, I hypothesized that cells resistant to G1-targeting agents, such as ICI 182,780, would remain sensitive to CEP-1347, and the combination might therefore decrease the occurrence of resistance.

In MCF-7 xenograft studies, CEP-1347 alone slowed the growth of tumors, but ICI 182,780 alone and in combination with CEP-1347 were more effective and indistinguishable from each other. However, the behavior of tumors after cessation of treatment suggests that the combination may provide a significant advantage. CEP-1347 treated MCF-7 tumors more than doubled in volume in 60 days following treatment, and tumors treated with ICI 182,780 also nearly doubled in volume. Interestingly, tumors treated with the combination of CEP-1347 plus ICI 182,780 did not increase in volume during the 60 day regrowth period. The effects of ICI 182,780 in our experiments were predominantly to block cell proliferation, as evidenced by the G1 cell cycle arrest observed in vitro and decreased BrdU incorporation in vivo. In contrast, no significant effect of ICI 182,780 on TUNEL staining was observed in vivo or in vitro. The effect of ICI 182,780 on apoptosis in the literature is inconsistent, with some reports indicating induction of apoptosis [36-38] and others showing no effect [41-43]. In contrast to ICI 182,780, the primary effect in vivo of CEP-1347 was to increase cell death. As previously reported, CEP-1347 treatment in vitro caused an accumulation of cells in mitosis and the appearance of a polyploid (>4n) population, both of which can result in increased cell death [44-46]. Polyploidy can also lead to genome instability,

which can result in tumor progression and/or therapeutic resistance [47-49]. However, other therapies used clinically, such as taxol, lead to a mitotic arrest and development of polyploidy, but eventually result in cell death [50]. Our results suggest that combination treatment may prevent the development of genome instability and resistance because the polyploid population was smaller in cells treated with CEP-1347 plus ICI 182,780 relative to CEP-1347 alone. Our interpretation of this is that a percentage of CEP-1347 treated cells eventually enter G1 without going through a normal mitosis and cytokinesis, giving rise to a G1 population with 4n DNA content, which can then continue to cycle. Concurrent treatment with ICI 182,780 arrests these cells in their 4n G1 state, thereby preventing their continued cycling, and subsequent genome instability, and reducing the likelihood of developing more aggressive and therapy resistant disease. This may also contribute to the prevention of regrowth observed in vivo after cessation of treatment.

The effects of CEP-1347 in endocrine resistant LCC9 cells are also intriguing. ICI 182,780 alone had little to no effect on LCC9 cell proliferation or cell death in vitro. However, as in MCF-7 cells, CEP-1347 induced a mitotic arrest, polyploidy, and cell death. In addition, combination treatment resulted in increased cell death and decreased colony formation. The benefits of combination therapy were also observed in vivo. Treatment with either CEP-1347 or ICI 182,780 alone slightly slowed the growth of LCC9 tumors, although neither was statistically significant. In contrast, the combination of both significantly slowed tumor growth. Analysis of LCC9 tumors after long term treatment revealed no effect of individual ICI 182,780 or CEP-1347 treatment, but the

combination revealed a significant decrease in BrdU incorporation and increase in TUNEL staining. The same trends were observed in the short term experiment, although they did not reach statistical significance. It is somewhat surprising that no increase in TUNEL staining was observed in LCC9 tumors treated with CEP-1347 alone, since they respond to this drug in vitro. This could be a result of sensitivity, since previous dose-response curves of MCF-7 and LCC9 curves suggest that the IC50 of CEP-1347 is higher in LCC9 cells [21]. This may also explain the lack of a significant effect of combination treatment in the short term study, since the length of treatment may not have been sufficient.

In summary, our results reveal that CEP-1347 may be an effective therapeutic for ER+ breast cancer, particularly in combination with an endocrine agent such as the SERM ICI 182,780. As with many kinase inhibitors, the development of therapeutic resistance is a potential problem, but increasing the concentration of CEP-1347, and/or combining it with ICI 182,780, decreases its occurrence. The finding that the combination of CEP-1347 plus ICI 182,780 was effective for LCC9 tumors is particularly exciting since this cell line is a model for advanced disease that is resistant to all endocrine therapies. Interestingly, LCC9 cells grew detectable micrometastases in the lungs of several animals. Few models of metastatic breast cancer exist; this is the first report of LCC9 metastasis in vivo and this finding provides an opportunity for future studies on the effects of treatment in metastatic disease. Finally, the fact that CEP-1347 previously went through Phase II/III clinical trials for PD [19, 20, 23], where its safety and lack of toxicity was established, warrants further study of its potential as a breast cancer

therapeutic. Such studies could evaluate its effects on dormancy, metastasis, and the development of resistance in vivo.

Materials and Methods

Cell culture and reagents

MCF-7 and MCF-7/LCC9 cells were provided by Dr. Robert Clarke (Lombardi Comprehensive Cancer Center, Georgetown University). They were cultured in improved modified Eagle's medium (Invitrogen) supplemented with 5% fetal bovine serum (Hyclone), 100 units/mL penicillin, and 100 units/mL streptomycin. To engineer RFP/Luc clones, MCF-7 and LCC9 cells were infected with a lentivirus containing red fluorescent protein (RFP), luciferase, and blasticidin resistance under an EF1a promotor (Cat # LVP439, GenTarget). Infected cells were sorted based on intensity of RFP fluorescence (BD Influx). Individual colonies were amplified, and RFP and luciferase expression, and hormone sensitivity were confirmed (Supplemental Figure 4). RFP/Luc cells were cultured in media supplemented with 2 µg/mL blasticidin (Sigma, 15205) for selection. All cells were cultured at 37 °C with 5% CO2. Cell line identities were confirmed using STR analysis at Michigan State University. Drug treatments included vehicle (DMSO), 10 nM ICI 182,780 182,780 in ethanol (Selleckchem), and 100, 150, or 200 or 400 nM CEP-1347 in DMSO (provided by Teva Pharmaceuticals).

Flow cytometry

For apoptosis and cell cycle assays using cell lines, 10^6 cells were plated per 10 cm dish. Treatments were added after 24 hours and continued for 72 hours. For cell cycle

analysis, cells were trypsinized, fixed in 70% ethanol overnight at -20 °C, and washed two times with 5% FBS/95% PBS, then resuspended in PBS containing 50 µg/mL propidium iodide and 50 µg/mL RNaseA for 15 minutes at 37 °C. Cells were analyzed using a FACS Vantage flow cytometer and data were analyzed using ModFit software. 10,000 events were analyzed for each sample.

Cell viability, and colony formation assays

To measure the effects of treatment on cell viability, $2x10^5$ cells were plated in 10 cm dishes and treated with vehicle, 10 nM ICI 182,780, 100 nM CEP-1347, or 100 nM CEP-1347 plus 10 nM ICI 182,780 for 7 days, with fresh medium added on day 3. On day 7, cells were trypsinized and live and dead cells were quantified by trypan blue exclusion (-Thermo Fisher, T10282). 100 live cells were re-plated in fresh growth medium without drug treatments, and colonies were allowed to form for 19 days. Plates were washed with PBS, fixed in 3.7% formaldehyde, stained with 0.01% crystal violet, and colonies were quantified. To assay for the development of drug resistance, $2.5x10^4$ cells per well were plated in 6-well plates and treated continuously with 100, 150, or 200 nM CEP-1347 with and without 10 nM ICI 182,780 for 37-39 days. Fresh medium was added every 4-5 days. Plates were fixed and stained as described above, and colonies were quantified.

Tumor Studies

All animal studies were carried out following the Michigan State University Institutional Animal Care and Use Committee guidelines. For long term growth curves, $5x10^6$ MCF7

RFP/Luc or LCC9 RFP/Luc cells were injected orthotopically into the 4th inguinal mammary fat pad of 40 Nu/Nu athymic mice (Charles River) for 10 mice per treatment group. Concurrently, a 0.5 mg 17-β estradiol beeswax pellet was implanted subcutaneously between the shoulders to provide sufficient estrogen supplementation to support tumor growth. Tumor volume was measured twice a week with digital calipers, and the formula L*W*H*0.523 was used to calculate tumor volume. Once tumors reached 0.075-0.225 mm^3 (day 19 for MCF-7 and day 17 for LCC9), ten animals were randomized into each group, and treatments were initiated. Animals were excluded from analyses if they did not survive the entire 6 week treatment, or if tumor volume fell outside a predetermined range at the initiation of treatment. Body weight measurements across the study indicated that treatments were not detrimental to animal health (Supplemental Figure 2-5). 5 mg of ICI 182,780 in castor oil (Sigma) was injected subcutaneously once weekly [51] and CEP-1347 in 3:1 Gelucire 44/14 (Gattefosse) and propylene glycol (Sigma) was dosed orally at 60 mg/kg every other day. ICI 182,780 dosing conditions were based on the literature [52] and optimal CEP-1347 dosing conditions were established in pilot tumor studies. Treatments were carried out for 6 weeks with bi-weekly monitoring of tumor growth and animal weight. Upon reaching the study endpoint, the majority of animals in each treatment group were sacrificed and tumors harvested for further analysis. Three animals from each responding treatment group were reserved and monitored for tumor regrowth for 6 additional weeks in the absence of treatment. For short term studies, 5x105 MCF-7RFP/luc or LCC9 RFP/luc cells were injected into 20 Nu/Nu athymic mice for each cell line (5 mice per treatment), with concurrent implantation of a 0.5 mg 17-β estradiol

beeswax pellet. Tumor volumes were monitored twice weekly by caliper measurements. Once tumors reached approximately 0.250 mm^3, treatments were initiated. A single dose of ICI 182,780 was given on day 1 and CEP-1347 was dosed for five consecutive days. Twenty-four hours after the last dose, animals were euthanized and tumors were harvested for further analysis. For BrdU analysis of proliferating cells, animals were injected intraperitoneally with 70 mg/kg BrdU 2 hours prior to euthanasia.

For PDX amplifications, NOD/SCID mice were obtained from Jackson Labs. A 1 mm3 tumor fragment was implanted into a cleared fat pad [53]. HCI-011 and HCI-013 are derived from pleural effusions. HCI-011 exhibits ductal histopathology, while HCI-013 shows lobular histopathology. HCI-013 EI is an estrogen-independent derivative of HCI-013 that developed after long-term passage of HCI-013 in ovariectomized mice [54]. Mice implanted with HCI-011 or HCI-013 were supplemented with a 0.5 mg 17-β estradiol beeswax pellet implanted subcutaneously between the shoulder blades. Tumor volume and animal weight were monitored biweekly. Once tumors reached 1.5 cm3, tissue was harvested and processed into organoids as described [55]. ER status of all tumors were confirmed by IHC (Supplemental Figure 2-6).

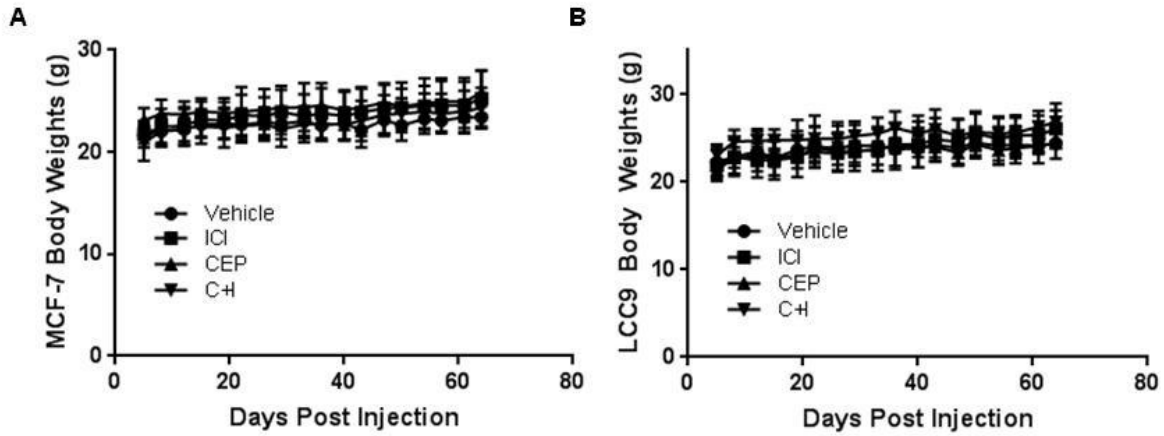

Supplemental Figure 2-5: Effects of CEP-1347 and ICI 182,780 on body weight.

Body weight measurements of mice bearing MCF-7 (A) or LCC9 (B) tumors.

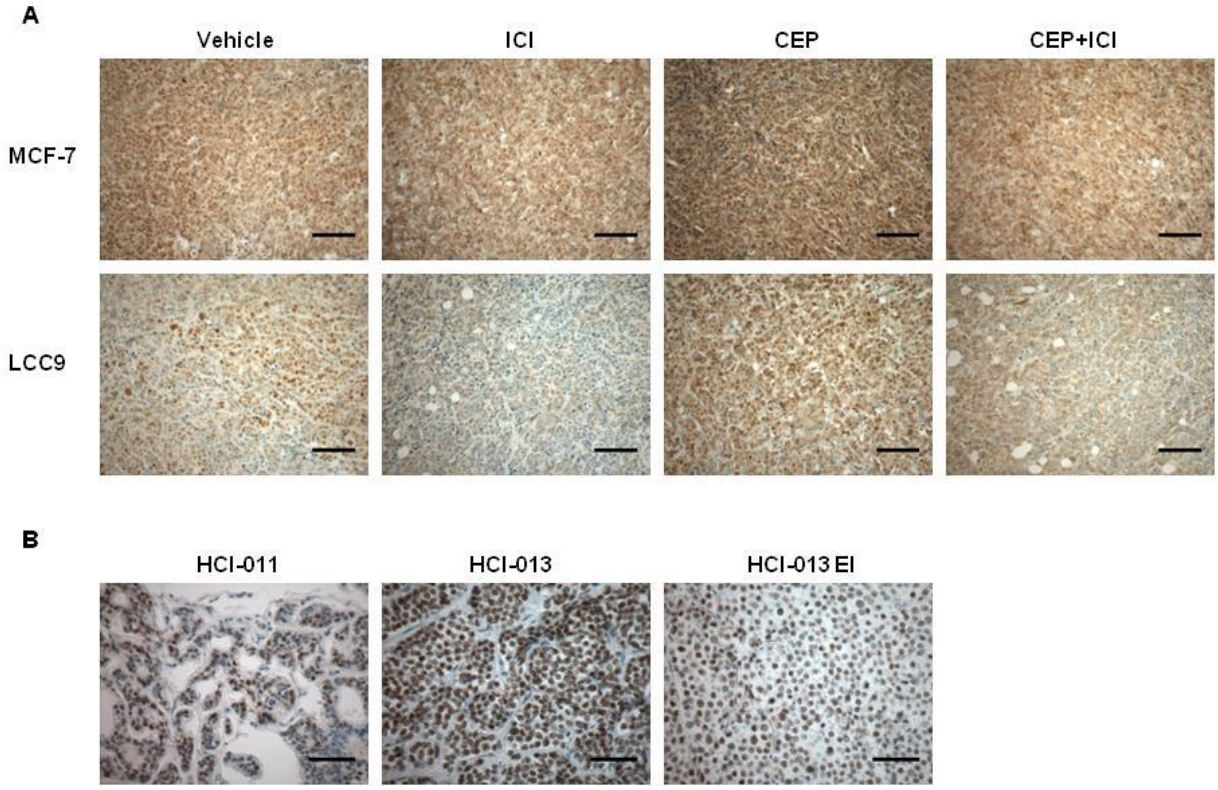

Supplemental Figure 2-6: ER staining of xenograft and PDX tumor sections. (A). MCF-7 and LCC9 tumors were stained with anti-ER alpha after treatment to confirm ER status. (B). PDX tumors were stained upon harvest to ensure ER positivity.

Immunohistochemistry

For all immunohistochemistry staining, animal specimens were fixed in 10% Neutral Buffered Formalin, dehydrated in ascending grades of ethanol, embedded in paraffin and sectioned on a rotary microtome at 4 µm. The slides were deparaffinized and hydrated through descending grades of ethyl alcohol. For cell lines, cells were cultured and treated on coverslips and fixed in 10% Neutral Buffered Formalin. For H&E, slides were stained with hematoxylin (Cancer Diagnostics Inc.), followed by a clarifying rinse in 1% glacial acetic acid. Slides were placed in 95% ethanol, then stained with 1% eosin with phloxine. For BrdU staining, slides were treated with 4.0 M HCl, then subjected to enzyme induced epitope retrieval using 0.4% pepsin. Sections were then incubated with the primary antibody (BD Biosciences, catalog #347580), followed by reaction development with Romulin AEC™ Chromogen (Biocare) and counterstained with Cat Hematoxylin. For TUNEL staining, slides underwent enzyme induced epitope retrieval using 20 µl/ml of Proteinase K in PBS (A.G. Scientific, catalog #P-1265), and staining was completed following the manufacturer's protocol (Millipore, ApopTag Peroxidase In Situ Apoptosis Detection Kit, catalog #S7100). Slides were counterstained in methyl green for 10 seconds and allowed to air dry overnight. All staining was completed at room temperature on the IntelliPath™ Flex Autostainer, and all slides were cover slipped using a synthetic mounting medium (Mercedes Medical). For BrdU and TUNEL analyses, ten fields of view were taken from the periphery of one section per tumor. Each data point represents the average percent positive of the ten images for each individual animal.

Statistical analyses

A two-way student's T-Test was used to determine statistical significance between two treatment groups, and one-way ANOVA was used to determine statistical significance among three or more treatment groups with Tukey used for post-hoc analyses. An alpha of 0.05 was utilized to indicate statistical significance. Results are expressed as mean +/- SD, unless otherwise specified.

Acknowledgements

The authors wish to thank the Investigative Histopathology Laboratory at Michigan State University for their assistance with immunohistochemistry, Dr, Louis King for assistance with flow cytometry, Dr. Robert Clarke for providing cell lines, and Dr. Alana Welm for providing patient derived xenograft lines. This research was supported by grants from the Department of Defense (W81XWH-15-1-0018), The Clinical and Translational Sciences Institute at Michigan State University, and the Aitch Foundation.

REFERENCES

REFERENCES

1. Siegel, R.L., K.D. Miller, and A. Jemal, Cancer Statistics, 2017. CA Cancer J Clin, 2017. 67(1): p. 7-30.

2. Sims, A.H., et al., Origins of breast cancer subtypes and therapeutic implications. Nat Clin Pract Oncol, 2007. 4(9): p. 516-25.

3. Wolf, D.M., et al., Investigation of the mechanism of tamoxifen-stimulated breast tumor growth with nonisomerizable analogues of tamoxifen and metabolites. J Natl Cancer Inst, 1993. 85(10): p. 806-12.

4. Zwart, W., V. Theodorou, and J.S. Carroll, Estrogen receptor-positive breast cancer: a multidisciplinary challenge. Wiley Interdiscip Rev Syst Biol Med, 2011. 3(2): p. 216-30.

5. Osborne, C.K. and R. Schiff, Mechanisms of endocrine resistance in breast cancer. Annu Rev Med, 2011. 62: p. 233-47.

6. Yardley, D.A., et al., Everolimus plus exemestane in postmenopausal patients with HR(+) breast cancer: BOLERO-2 final progression-free survival analysis. Adv Ther, 2013. 30(10): p. 870-84.

7. Bachelot, T., et al., Randomized phase II trial of everolimus in combination with tamoxifen in patients with hormone receptor-positive, human epidermal growth factor receptor 2-negative metastatic breast cancer with prior exposure to aromatase inhibitors: a GINECO study. J Clin Oncol, 2012. 30(22): p. 2718-24.

8. Finn, R.S., et al., Palbociclib and Letrozole in Advanced Breast Cancer. N Engl J Med, 2016. 375(20): p. 1925-1936.

9. Turner, N.C., et al., Palbociclib in Hormone-Receptor-Positive Advanced Breast Cancer. N Engl J Med, 2015. 373(3): p. 209-19.

10. Fasching PA, J.G., Pivot X, Martin M, De Laurentiis M, Blackwell K, Esteva FJ, Paquet-Luzy T, Tang Z, Lorenc KR, Slamon DJ. Phase III study of ribociclib (LEE011) in combination with fulvestrant for the treatment of postmenopausal patients (pts) with hormone receptor-positive (HR+), HER2-negative (HER2–) advanced breast cancer (aBC) who have received no or only one line of prior endocrine treatment: MONALEESA-3. in Proceedings of the Thirty-Eighth Annual CTRC-AACR San Antonio Breast Cancer Symposium. 2016. San Antonio, TX: AACR; Cancer Research.

11. Piccart, M., et al., Everolimus plus exemestane for hormone-receptor-positive, human epidermal growth factor receptor-2-negative advanced breast cancer:

overall survival results from BOLERO-2dagger. Ann Oncol, 2014. 25(12): p. 2357-62.

12. Rocca, A., et al., Progress with palbociclib in breast cancer: latest evidence and clinical considerations. Ther Adv Med Oncol, 2017. 9(2): p. 83-105.

13. Herrera-Abreu, M.T., et al., Early Adaptation and Acquired Resistance to CDK4/6 Inhibition in Estrogen Receptor-Positive Breast Cancer. Cancer Res, 2016. 76(8): p. 2301-13.

14. Bihani, T., et al., Resistance to everolimus driven by epigenetic regulation of MYC in ER+ breast cancers. Oncotarget, 2015. 6(4): p. 2407-20.

15. Herynk, M.H. and S.A. Fuqua, Estrogen receptor mutations in human disease. Endocr Rev, 2004. 25(6): p. 869-98.

16. Chen, J. and K.A. Gallo, MLK3 regulates paxillin phosphorylation in chemokine-mediated breast cancer cell migration and invasion to drive metastasis. Cancer Res, 2012. 72(16): p. 4130-40.

17. Swenson, K.I., K.E. Winkler, and A.R. Means, A new identity for MLK3 as an NIMA-related, cell cycle-regulated kinase that is localized near centrosomes and influences microtubule organization. Mol Biol Cell, 2003. 14(1): p. 156-72.

18. Huang, C., K. Jacobson, and M.D. Schaller, A role for JNK-paxillin signaling in cell migration. Cell Cycle, 2004. 3(1): p. 4-6.

19. Saporito, M.S., R.L. Hudkins, and A.C. Maroney, Discovery of CEP-1347/KT-7515, an inhibitor of the JNK/SAPK pathway for the treatment of neurodegenerative diseases. Prog Med Chem, 2002. 40: p. 23-62.

20. Sweeney, Z.K. and J.W. Lewcock, ACS chemical neuroscience spotlight on CEP-1347. ACS Chem Neurosci, 2011. 2(1): p. 3-4.

21. Wang, L., K.A. Gallo, and S.E. Conrad, Targeting mixed lineage kinases in ER-positive breast cancer cells leads to G2/M cell cycle arrest and apoptosis. Oncotarget, 2013. 4(8): p. 1158-71.

22. Cha, H., et al., Inhibition of mixed-lineage kinase (MLK) activity during G2-phase disrupts microtubule formation and mitotic progression in HeLa cells. Cell Signal, 2006. 18(1): p. 93-104.

23. Mixed lineage kinase inhibitor CEP-1347 fails to delay disability in early Parkinson disease. Neurology, 2007. 69(15): p. 1480-90.

24. Osmani, A.H., et al., Activation of the nimA protein kinase plays a unique role during mitosis that cannot be bypassed by absence of the bimE checkpoint. EMBO J, 1991. 10(9): p. 2669-79.

25. Chen, J., E.M. Miller, and K.A. Gallo, MLK3 is critical for breast cancer cell migration and promotes a malignant phenotype in mammary epithelial cells. Oncogene, 2010. 29(31): p. 4399-411.

26. Rattanasinchai, C., et al., MLK3 regulates FRA-1 and MMPs to drive invasion and transendothelial migration in triple-negative breast cancer cells. Oncogenesis, 2017. 6(6): p. e345.

27. Zhan, Y., et al., Mixed lineage kinase 3 is required for matrix metalloproteinase expression and invasion in ovarian cancer cells. Exp Cell Res, 2012. 318(14): p. 1641-8.

28. Cronan, M.R., et al., Defining MAP3 kinases required for MDA-MB-231 cell tumor growth and metastasis. Oncogene, 2012. 31(34): p. 3889-900.

29. Okada, M., et al., Repositioning CEP-1347, a chemical agent originally developed for the treatment of Parkinson's disease, as an anti-cancer stem cell drug. Oncotarget, 2017. 8(55): p. 94872-94882.

30. Soule, H.D., et al., A human cell line from a pleural effusion derived from a breast carcinoma. J Natl Cancer Inst, 1973. 51(5): p. 1409-16.

31. Lee, A.V., S. Oesterreich, and N.E. Davidson, MCF-7 cells--changing the course of breast cancer research and care for 45 years. J Natl Cancer Inst, 2015. 107(7).

32. Brunner, N., et al., MCF7/LCC9: an antiestrogen-resistant MCF-7 variant in which acquired resistance to the steroidal antiestrogen ICI 182,780 confers an early cross-resistance to the nonsteroidal antiestrogen tamoxifen. Cancer Res, 1997. 57(16): p. 3486-93.

33. Komarova, N.L. and D. Wodarz, Drug resistance in cancer: principles of emergence and prevention. Proc Natl Acad Sci U S A, 2005. 102(27): p. 9714-9.

34. Sikora, E., Mosieniak, G., Sliwinska, M. A., Morphological and Functional Characteristic of Senescent Cancer Cells. Curr Drug Targets, 2016. 17(4): p. 377-387.

35. DeRose, Y.S., et al., Tumor grafts derived from women with breast cancer authentically reflect tumor pathology, growth, metastasis and disease outcomes. Nat Med, 2011. 17(11): p. 1514-20.

36. Diel, P., K. Smolnikar, and H. Michna, The pure antiestrogen ICI 182780 is more effective in the induction of apoptosis and down regulation of BCL-2 than tamoxifen in MCF-7 cells. Breast Cancer Res Treat, 1999. 58(2): p. 87-97.

37. Ellis, P.A., et al., Induction of apoptosis by tamoxifen and ICI 182780 in primary breast cancer. Int J Cancer, 1997. 72(4): p. 608-13.

38. Lim, K.B., et al., Induction of apoptosis in mammary gland by a pure anti-estrogen ICI 182780. Breast Cancer Res Treat, 2001. 68(2): p. 127-38.

39. Kornblum, N., et al., Randomized Phase II Trial of Fulvestrant Plus Everolimus or Placebo in Postmenopausal Women With Hormone Receptor-Positive, Human Epidermal Growth Factor Receptor 2-Negative Metastatic Breast Cancer Resistant to Aromatase Inhibitor Therapy: Results of PrE0102. J Clin Oncol, 2018: p. JCO2017769331.

40. The safety and tolerability of a mixed lineage kinase inhibitor (CEP-1347) in PD. Neurology, 2004. 62(2): p. 330-2.

41. Jansen, G.H., et al., Effects of fulvestrant alone or combined with different steroids in human breast cancer cells in vitro. Climacteric, 2008. 11(4): p. 315-21.

42. Dolfi, S.C., et al., Fulvestrant treatment alters MDM2 protein turnover and sensitivity of human breast carcinoma cells to chemotherapeutic drugs. Cancer Lett, 2014. 350(1-2): p. 52-60.

43. Osipo, C., et al., Paradoxical action of fulvestrant in estradiol-induced regression of tamoxifen-stimulated breast cancer. J Natl Cancer Inst, 2003. 95(21): p. 1597-608.

44. Arthur, C.R., et al., Autophagic cell death, polyploidy and senescence induced in breast tumor cells by the substituted pyrrole JG-03-14, a novel microtubule poison. Biochem Pharmacol, 2007. 74(7): p. 981-91.

45. Xu, W.S., et al., Induction of polyploidy by histone deacetylase inhibitor: a pathway for antitumor effects. Cancer Res, 2005. 65(17): p. 7832-9.

46. Verdoodt, B., et al., Induction of polyploidy and apoptosis after exposure to high concentrations of the spindle poison nocodazole. Mutagenesis, 1999. 14(5): p. 513-20.

47. Zasadil, L.M., E.M. Britigan, and B.A. Weaver, 2n or not 2n: Aneuploidy, polyploidy and chromosomal instability in primary and tumor cells. Semin Cell Dev Biol, 2013. 24(4): p. 370-9.

48. Puig, P.E., et al., Tumor cells can escape DNA-damaging cisplatin through DNA endoreduplication and reversible polyploidy. Cell Biol Int, 2008. 32(9): p. 1031-43.

49. Coward, J. and A. Harding, Size Does Matter: Why Polyploid Tumor Cells are Critical Drug Targets in the War on Cancer. Front Oncol, 2014. 4: p. 123.

50. Stepien, A., et al., Taxol-induced polyploidy and cell death in CHO AA8 cells. Acta Histochem, 2010. 112(1): p. 62-71.

51. Osborne, C.K., et al., Comparison of the effects of a pure steroidal antiestrogen with those of tamoxifen in a model of human breast cancer. J Natl Cancer Inst, 1995. 87(10): p. 746-50.

52. Bross, P.F., et al., FDA drug approval summaries: fulvestrant. Oncologist, 2002. 7(6): p. 477-80.

53. Lawson, D.A., et al., The Cleared Mammary Fat Pad Transplantation Assay for Mammary Epithelial Organogenesis. Cold Spring Harb Protoc, 2015. 2015(12): p. pdb prot078071.

54. Sikora, M.J., et al., Invasive lobular carcinoma cell lines are characterized by unique estrogen-mediated gene expression patterns and altered tamoxifen response. Cancer Res, 2014. 74(5): p. 1463-74.

55. DeRose, Y.S., et al., Patient-derived models of human breast cancer: protocols for in vitro and in vivo applications in tumor biology and translational medicine. Curr Protoc Pharmacol, 2013. Chapter 14: p. Unit14 23.

Chapter 3: Exploration of the Cellular and Nuclear Mitotic Phenotype Resulting from Treatment with CEP-1347

Abstract

Kinase inhibitors are often used to treat a number of diseases with the added benefit of specificity in therapy. CEP-11004 and CEP-1347 are kinase inhibitors that were initially investigated for their role in MLK inhibition. A unique nuclear morphology has been reported after treatment with CEP-11004, but cellular phenotype after treatment with CEP-1347 has not been investigated. In this report, I explored the cellular and nuclear morphology that results from treatment with CEP-1347 using estrogen receptor positive breast cancer cells as an experimental model. I further investigated the kinase target or targets that may be responsible for producing the phenotypes observed and identified an alternate kinase pathway whose activity is modulated by CEP-1347.

Introduction

The advent of targeted therapies has drastically changed treatment options for a number of diseases including cancer, autoimmune disorders, and degenerative diseases [1, 2]. Dysregulation of kinase function has been widely implicated in disease, and therapies often target kinase activity. The specificity of these compounds allows for inhibition of enzyme activity which often reduces side effect profiles and enhances therapeutic efficacy [1, 3]. Kinase inhibitors have been studied for decades, and multiple agents are now clinically available for estrogen receptor positive (ER+) breast cancer, including the recently approved CDK 4/6 inhibitors palbociclib, abemaciclib, and ribociclib [4]. Furthermore, small molecule kinase inhibitors, such as neratinib [5], or

monoclonal antibodies, such as traztuzumab [5, 6] and pertuzumab [6] are able to target the receptor tyrosine kinase HER2 in cancers that overexpress this cell surface receptor.

CEP-1347 and CEP-11004 are indolocarbazole derivatives of K252a, an analog of staurosporine [7]. They act as competitive inhibitors that bind to the adenosine triphosphate (ATP) binding site of protein kinases, and have primarily been studied as inhibitors of the MLK family of serine/threonine kinases, specifically MLK3 [7]. MLKs act as mitogen activated protein kinase kinase kinases (MAP3K) which phosphorylate and activate mitogen activated protein kinase kinases (MAP2Ks). MAP2Ks in turn phosphorylate and activate mitogen activated protein kinases (MAPKs), which can then phosphorylate transcription factors or cytoplasmic substrates. The end outcome of this phosphorylation cascade is to activate transcription of genes involved in cellular growth and survival, and to promote cytoskeletal rearrangements, cell migration, and invasion [8-10].

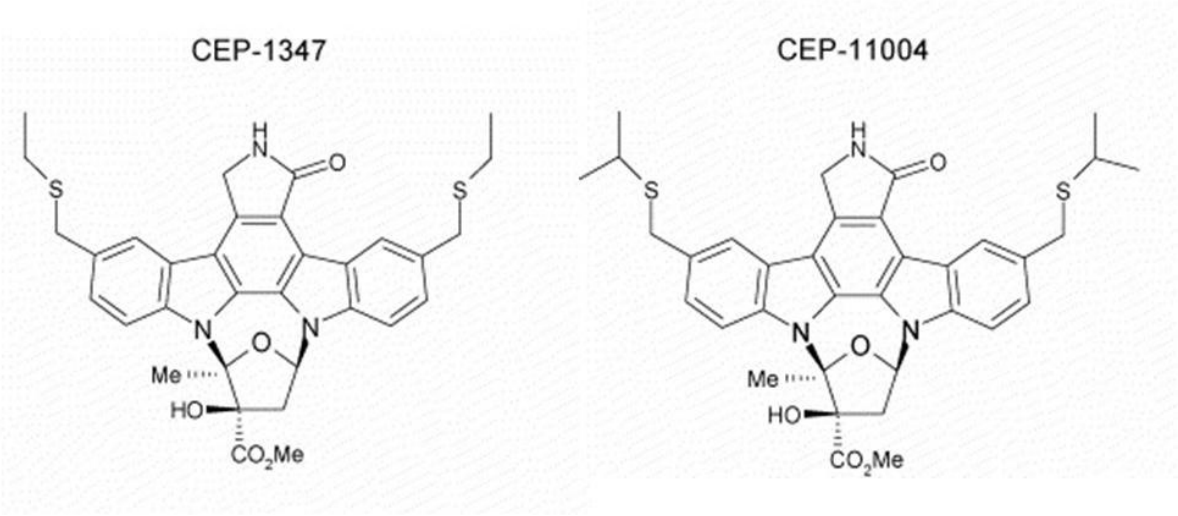

Figure 3-1: Chemical structures of CEP-1347 and CEP-11004. (Adapted from [11]).

The mechanism of CEP-1347 action was initially studied in the context of Parkinson's Disease (PD) with the intent of inhibiting apoptosis of dopaminergic neurons in the substantia nigra to prevent disease progression [7]. These studies identified MLK3 as a major target of CEP-1347, and determined that the activity of the MAPK c-Jun N-terminal kinase/stress-activated protein kinase (JNK/SAPK) was inhibited downstream of MLK3, with little to no effect on the MAPKs extracellular-signal regulated kinase (ERK) and p38 [7]. The inhibition of JNK phosphorylation caused increased neuron survival in cell culture and in animal studies [7, 12]. Promising results *in vitro* and *in vivo* led to the initiation of a Phase I clinical trial to establish safety and tolerability in humans, but was ineffective in preventing disease progression in a Phase II/III trial (PRECEPT) [13]. Because CEP-1347 was well tolerated in humans, it continued to be studied, along with CEP-11004. Subsequent studies found that treatment with CEP-1347 slowed or reversed progression of Huntington's disease [14, 15], Alzheimer's disease [7], and auditory disorders [16] in animal models. Furthermore, CEP-1347 was found to exhibit anti-inflammatory activities in the brain [17, 18] and pancreas [19], and its potential as an anti-cancer agent was also explored [20, 21].

Chemically, these compounds differ in their side chains: CEP-1347 contains two ethyl groups while in CEP-11004 these ethyl groups are substituted for isopropyl groups (Figure 3-1). However, biologically, both compounds selectively decreased viability of transformed cell lines, while having no detectable effect on non-transformed cell lines at concentrations used [21, 22]. Treatment of transformed cell lines with these compounds resulted in an early mitotic arrest [21, 22], which has been our primary focus. Further

study of the mechanism of action of CEP-11004 discovered that treatment led to the development of abnormal mitotic spindles and aberrant DNA condensation without affecting centrosome duplication and separation [22]. While the mechanism of action and phenotype resulting from treatment with CEP-11004 has been better studied than CEP-1347, the latter compound more effectively inhibited phosphorylation of JNK in neuronal cells [23]. Furthermore, unlike CEP-1347, the safety and efficacy of CEP-11004 has not been established, making it desirable to further elucidate the mechanism of action of CEP-1347.

Binding studies completed with CEP-1347 indicate that it is able to bind not only to MLK3, but also to additional kinases including Aurora A, Aurora B, MLKs 1 and 2, adenosine monophosphate-activated protein kinase (AMPK), and its downstream target S6 kinase (p70s6k), among others [24]. However, the ability of CEP-1347 to inhibit the activity of all of these kinases *in vitro* and *in vivo*, as well as the relative IC_{50}s, have not been very well studied.

Based on previous research describing the cellular and nuclear phenotype apparent after treatment with CEP-11004, I hypothesized that a similar mitotic phenotype might exist after exposure to CEP-1347, and that the kinase target of this compound would be active in mitosis. Centrosome duplication occurs during S phase, prior to entry into mitosis. During the G2/M transition, centrosomes migrate to opposite sides of the cell due to both pulling forces from astral microtubules that attach centrosomes to cell membranes, and pushing forces between centrosomes [25]. This process establishes

appropriate bipolarity for subsequent cell division. Spindle microtubules grow from centrosomes towards kinetochores, which are located at chromosome centromeres, and tension facilitates alignment of DNA along the metaphase plate. The absence of tension at one or more pairs of sister chromatids activates the spindle assembly checkpoint (SAC), which prevents entry into anaphase.

A number of kinases are involved in mitotic progression. Aurora A localizes to centrosomes and functions in centrosome duplication [26]. Polo-like kinase 1 (PLK1) plays a role in multiple steps of mitosis including centrosome separation and migration [25, 27, 28], as do never in mitosis gene-A (NIMA) related kinases Nek2 and Nek9 [25]. Aurora B facilitates kinetochore attachment to microtubules until metaphase, and then migrates to the spindle midbody for the remainder of mitosis [26]. The lack of appropriate activity of Aurora A, Aurora B, or PLK1 results in inappropriate chromosome alignment during metaphase, disrupts mitotic spindle formation and polarization, and often results in apoptosis [26, 29-32].

The primary target of CEP-1347, MLK3 [7], also localizes to centrosomes during mitosis [33]. Overexpression of MLK3 disrupts cytoplasmic microtubule formation during interphase and inhibits astral microtubule formation, indicating a possible role in mitotic progression [33]. Furthermore, MLK3 displays sequence homology with NIMA kinases [33], which are required for the G2/M transition in *Aspergillis nidulans*, further supporting the possibility that MLK3 is important for progression into mitosis [34].

In this study, I characterized the phenotype created by treatment with CEP-1347 and its kinase targets in breast cancer cells. While MLK3 is the most studied target of CEP-1347, this compound binds to multiple kinases [35], suggesting that additional targets may exist. I hypothesized that CEP-1347 is capable of binding to and inhibiting the activity of kinases outside of MLK3 and that these other kinases will be actively involved in cellular progression through mitosis. Using reverse phase protein array (RPPA) analysis, I identified adenosine monophosphate-activated protein kinase (AMPK) as a novel kinase whose activity is modulated by treatment with CEP-1347, and studied its role in cell cycle progression and mitotic spindle formation and orientation.

Results

CEP-1347 treated cells exhibit aberrant mitotic DNA alignment and spindle formation

As previously described, CEP-1347 induces a mitotic arrest of transformed cells, and prolonged treatment leads to the formation of abnormally large cells with expanded cytoplasms and at times, multiple nuclei [21, 33]. I reasoned that because treatment with CEP-1347 leads to a mitotic arrest, and CEP-11004 treated cells exhibit aberrant mitotic spindle formation, CEP-1347 treatment might exhibit a similar nuclear phenotype. To fully characterize the nuclear effects of CEP-1347, I analyzed the nuclear morphology of cells throughout mitosis. Cells were synchronized in G1, then allowed to progress through the cell cycle in the presence or absence of CEP-1347. Cells were harvested at various times, and analysis of DNA content indicated that cells entered mitosis between 27 and 30 hours after release (Figure 3-2A). By 30 and 33 hours after release, vehicle treated cells returned to G1 after cytokinesis. Consistent with our

previous report [21], at these time points, CEP-1347 caused an accumulation of cells in G2/M by DNA content. Nuclei were examined using DAPI to visualize DNA and anti-alpha-tubulin antibody to visualize mitotic spindles. Vehicle and CEP-1347 treated cells were in interphase at 24 hours and progressed into prophase of mitosis by 27 hours. At 30 and 33 hours, vehicle treated cells displayed complete DNA condensation and uniform chromosome alignment, consistent with metaphase (Figure 3-2B). The chromosomes in these cells also exhibited clear sister chromatid separation during anaphase, telophase, and cytokinesis (Supplemental Figure 3-1). Interestingly, at 30 and 33 hours, cells treated with CEP-1347 were incompletely aligned along the metaphase plate, and the presence of lagging chromosomes was apparent (Figure 3-2B, arrows).

Examination of mitotic spindles revealed that vehicle treated cells formed organized bipolar metaphase spindles. However, cells treated with CEP-1347 formed disordered and asymmetric spindles, often without distinct bipolarity. Quantification of mitotic spindles revealed that the majority of cells treated with vehicle generated spindles with a normal bipolar appearance (Figure 3-2C, Supplemental Figure 3-2). The very few vehicle treated cells that exhibited abnormal spindles were multipolar rather than bipolar (Supplemental Figure 3-1). Unexpectedly, the vast majority of mitotic spindles that formed in cells treated with CEP-1347 appeared irregular and asymmetric, and none of these spindles exhibited multipolarity.

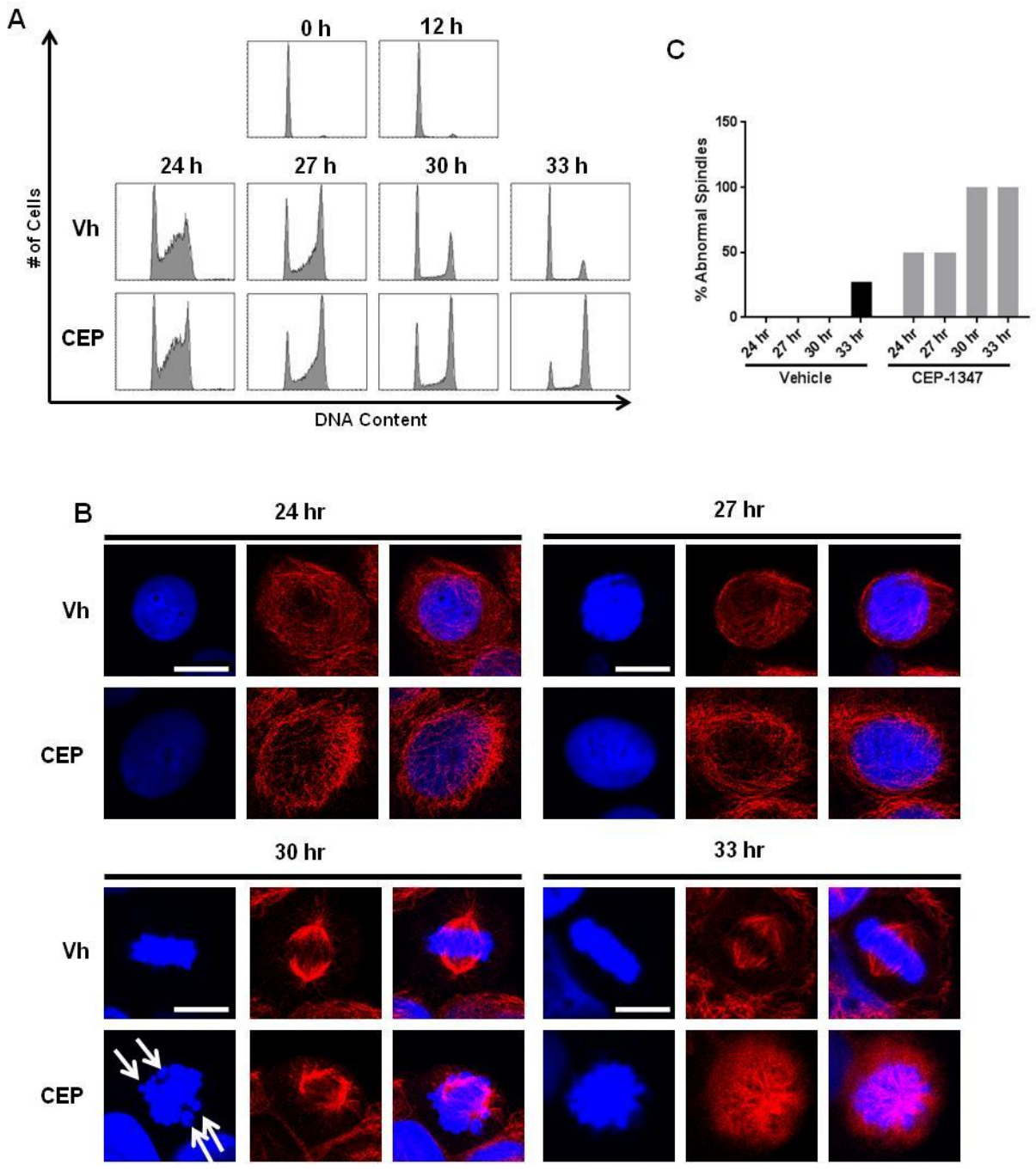

Figure 3-2: Treatment with CEP-1347 leads to an early mitotic arrest. MCF-7 cells were treated with 10 nM ICI 182,780 for 48 hours to synchronize in G1. ICI 182,780 was then washed out and replaced with media containing 10 nM 17-β estradiol to initiate cycling; this was considered the 0 hour time point. Synchronized MCF-7 cells were

Figure 3-2 (cont'd)

treated with vehicle or 100 nM CEP-1347 at 12 hours and followed through the cell cycle. Cell cycle distribution at 24-33 hours reveal accumulation of CEP-1347 treated cells in G2/M (A). DNA condensation (DAPI, blue) and mitotic spindle formation (alpha-tubulin, red) were analyzed at all mitotic time points (B). Quantification of mitotic spindles (C). Scale bar represents 10 μm.

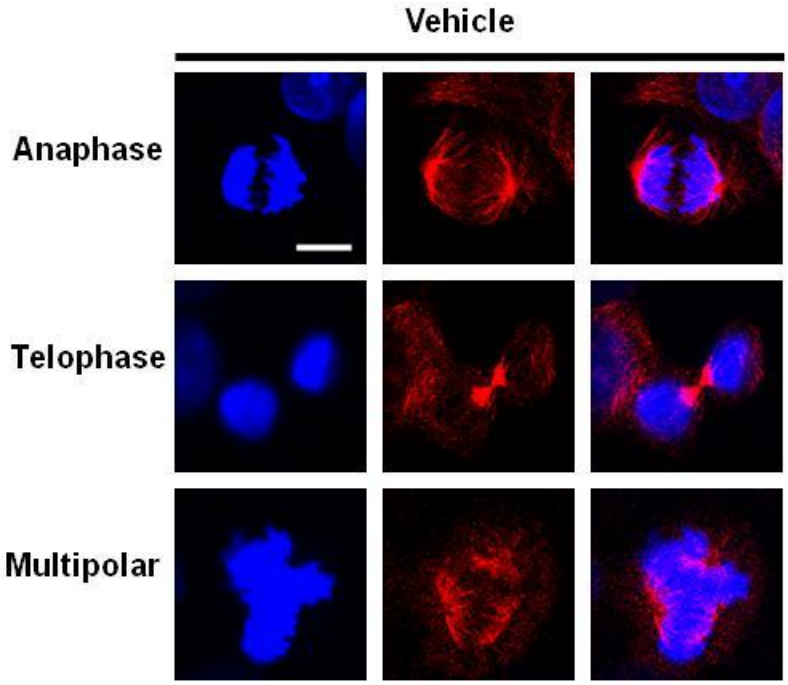

Supplemental Figure 3-1: Late mitotic and abnormal mitotic formations of vehicle treated cells. Scale bar represents 10 μm.

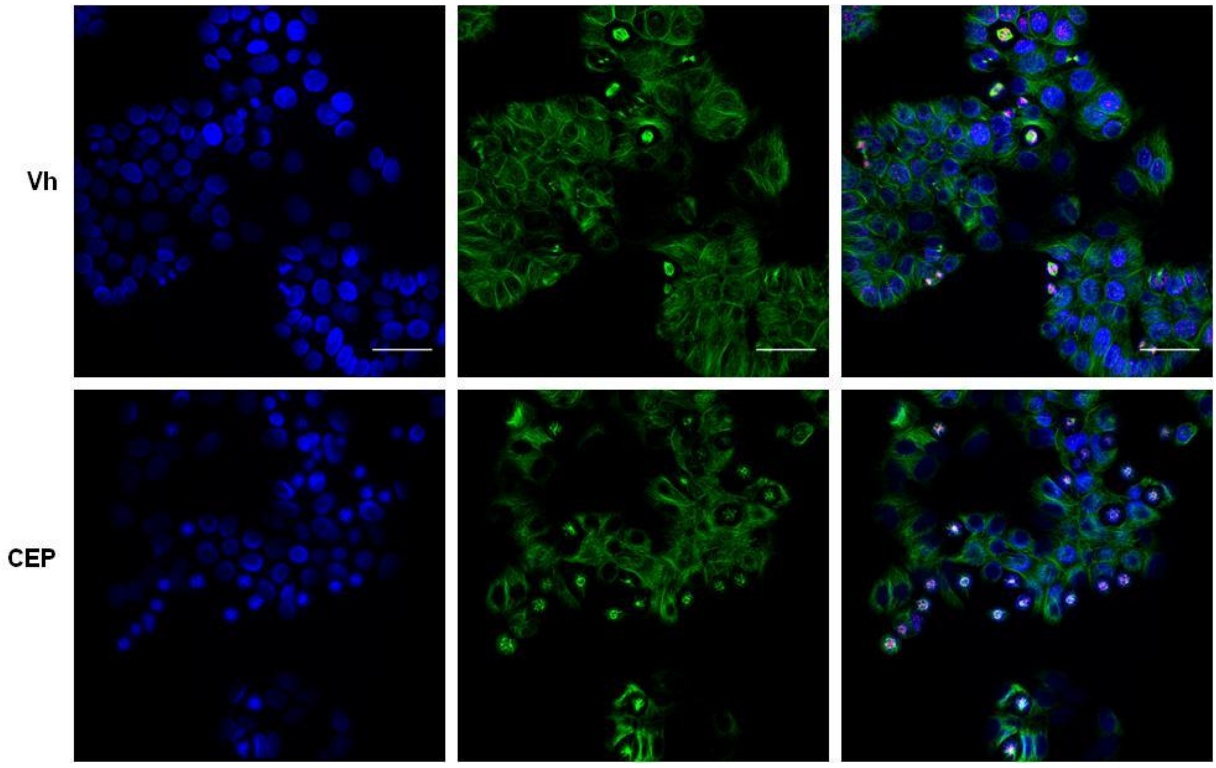

Supplemental Figure 3-2: Lower magnification images of vehicle and CEP-1347 treated cells. Scale bar represents 50 μm.

CEP-1347 treatment leads to presence of multiple chromosome misalignment phenotypes

To further investigate the effect of CEP-1347 on spindle formation, I analyzed chromosome alignment in mid-mitosis. Synchronized cells were harvested and stained with anti-centromere antibody (ACA) to visualize centromeres, anti-alpha-tubulin to examine spindles, and DAPI to visualize DNA. In early mitosis, (27 hours), vehicle treated cells exhibited condensing DNA consistent with prophase. ACA staining was punctate and central to the nucleus with mitotic spindles not yet formed. DNA in CEP-1347 treated cells was less condensed, with more spread out centromeres and microtubules seeming to form from a central point. At 30 and 33 hours, vehicle treated

metaphase cells exhibited discrete punctate ACA staining along the metaphase plate, indicating appropriate alignment of DNA. This was not apparent in cells treated with CEP-1347, where a number of distinct nuclear morphologies were observed. In the first and most common, condensed DNA was organized in a circular configuration, but centromeres were clustered central to the DNA (Figure 3-3 a,d). In these nuclei, disordered microtubules surrounded the DNA without clear spindle-like organization. This morphology made up approximately 50-60% of all mitotic nuclei in CEP-1347 treated samples. In the second configuration, DNA was observed in a circular configuration with the majority of centromeres centrally oriented and closely clustered in the center of the DNA (Figure 3-3b). In this case, mitotic spindles were severely misformed with microtubules emanating from a single central point, and some centromeres were outside of the central core. This configuration made up approximately 30-40% of all mitotic nuclei in CEP-1347 treated samples. Finally, some nuclei displayed near-normal looking spindles with most of the DNA aligned at a metaphase plate, but even in these cases lagging chromosomes were visible (Figure 3-3 c,e). These nuclei made up approximately 10% of all mitotic nuclei in CEP-1347 treated samples. The approximate distributions of nuclear morphologies were consistent from 27 hours through 33 hours.

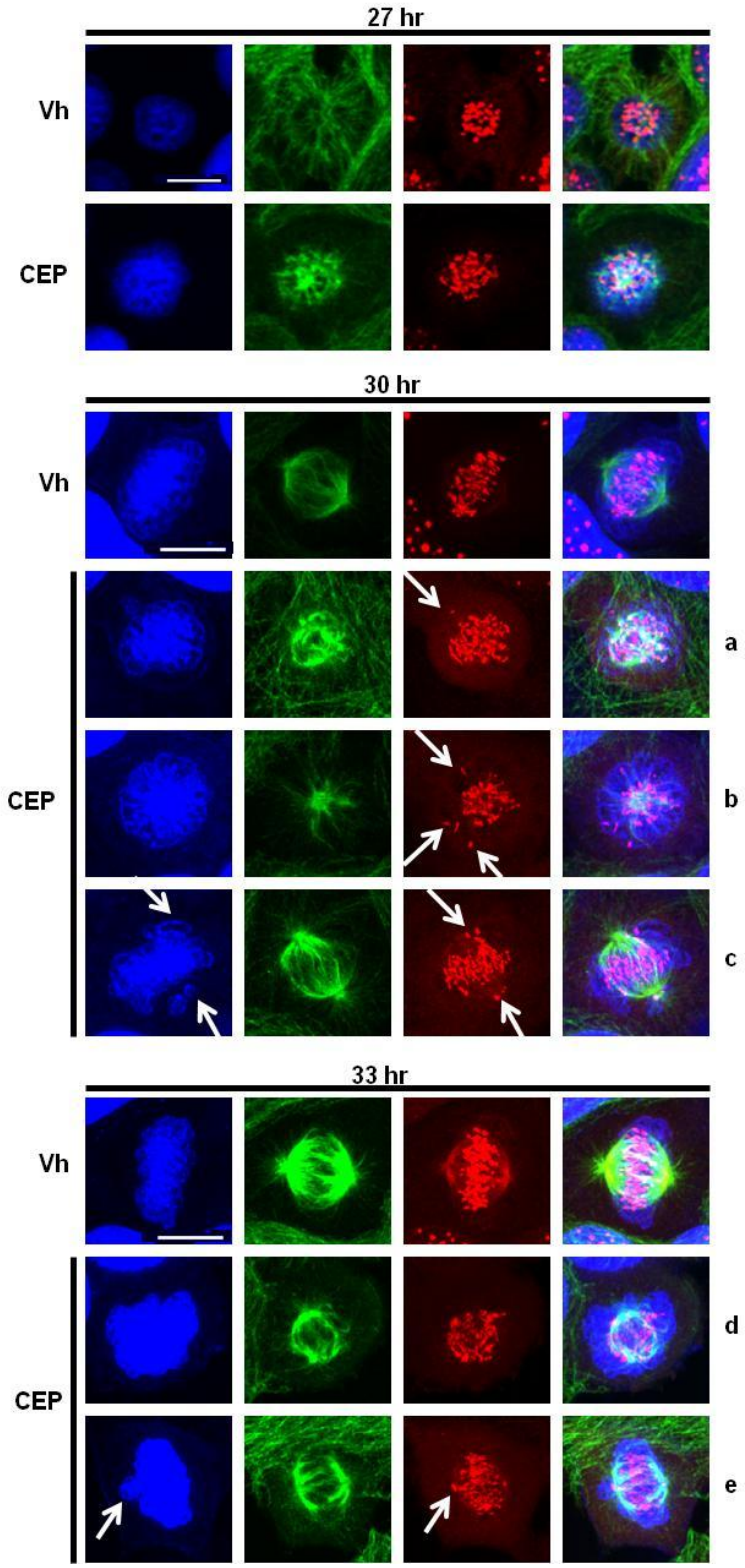

Figure 3-3: Treatment with CEP-1347 alters centromere alignment. Synchronized MCF-7 cells were treated with vehicle or 100 nM CEP-1347 and followed through the

Figure 3-3 (cont'd)

cell cycle. DNA condensation (DAPI, blue) and mitotic spindle formation (alpha-tubulin, green), and centromeres (anti-centromere antibody, red) were analyzed at all mitotic time points. Scale bar represents 10 μm.

Centrosome duplication is unaffected by treatment with CEP-1347

Centrosome duplication occurs in S phase, prior to entry into mitosis. In late G2 and early mitosis, duplicated centrosomes migrate to opposite sides of the cell to create a bipolar mitotic spindle and, after nuclear envelope breakdown, spindle microtubules attach to kinetochores at centromeres of condensed chromosomes. Based on the irregular mitotic microtubule structures observed, I hypothesized that CEP-1347 treatment might inhibit centrosome duplication. To test this, I analyzed centrosomes after treatment with CEP-1347 by harvesting synchronized cells at 27-33 hours, and staining with anti-gamma-tubulin antibody. Interestingly, I found that centrosome duplication was unaffected by treatment with CEP-1347 at all time points (Figure 3-4). Duplicated centrosomes were evident in both vehicle and CEP-1347 treated cultures, and were visible in cells with both interphase and mitotic DNA. Intriguingly, while centrosomes in vehicle treated cells migrated to opposite poles, the duplicated centrosomes in CEP-1347 treated mitotic cells that exhibited the first or second nuclear morphology mentioned previously remained in close proximity, and were surrounded by condensed DNA. In the rare cases where DNA was partially aligned along the metaphase plate, correlating to the third nuclear morphology described, centrosomes in CEP-1347 treated cells had migrated to opposite sides of the condensed DNA to

somewhat allow formation of a bipolar spindle. Together, this suggests that one mechanism of action of CEP-1347 is to inhibit centrosome separation and migration, thereby preventing appropriate cellular polarization. In the instances where centrosomes separate and migrate away from each other, mitotic spindles are still irregular, indicating that CEP-1347 may have additional effects.

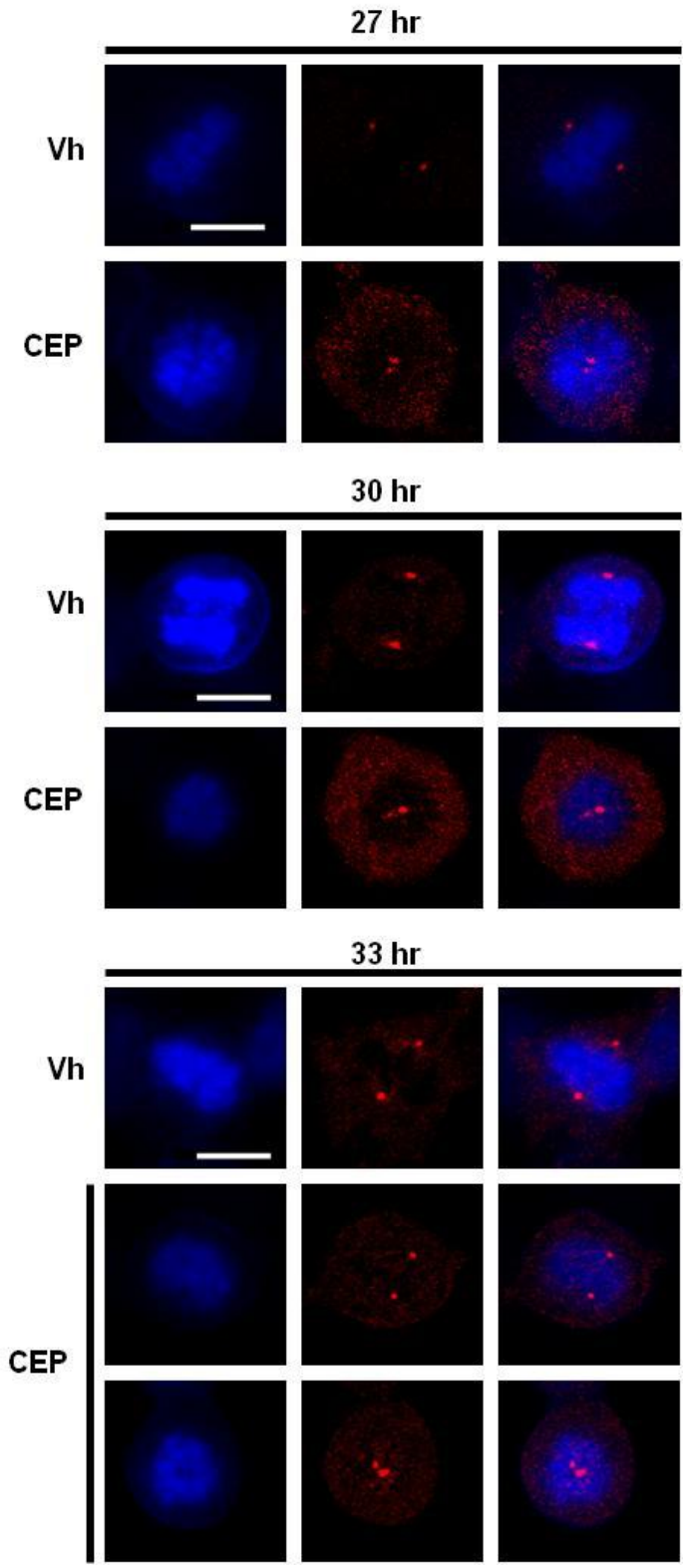

Figure 3-4: Treatment with CEP-1347 disrupts centrosome separation and migration. Synchronized MCF-7 cells were treated with vehicle or 100 nM CEP-1347

Figure 3-4 (cont'd)

and followed through the cell cycle. DNA condensation (DAPI, blue) and mitotic spindle formation (alpha-tubulin, green), and centromeres (anti-centromere antibody, red) were analyzed at all mitotic time points. Scale bar represents 10 μm.

Studying the targets of CEP-1347

Having carefully studied the phenotype resulting from treatment with CEP-1347, I next addressed the question of whether inhibition of MLK3 activity was responsible for causing the observed changes in cellular morphology. As previously stated, MLK3 is the best studied kinase inhibited by CEP-1347 and is known to localize to centrosomes during mitosis [33]. In addition, overexpression of MLK3 alters mitotic microtubule formation [22]. However, as also previously stated, CEP-1347 can bind to a number of kinases [35]. Of these, Aurora kinases A and B have well characterized roles in mitotic progression. Aurora kinase A localizes to and functions at centrosomes to facilitate duplication [30], while Aurora B localizes and functions at centromeres until metaphase when it re-localizes to the cell midbody [26]. Aurora B is the canonical kinase that phosphorylates histone H3; thus, inhibition of Aurora B decreases expression of phosphorylated histone H3 [36]. Inhibition of either of these Aurora kinases individually, or both together, leads to mitotic arrest and accumulation of polyploid cells, and results in apoptosis [29, 31, 32, 37], all of which are similar to the phenotype seen upon treatment with CEP-1347. However, unlike the phenotype that was see upon treatment with CEP-1347, Aurora A kinase inhibitors prevent centrosome duplication, and as previously reported, treatment with CEP-1347 leads to an accumulation of phospho-

histone H3 (data not shown) [21], leading us to conclude that CEP-1347 does not directly target either Aurora A or B.

MLK3 as the target of CEP-1347

MLK3 localizes to centrosomes [33] and centrosome separation is altered by CEP-1347 treatment. Furthermore, overexpression of MLK3 was able to reverse CEP-11004 induced cell cycle arrest [22]. To investigate if inhibition of MLK3 activity is responsible for the effects of CEP-1347, I utilized two approaches: overexpression and knockdown. To examine if MLK3 overexpression altered the CEP-1347 induced decrease in cell viability, I utilized MCF-7 cells engineered to inducibly overexpress MLK3 [38]. I hypothesized that MLK3 overexpression would alter sensitivity to CEP-1347 by changing the pharmacodynamics of ligand-protein interactions, and expected MLK3 overexpression to make cells more resistant to CEP-1347. While the majority of cells overexpressed MLK3 (Supplemental Figure 3-3), this overexpression had no effect on sensitivity to CEP-1347, even after 6 days of treatment (Figure 3-5A). To directly analyze the role of MLK3 in cell cycle, its expression was knocked down using RNA interference, and DNA content was analyzed. As shown in Figure 3-5B, although MLK3 protein expression was reduced by approximately 85% compared to control, cell cycle distribution was unaffected, while CEP-1347 caused the expected G2/M accumulation. The lack of an effect of knockdown on cell cycle may be due to residual MLK3 activity, but may also suggest that an alternate target of CEP-1347 causes the cell cycle arrest phenotype.

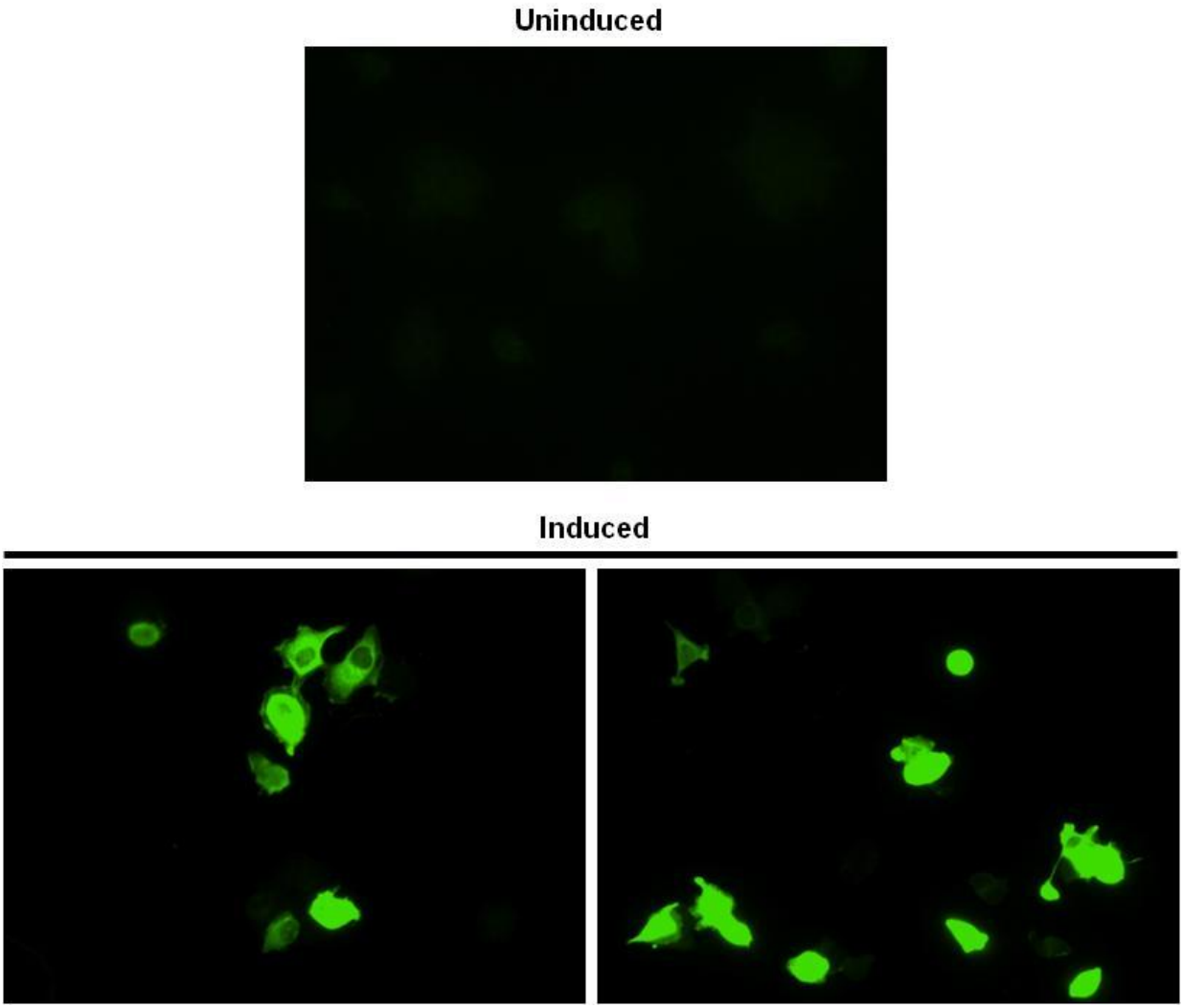

Supplemental Figure 3-3: MLK3 is overexpressed after induction. MCF-7iMLK3 cells were treated with 50 nM of the inducer AP21967 and stained with anti-MLK3 (green) to analyze overexpression. Images are representative uninduced and induced cells.

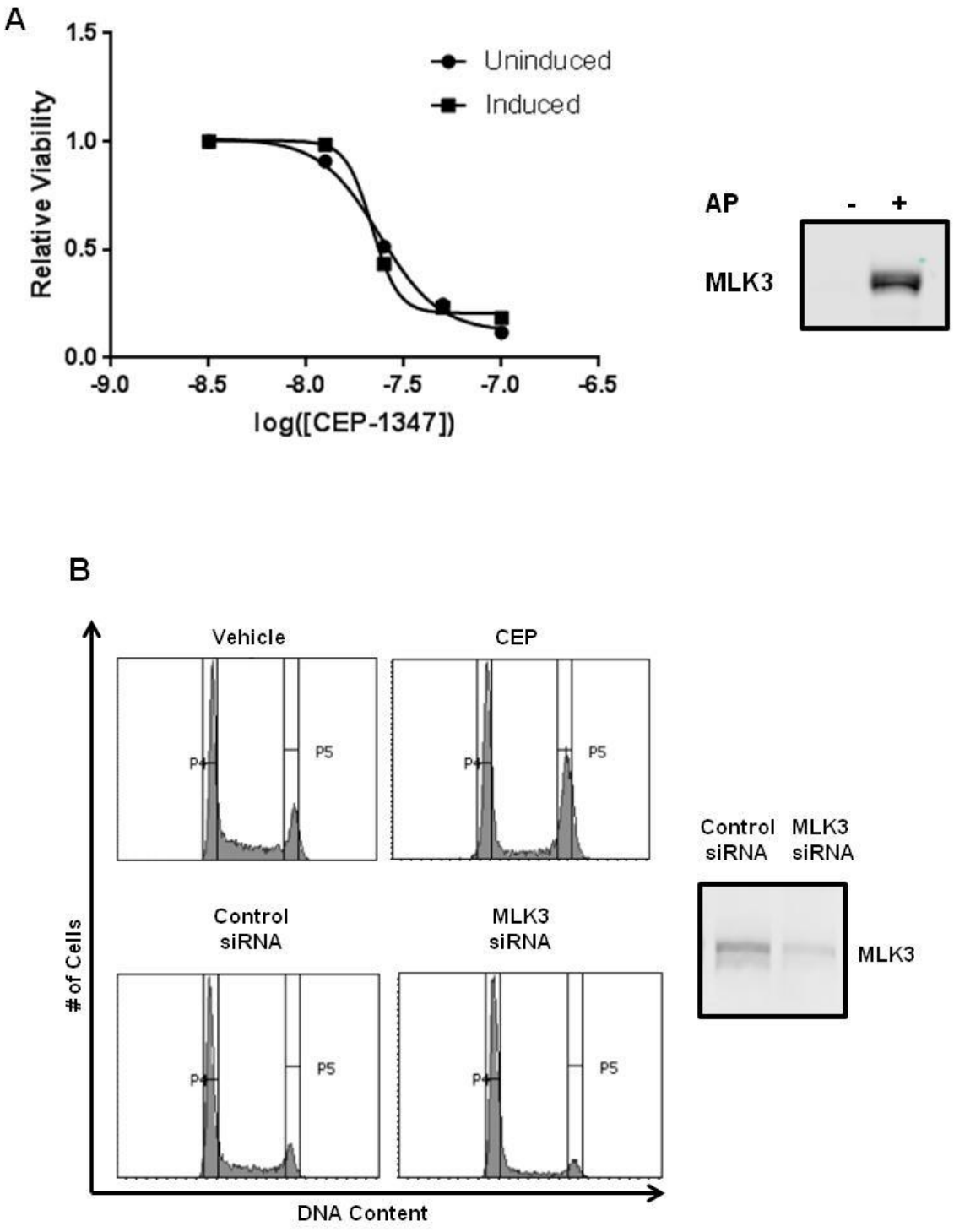

Figure 3-5: Investigating MLK3 as the target of CEP-1347. MCF-7iMLK3 cells were treated with various concentrations of CEP-1347 +/- 50 nM AP21967 to induce MLK3 expression. After 6 days of treatment, viability was assessed using the CCK-8

Figure 3-5 (cont'd)

spectrophotometric assay (A). siRNA against MLK3 was used to knockdown expression. 48 hours after knockdown, cell cycle distribution was analyzed using cells treated with vehicle and 100 nM CEP-1347 as controls (B).

RPPA analysis of CEP-1347 treated cells

To investigate if there are additional targets of CEP-1347 during mitosis, I utilized a reverse phase protein phosphorylation array (RPPA). The RPPA at Baylor College of Medicine includes 216 validated antibodies for total and phospho-proteins, a list of which is available here. While MLK3 is not on this array, multiple MAP2Ks, MAPKs and other signaling proteins are represented. In preparation for this study, I completed a time course in which synchronized MCF-7 cells were treated with CEP-1347 for varying lengths of time and harvested to analyze DNA content at the same late-mitotic time point. The goal of this study was to identify at what phase of the cell cycle treatment with CEP-1347 has the greatest impact on cell cycle distribution and kinase inhibition, leading to accumulation of the greatest number of cells in G2/M (Figure 3-6). Using the data from this experiment, I selected times for the RPPA assay. To determine if CEP-1347 treatment affected expression or phosphorylation of any of these proteins, I synchronized MCF-7 cells in G1, released them with estrogen treatment, then added CEP-1347 or vehicle after 23 hours, just prior to entry into mitosis. Cells were harvested after 2 and 6 hours of treatment, at which point vehicle treated cells were in early and late mitosis, respectively. Consistent with its role as an MLK inhibitor, the majority of proteins whose expression or phosphorylation were altered by CEP-1347 are involved

in MAPK signaling pathways (Figure 3-7). Phospho-JNK, p-c-Jun and total c-Jun all significantly decreased after 2 and 6 hours of treatment. Phospho-ERK1/2 and p-MEK1/2 also decreased by 6 hours of treatment. Phospho-p38 was increased at both time points, which is in agreement with previous reports that inhibiting JNK leads to a compensatory increase in p-p38 [39]. Aurora B is not present on the array, but both phospho- and total Aurora A increased in CEP-1347 treated cultures.

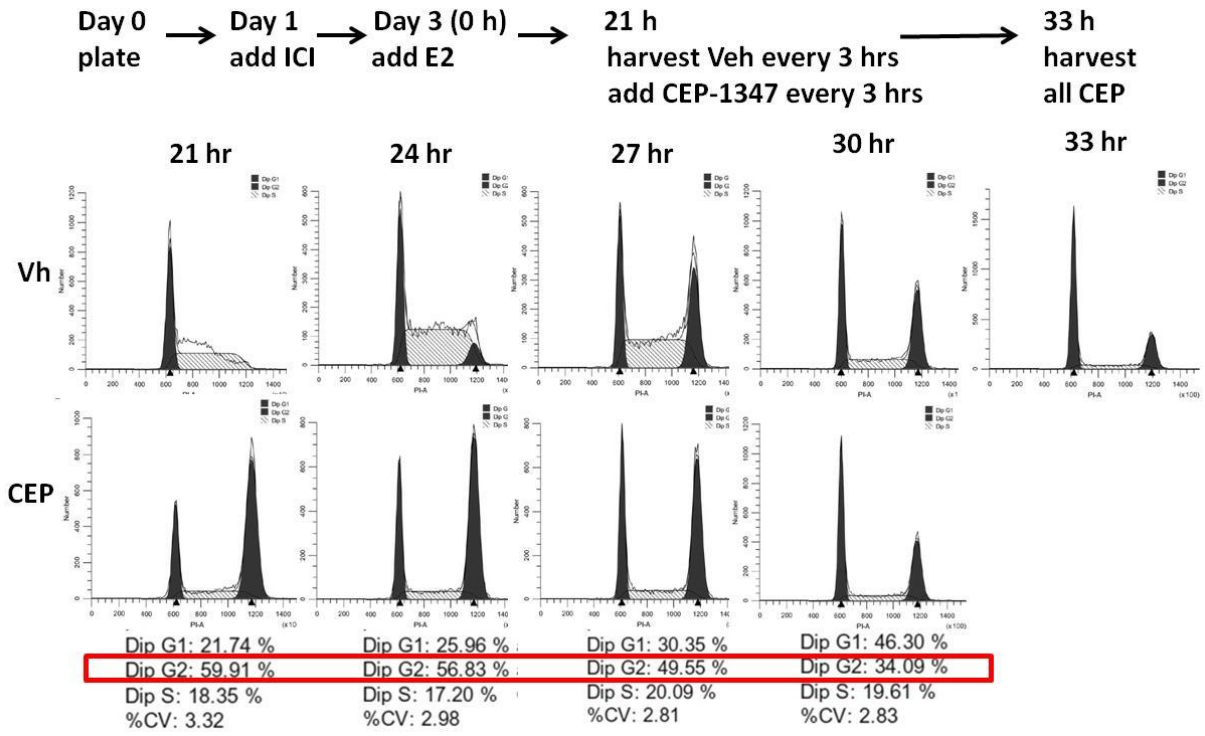

Figure 3-6: Treatment with CEP-1347 at multiple time points leads to G2/M arrest. CEP-1347 was added to synchronized MCF-7 cells every 3 hours from 21 h-30 h and all cells were harvested at 33 h. Accumulation of cells in G2/M was most evident after addition of CEP-1347 at 21 hours.

One of the proteins whose phosphorylation was most inhibited by CEP-1347 treatment at both time points was phospho-AMPK, specifically its phosphorylation at Thr172. Phosphorylation of Akt at Thr308 was also reduced, although to a much less extent, and only at the late time point. Akt phosphorylation of mTOR has been well studied; however, AMPK is also able to activate mTOR independently of Akt. After activation by either Akt or AMPK, mTOR phosphorylates p70s6k, another kinase whose activation was decreased in CEP-1347 treated cultures. Thus, in addition to MAPK pathways, activity of the Akt-AMPK/mTOR/p70s6k pathway is also decreased by CEP-1347. Whether this pathway is dependent or independent of MLK3 remains to be determined. The best characterized upstream activator of AMPK is LKB1 [40], but there are also reports that AMPK can be phosphorylated by MLK3 [41]. In either case, the finding that AMPK phosphorylation is decreased by CEP-1347 provides a novel path for investigation of the mechanism of action of this kinase inhibitor.

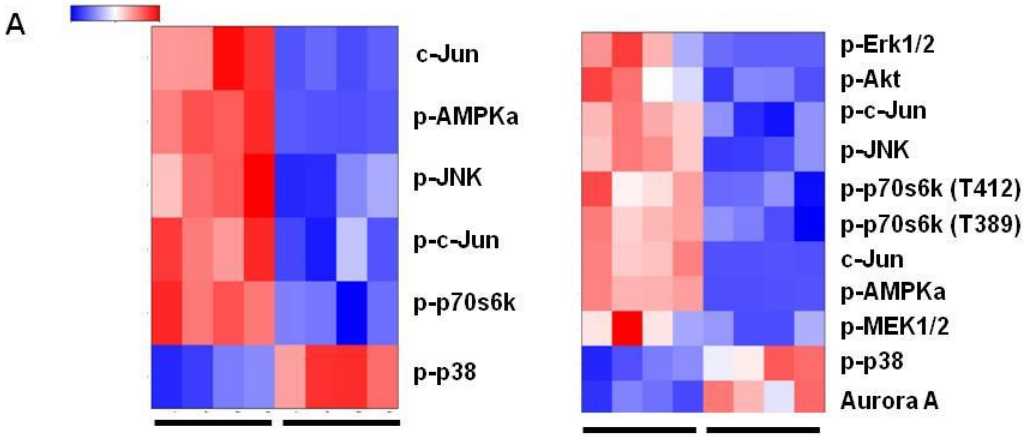

Protein	Fold Change
p-p38	4.377175
p-p70S6K	0.747425
p-SAPK/JNK	0.558644
c-Jun	0.356013
p-c-Jun	0.220676
p-AMPKa	0.190782

Protein	Fold Change
p-p38	2.056228
AuroraA	1.569168
p-p70S6K	0.742262
p-p70S6K	0.732043
p-Akt	0.678302
p-MEK1/2	0.646176
p-SAPK/JNK	0.528509
p-c-Jun	0.279322
p-p44/42MAPK(Erk1/2)	0.267943
p-AMPKa	0.217638
c-Jun	0.08362

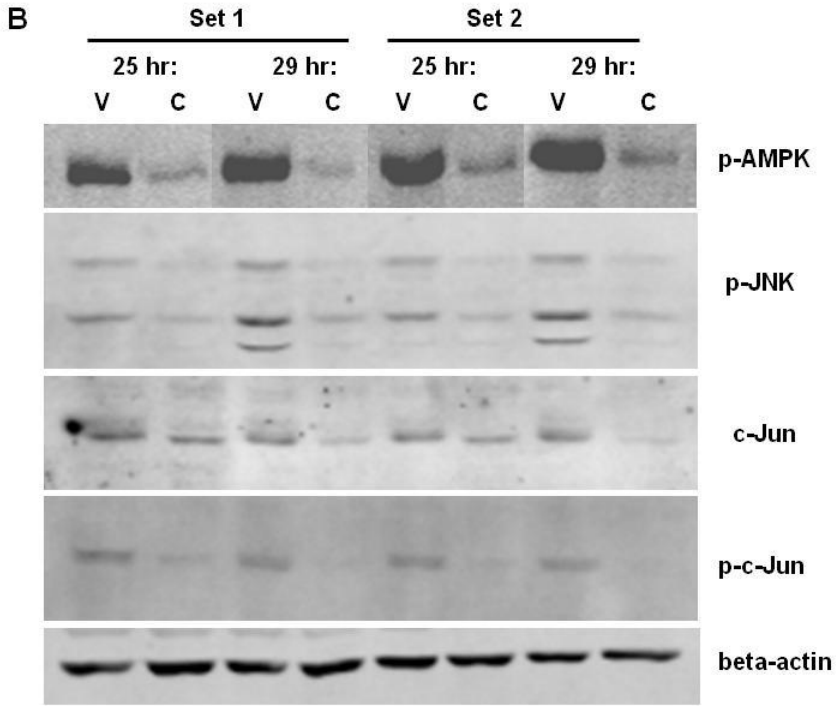

Figure 3-7: RPPA analysis of CEP-1347 treated cells. Synchronized MCF-7 cells were treated with vehicle or 100 nM CEP-1347 for 2 hours (25 hour time point) or 6

Figure 3-7 (cont'd)

hours (29 hour time point) and lysates were harvested for RPPA analysis. Fold change of protein expression is represented in heat maps with red representing increase in expression and blue indicating decrease in expression (A). Western blot confirmation of RPPA results (B).

AMPK as the target of CEP-1347

Because AMPK phosphorylation was among the most inhibited upon treatment with CEP-1347, I hypothesized that AMPK inhibition might be involved in creating the mitotic phenotype seen in CEP-1347 treated cells. To test this possibility, I treated cells with the AMPK inhibitor, Compound C, and analyzed DNA content with flow cytometry. After 24 hours of treatment, AMPK inhibition led to accumulation of cells in G2/M of the cell cycle (Figure 3-8A). This result was consistent in endocrine sensitive (MCF-7) and resistant (LCC9) ER+ breast cancer cell lines, and was very similar to the effect seen in CEP-1347 treated cells.

To determine if the nuclear morphology in Compound C treated cells was similar to that seen upon CEP-1347 treatment, synchronized cells were treated with Compound C, then stained with anti-alpha tubulin antibody to examine microtubule formation, anti-centromere antibody to visualize centromeres, and DAPI to analyze DNA condensation. While vehicle treated cells displayed normal mitoses, nearly 95% of cells treated with Compound C between 27 and 33 hours appeared to be in interphase rather than in mitosis based on microtubule formation and DNA condensation (Figure 3-8B,

Supplemental Figure 3-4). Rarely, cells treated with Compound C displayed condensed DNA consistent with prophase. In these cells, microtubule staining was more intense around the periphery of the cell rather than throughout the whole cell, producing a phenotype that was drastically different than that seen with treatment with CEP-1347. Together, this suggests that CEP-1347 mediated inhibition of AMPK is not the cause of the abnormal nuclear phenotype that I have described.

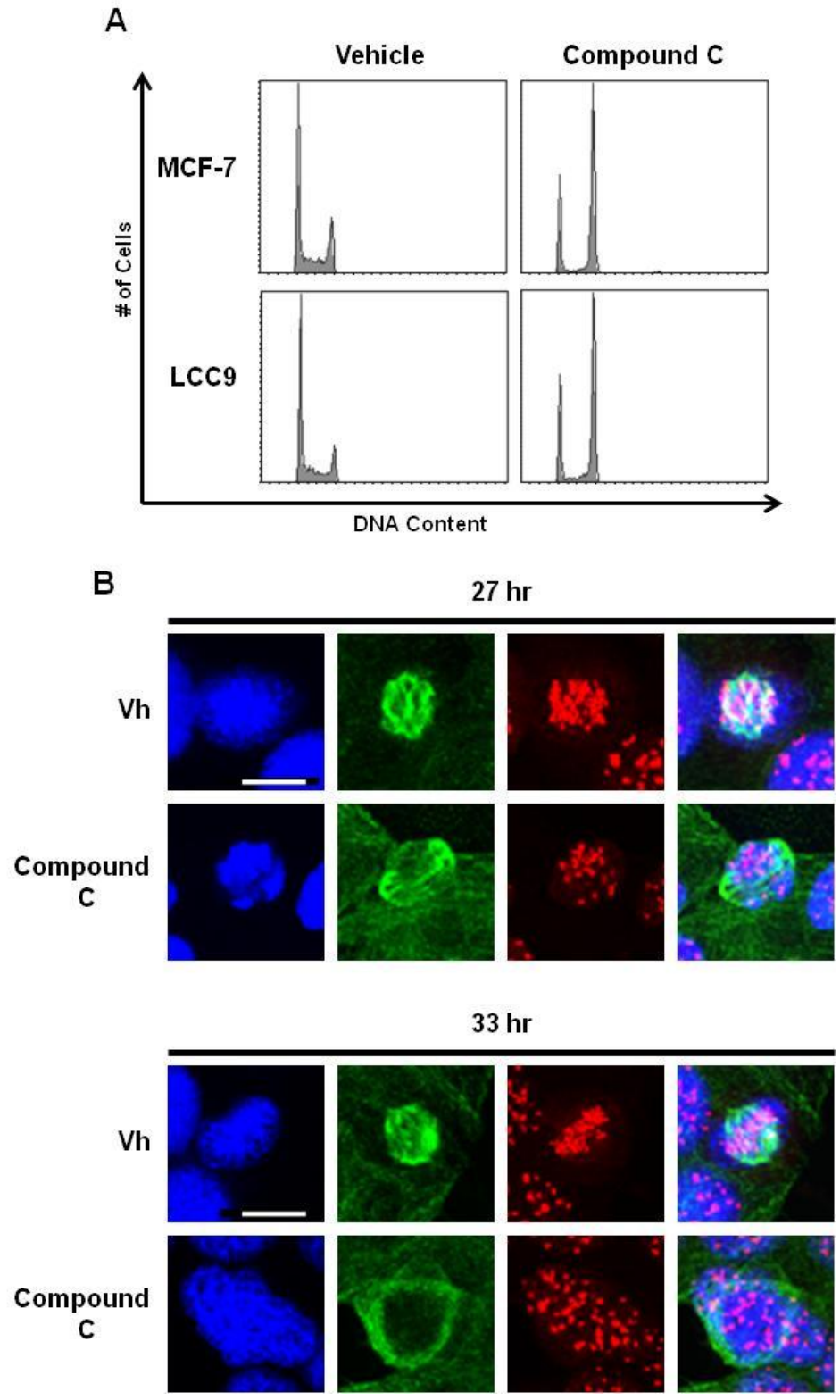

Figure 3-8: Effects of treatment with Compound C. Cycling populations of MCF-7 cells were treated with vehicle or 20 μM Compound C and cell cycle distribution was

Figure 3-8 (cont'd)

analyzed with flow cytometry (A). Synchronized MCF-7 cells were treated with vehicle or 20 μM Compound C and followed through the cell cycle. DNA condensation (DAPI, blue) and mitotic spindle formation (alpha-tubulin, green), and centromeres (anti-centromere antibody, red) were analyzed at all mitotic time points. Scale bar represents 10 μm.

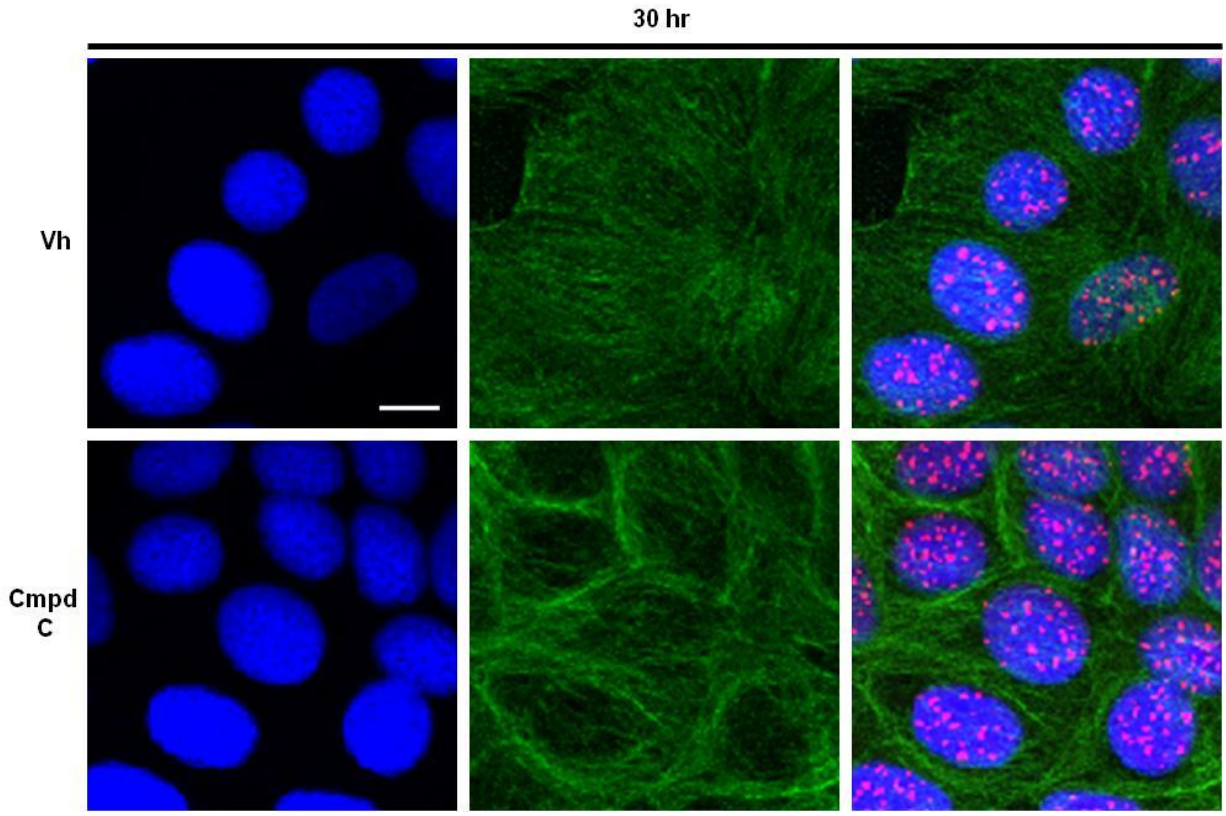

Supplemental Figure 3-4: Interphase cell population after treatment with Compound C. Synchronized MCF-7 cells were treated with vehicle or 20 μM Compound C and followed through the cell cycle. DNA condensation (DAPI, blue) and mitotic spindle formation (alpha-tubulin, green), and centromeres (anti-centromere antibody, red) were analyzed at all mitotic time points. Interphase cells at all time points

Supplemental Figure 3-4 (cont'd)

display altered alpha-tubulin distribution after treatment with Compound C. Scale bar represents 10 μm.

Discussion

The presence of dysregulated kinase expression and activity in many cancers has led to the development and characterization of kinase inhibitors as cancer therapeutics. Kinase inhibitors provide a therapeutic advantage by targeting a specific substrate and minimizing off-target effects that lead to deleterious side effect profiles. They also allow for a more personalized approach to cancer treatment based on the protein expression and pathway activation profiles of individual tumors. CEP-1347 and CEP-11004 are kinase inhibitors best known for their ability to inhibit MLKs, specifically MLK3. Their effects are selective for tumorigenic cell lines, and investigation into their mechanism of action demonstrated that treatment with CEP-11004 leads to an early mitotic arrest, chromosome misalignment along the metaphase plate, and disrupted mitotic spindle formation. In this study, I examined the mechanism of action of CEP-1347 and attempted to identify the kinase or kinases responsible for its mitotic phenotype.

As previously reported, CEP-1347 induces a mitotic arrest [21, 22, 33]. To further characterize this arrest, I analyzed the cellular and nuclear configurations of centrosomes, centromeres, microtubules, and DNA after treatment with CEP-1347 at different phases of the cell cycle. Interestingly, it appeared that the mitotic arrest arose from the inability of centrosomes to generate a bipolar spindle. Rather, cells treated with

CEP-1347 exhibited duplicated centrosomes that were centrally located and surrounded by condensed DNA and irregularly formed mitotic spindles. In cases where centrosomes were able to segregate, mitotic spindles appeared irregular, and metaphase DNA alignment frequently exhibited lagging chromosomes. Both of these configurations would lead to a lack of tension at one or more pairs of sister chromatids, and would activate the SAC.

To identify the mitotic target of CEP-1347, I first interrogated the role of MLK3. Overexpression of MLK3 did not alter IC_{50} to CEP-1347 in a viability assay. While MLK3 expression was dramatically induced in the majority of cells, it was not present in 100% of cells. Because of this, the effect of overexpression on viability, if present, may have been somewhat muted and this may have impacted the sensitivity of this assay to detect changes between induced and uninduced conditions. To directly test whether MLK3 is required for mitotic progression, the effects of knockdown on cell cycle were examined. Although expression was reduced by 85%, cell cycle distribution was unaltered. There are several possible explanations for this result. The remaining 15% of MLK3 expression may have provided sufficient enzyme activity to prevent arrest, or other MLKs may be have been present and were able to compensate for the loss of MLK3. Finally, the activity of mitotic kinases other than MLKs might be inhibited by CEP-1347 and their inhibition may be responsible for the phenotypes observed.

To identify proteins whose expression or phosphorylation are inhibited by CEP-1347 during mitosis, I utilized an RPPA. This analysis expectedly revealed that multiple

kinases in the MAPK cascade were inhibited upon treatment with CEP-1347. Interestingly, RPPA analysis revealed that CEP-1347 was also able to inhibit activation of the Akt-AMPK/mTOR/p70s6k pathway. AMPK is primarily known for its role in energy homeostasis and metabolism [40, 42]. It is canonically activated by liver kinase B1 (LKB1), or calmodulin-dependent kinase kinase beta (CaMKKβ) in instances of high intracellular calcium [40]. AMPK activation downstream of MLK3 has been described [41], as well as AMPK signaling downstream to JNK [43-45]. Furthermore, AMPK activation is induced during mitosis and it has been described to play a role in mitotic spindle orientation and cellular polarity [46-49].

To determine the role of this pathway in creating the phenotype observed by treatment with CEP-1347, I utilized an AMPK inhibitor, Compound C, and analyzed cell cycle progression and cellular and nuclear morphology. While treatment with Compound C caused an accumulation of cells in G2/M, similar to that seen after treatment with CEP-1347, analysis of centromeres, microtubules, and DNA revealed that Compound C induced cell cycle arrest is more likely in G2 rather than in mitosis, as the vast majority of cells appeared to be in interphase. A minority of cells exhibited condensing DNA with an accumulation of microtubules surrounding the periphery of the cell. The morphology of these cells is very similar to that which was observed upon MLK3 overexpression [33], perhaps suggesting another link to MLK3 involvement. While Compound C is the most commonly used inhibitor for AMPK activity, it is not completely specific and has some activity against multiple other kinases [50]. Thus, it is possible that the G2 arrest and nuclear phenotype observed after treatment with Compound C in this experimental

setting resulted from inhibition of another target. Together, these data suggest that perhaps AMPK is not the target of CEP-1347 that leads to the phenotype observed, and further study of MLK3 and AMPK, as well as investigation into other kinase targets should be completed.

Pharmacological inhibition of MLK3 using a known MLK3 inhibitor may be useful in elucidating the cell cycle effects of MLK3 inhibition, and evaluating expression of alternate MLKs in these cell models may facilitate identification of other kinases that may compensate for MLK3 activity. While overexpression of MLK3 has no effect on sensitivity to CEP-1347, the effect of MLK3 knockdown on drug sensitivity has not been studied. To further examine the role of AMPK in CEP-1347 mediated cell cycle arrest, a more specific method using RNA interference rather than pharmacological inhibition of activity may be prudent. Assessment of the effect of reduced expression of AMPK on sensitivity to CEP-1347 may provide useful insight on the role of this kinase in the mechanism of CEP-1347 action. Finally, it would be informative to further investigate the function of alternate mitotic kinases, including Aurora A, Aurora B, and PLK1.

Materials and Methods

Cell culture and reagents

MCF-7 and MCF-7/LCC9 cells were provided by Dr. Robert Clarke (Lombardi Comprehensive Cancer Center, Georgetown University), and MCF-7iMLK3 cells were provided by Dr. Kathy Gallo (Michigan State University). All cells were cultured in improved modified Eagle's medium (Invitrogen) supplemented with 5% fetal bovine

serum (Hyclone), 100 units/mL penicillin, and 100 units/mL streptomycin and cultured at 37 °C with 5% CO_2. Drug treatments included vehicle (DMSO), 10 nM ICI 182,780 in ethanol (Selleckchem), 10 nM 17β-estradiol in ethanol (Sigma), 100 nM CEP-1347 in DMSO (donated by Teva Pharmaceuticals), 20 μM Compound C in DMSO (Sigma).

Flow cytometry

For cell cycle assays 10^6 cells were plated per 10 cm dish. After designated treatment, cells were trypsinized, fixed in 70% ethanol overnight at -20 °C, and washed two times with 5% FBS/95% PBS, then resuspended in PBS containing 50 μg/mL propidium iodide and 50 μg/mL RNaseA for 15 minutes at 37 °C. Cells were analyzed using a FACS Vantage flow cytometer and data were analyzed using ModFit software. 10,000 events were analyzed for each sample.

Cell viability assay

1000 MLK3-inducible MCF-7 cells were plated in 96 well plates. After 24 hours, vehicle or CEP-1347 was added concurrent with 50 nM AP21967 to induce MLK3 expression. Cells were treated for 6 days with fresh media added on day 3. On day 6, 10 μL of CCK-8 reagent (Dojindo) was added and optical density at 490 nm was read on a plate spectrophotometer.

siRNA knockdown of MLK3

MLK3 siRNA (Invitrogen) and control siRNA (Dharmacon) were provided by Kathy Gallo. Cells were transfected with 10 nM siRNA for 48 hours and harvested as described for analysis of DNA content by flow cytometry.

Reverse Phase Protein Array

$5x10^6$ cells were plated in 10 cm dishes and synchronized in G1 with 48 hours of treatment with ICI 182,780, which was washed out followed by addition of 10 nM 17-β-estradiol to release the cells from G1 arrest and allow synchronous progression through the cell cycle. The addition of 17-β-estradiol marked the 0 hour time point. Vehicle or CEP-1347 was added at 23 hours and protein lysates were harvested at 25 or 29 hours per the Baylor College of Medicine RPPA Core protocols. Treatments were completed and analyzed in quadruplicate.

Immunofluorescence

$5x10^4$ MCF-7 cells were plated on coverslips in 6-well dishes. After 24 hours they were treated with 10 nM ICI 182,780 to synchronize them in G1. After 48 hours, ICI 182,780 was washed out and 10 nM 17-β-estradiol was added to release the cells from G1 arrest and allow synchronous progression through the cell cycle. This was considered the zero hour timepoint. At 12 hours post release, drug treatments were added, and cells were harvested at designated timepoints. After harvest, coverslips were washed in PBS and fixed in 100% methanol at -20 °C for at least 30 minutes to fix, washed in PBS, blocked and permeabilized in 2% bovine serum albumin (BSA) plus 0.5% triton-X in

PBS for 1 hour, and incubated with primary antibody overnight at 4 °C. Coverslips were incubated with secondary antibody for 1 hour at room temperature, counterstained with 1 μg/mL DAPI for 15 minutes, mounted on slides with Fluoromount-G (Thermo Fisher). Images were obtained using a FluoView 1000 Confocal Microscope. Antibodies included 1:1000 alpha-tubulin (T9026, Sigma), 1:2000 gamma-tubulin (T6557, Sigma), 1:10 anti-centromere antibody (15-234, Antibodies Incorporated), DAPI (D9564, Sigma) and 1:200 secondary antibody (Invitrogen)

Western blotting

Cells were washed in PBS and lysed in CellLytic M lysis buffer (Sigma), supplemented with protease inhibitors (Complete Mini EDTA-free, Roche) and phosphatase inhibitors (PhosSTOP, Roche). Bradford assays (BioRad) were used to determine protein concentration. 20 μg of protein lysate was resolved on 10% SDS-polyacrylamide gels, transferred to PVDF membranes, and probed with primary antibody overnight at 4 °C and secondary antibody for 1 hour at room temperature. Fluorescence was analyzed using a Li-COR Odyssey (Li-COR Biosciences). Antibodies included 1:1000 p-AMPK (2535S, Cell Signaling), 1:1000 p-JNK (4668S, Cell Signaling), 1:1000 c-Jun (sc-1694, Santa Cruz), 1:1000 p-c-Jun (sc-822, Santa Cruz), p-histone H3 (9701L, Cell Signaling), 1:1000 beta-actin (A4700, Sigma), 1:1000 MLK3 (ab51068, Abcam), and 1:10,000 secondary antibody (Invitrogen).

REFERENCES

REFERENCES

1. Ferguson, F.M. and N.S. Gray, *Kinase inhibitors: the road ahead.* Nat Rev Drug Discov, 2018. **17**(5): p. 353-377.

2. Muller, S., et al., *The ins and outs of selective kinase inhibitor development.* Nat Chem Biol, 2015. **11**(11): p. 818-21.

3. Levitzki, A., *Protein kinase inhibitors as a therapeutic modality.* Acc Chem Res, 2003. **36**(6): p. 462-9.

4. Polk, A., et al., *Specific CDK4/6 inhibition in breast cancer: a systematic review of current clinical evidence.* ESMO Open, 2016. **1**(6): p. e000093.

5. Martin, M., et al., *Neratinib after trastuzumab-based adjuvant therapy in HER2-positive breast cancer (ExteNET): 5-year analysis of a randomised, double-blind, placebo-controlled, phase 3 trial.* Lancet Oncol, 2017. **18**(12): p. 1688-1700.

6. Gianni, L., et al., *Efficacy and safety of neoadjuvant pertuzumab and trastuzumab in women with locally advanced, inflammatory, or early HER2-positive breast cancer (NeoSphere): a randomised multicentre, open-label, phase 2 trial.* Lancet Oncol, 2012. **13**(1): p. 25-32.

7. Saporito, M.S., R.L. Hudkins, and A.C. Maroney, *Discovery of CEP-1347/KT-7515, an inhibitor of the JNK/SAPK pathway for the treatment of neurodegenerative diseases.* Prog Med Chem, 2002. **40**: p. 23-62.

8. Rattanasinchai, C. and K.A. Gallo, *MLK3 Signaling in Cancer Invasion.* Cancers (Basel), 2016. **8**(5).

9. Chen, J., E.M. Miller, and K.A. Gallo, *MLK3 is critical for breast cancer cell migration and promotes a malignant phenotype in mammary epithelial cells.* Oncogene, 2010. **29**(31): p. 4399-411.

10. Chen, J. and K.A. Gallo, *MLK3 regulates paxillin phosphorylation in chemokine-mediated breast cancer cell migration and invasion to drive metastasis.* Cancer Res, 2012. **72**(16): p. 4130-40.

11. Waldmeier, P., et al., *Recent clinical failures in Parkinson's disease with apoptosis inhibitors underline the need for a paradigm shift in drug discovery for neurodegenerative diseases.* Biochem Pharmacol, 2006. **72**(10): p. 1197-206.

12. Boll, J.B., et al., *Improvement of embryonic dopaminergic neurone survival in culture and after grafting into the striatum of hemiparkinsonian rats by CEP-1347.* J Neurochem, 2004. **88**(3): p. 698-707.

13. *Mixed lineage kinase inhibitor CEP-1347 fails to delay disability in early Parkinson disease.* Neurology, 2007. **69**(15): p. 1480-90.

14. Apostol, B.L., et al., *CEP-1347 reduces mutant huntingtin-associated neurotoxicity and restores BDNF levels in R6/2 mice.* Mol Cell Neurosci, 2008. **39**(1): p. 8-20.

15. Conforti, P., et al., *Blood level of brain-derived neurotrophic factor mRNA is progressively reduced in rodent models of Huntington's disease: restoration by the neuroprotective compound CEP-1347.* Mol Cell Neurosci, 2008. **39**(1): p. 1-7.

16. Pirvola, U., et al., *Rescue of hearing, auditory hair cells, and neurons by CEP-1347/KT7515, an inhibitor of c-Jun N-terminal kinase activation.* J Neurosci, 2000. **20**(1): p. 43-50.

17. Falsig, J., et al., *Specific modulation of astrocyte inflammation by inhibition of mixed lineage kinases with CEP-1347.* J Immunol, 2004. **173**(4): p. 2762-70.

18. Lund, S., et al., *Inhibition of microglial inflammation by the MLK inhibitor CEP-1347.* J Neurochem, 2005. **92**(6): p. 1439-51.

19. Wagner, A.C., et al., *CEP-1347 inhibits caerulein-induced rat pancreatic JNK activation and ameliorates caerulein pancreatitis.* Am J Physiol Gastrointest Liver Physiol, 2000. **278**(1): p. G165-72.

20. Okada, M., et al., *Repositioning CEP-1347, a chemical agent originally developed for the treatment of Parkinson's disease, as an anti-cancer stem cell drug.* Oncotarget, 2017. **8**(55): p. 94872-94882.

21. Wang, L., K.A. Gallo, and S.E. Conrad, *Targeting mixed lineage kinases in ER-positive breast cancer cells leads to G2/M cell cycle arrest and apoptosis.* Oncotarget, 2013. **4**(8): p. 1158-71.

22. Cha, H., et al., *Inhibition of mixed-lineage kinase (MLK) activity during G2-phase disrupts microtubule formation and mitotic progression in HeLa cells.* Cell Signal, 2006. **18**(1): p. 93-104.

23. Wang, L.H., A.J. Paden, and E.M. Johnson, Jr., *Mixed-lineage kinase inhibitors require the activation of Trk receptors to maintain long-term neuronal trophism and survival.* J Pharmacol Exp Ther, 2005. **312**(3): p. 1007-19.

24. Goodfellow, V.S., et al., *Discovery, Synthesis, and Characterization of an Orally Bioavailable, Brain Penetrant Inhibitor of Mixed Lineage Kinase 3.* J Med Chem, 2013.

25. Agircan, F.G., E. Schiebel, and B.R. Mardin, *Separate to operate: control of centrosome positioning and separation.* Philos Trans R Soc Lond B Biol Sci, 2014. **369**(1650).

26. Fu, J., et al., *Roles of Aurora kinases in mitosis and tumorigenesis.* Mol Cancer Res, 2007. **5**(1): p. 1-10.

27. Kumar, S., et al., *Regulatory functional territory of PLK-1 and their substrates beyond mitosis.* Oncotarget, 2017. **8**(23): p. 37942-37962.

28. Lee, S.Y., C. Jang, and K.A. Lee, *Polo-like kinases (plks), a key regulator of cell cycle and new potential target for cancer therapy.* Dev Reprod, 2014. **18**(1): p. 65-71.

29. Harrington, E.A., et al., *VX-680, a potent and selective small-molecule inhibitor of the Aurora kinases, suppresses tumor growth in vivo.* Nat Med, 2004. **10**(3): p. 262-7.

30. Wang, G., Q. Jiang, and C. Zhang, *The role of mitotic kinases in coupling the centrosome cycle with the assembly of the mitotic spindle.* J Cell Sci, 2014. **127**(Pt 19): p. 4111-22.

31. Wilkinson, R.W., et al., *AZD1152, a selective inhibitor of Aurora B kinase, inhibits human tumor xenograft growth by inducing apoptosis.* Clin Cancer Res, 2007. **13**(12): p. 3682-8.

32. Zhou, N., et al., *The investigational Aurora kinase A inhibitor MLN8237 induces defects in cell viability and cell-cycle progression in malignant bladder cancer cells in vitro and in vivo.* Clin Cancer Res, 2013. **19**(7): p. 1717-28.

33. Swenson, K.I., K.E. Winkler, and A.R. Means, *A new identity for MLK3 as an NIMA-related, cell cycle-regulated kinase that is localized near centrosomes and influences microtubule organization.* Mol Biol Cell, 2003. **14**(1): p. 156-72.

34. O'Connell, M.J., M.J. Krien, and T. Hunter, *Never say never. The NIMA-related protein kinases in mitotic control.* Trends Cell Biol, 2003. **13**(5): p. 221-8.

35. Marker, D.F., et al., *The new small-molecule mixed-lineage kinase 3 inhibitor URMC-099 is neuroprotective and anti-inflammatory in models of human immunodeficiency virus-associated neurocognitive disorders.* J Neurosci, 2013. **33**(24): p. 9998-10010.

36. Goto, H., et al., *Aurora-B phosphorylates Histone H3 at serine28 with regard to the mitotic chromosome condensation.* Genes Cells, 2002. **7**(1): p. 11-7.

37. Tsuda, Y., et al., *Mitotic slippage and the subsequent cell fates after inhibition of Aurora B during tubulin-binding agent-induced mitotic arrest.* Sci Rep, 2017. **7**(1): p. 16762.

38. Zhang, H., et al., *Hsp90/p50cdc37 is required for mixed-lineage kinase (MLK) 3 signaling.* J Biol Chem, 2004. **279**(19): p. 19457-63.

39. Wagner, E.F. and A.R. Nebreda, *Signal integration by JNK and p38 MAPK pathways in cancer development.* Nat Rev Cancer, 2009. **9**(8): p. 537-49.

40. Hardie, D.G. and D.R. Alessi, *LKB1 and AMPK and the cancer-metabolism link - ten years after.* BMC Biol, 2013. **11**: p. 36.

41. Luo, L., et al., *MLK3 phophorylates AMPK independently of LKB1.* PLoS ONE, 2015. **10**(4): p. e0123927.

42. Faubert, B., et al., *The AMP-activated protein kinase (AMPK) and cancer: many faces of a metabolic regulator.* Cancer Lett, 2015. **356**(2 Pt A): p. 165-70.

43. Guan, F.Y., et al., *Compound K protects pancreatic islet cells against apoptosis through inhibition of the AMPK/JNK pathway in type 2 diabetic mice and in MIN6 beta-cells.* Life Sci, 2014. **107**(1-2): p. 42-9.

44. Kang, S., et al., *The ginsenoside 20-O-beta-D-glucopyranosyl-20(S)-protopanaxadiol induces autophagy and apoptosis in human melanoma via AMPK/JNK phosphorylation.* PLoS ONE, 2014. **9**(8): p. e104305.

45. Lee, Y.M., et al., *AM251 suppresses the viability of HepG2 cells through the AMPK (AMP-activated protein kinase)-JNK (c-Jun N-terminal kinase)-ATF3 (activating transcription factor 3) pathway.* Biochem Biophys Res Commun, 2008. **370**(4): p. 641-5.

46. Koh, H. and J. Chung, *AMPK links energy status to cell structure and mitosis.* Biochem Biophys Res Commun, 2007. **362**(4): p. 789-92.

47. Thaiparambil, J.T., C.M. Eggers, and A.I. Marcus, *AMPK regulates mitotic spindle orientation through phosphorylation of myosin regulatory light chain.* Mol Cell Biol, 2012. **32**(16): p. 3203-17.

48. Vazquez-Martin, A., et al., *Polo-like kinase 1 regulates activation of AMP-activated protein kinase (AMPK) at the mitotic apparatus.* Cell Cycle, 2011. **10**(8): p. 1295-302.

49. Vazquez-Martin, A., C. Oliveras-Ferraros, and J.A. Menendez, *The active form of the metabolic sensor: AMP-activated protein kinase (AMPK) directly binds the mitotic apparatus and travels from centrosomes to the spindle midzone during mitosis and cytokinesis.* Cell Cycle, 2009. **8**(15): p. 2385-98.

50. Bain, J., et al., *The selectivity of protein kinase inhibitors: a further update.* Biochem J, 2007. **408**(3): p. 297-315.

Chapter 4: Conclusions and Future Directions

Resistance of ER+ breast cancers to clinically available therapeutics is a continuing problem that prevents adequate treatment of patient disease. Thus, there is a need to investigate novel compounds for use in patients who exhibit resistance to endocrine therapies, as well as identify therapies that prevent or slow the development of drug resistance. I investigated the efficacy of CEP-1347 in preventing the proliferation of endocrine sensitive and resistant ER+ breast cancer cells in culture and in pre-clinical animal models. I also further interrogated the kinase or kinases through which CEP-1347 induced its effects on ER+ breast cancers.

Efficacy of CEP-1347 as a breast cancer therapeutic

When used alone in culture, CEP-1347 led to an early mitotic arrest with the accumulation of a polyploid cell population. It also created disordered mitotic spindle formations and inhibited centrosome separation. Exposure to this compound led to a reduction in viability in both endocrine sensitive and resistant ER+ breast cancer cell lines. Additionally, treatment with CEP-1347 induced significant apoptosis in endocrine sensitive MCF-7 cells, and a more moderate induction of apoptosis in endocrine resistant LCC9 cells. When combined with the clinically used SERD, ICI 192,780, in culture, MCF-7 cells exhibited fewer cells with polyploidy, while the cell cycle phenotype in LCC9 remained unchanged. Furthermore, the combination treatment reduced the apoptotic population in MCF-7 cells while in contrast, the apoptotic population was significantly enhanced in LCC9 cells.

These *in vitro* results were largely reproduced when CEP-1347 was further studied *in vivo*. In xenograft models of ER+ breast cancer tumorigenesis, CEP-1347 alone significantly reduced proliferation in endocrine sensitive cells and slowed proliferation in endocrine resistant cells. This compound alone did not significantly reduce proliferation in endocrine sensitive or resistant tumors or exhibit any effect on apoptosis in endocrine resistant cells. However, it was able to drastically increase apoptosis in short term and long term studies of endocrine sensitive breast cancer. When combined with ICI 182,780, the effects of CEP-1347 *in vivo* were enhanced. This combination therapy effectively inhibited proliferation of both endocrine sensitive and resistant cells. However, this result was achieved by distinct mechanisms in each of the models used. Combination treatment primarily reduced proliferation of MCF-7 cells, while this effect was attained by both decreased proliferation and a considerable induction in apoptosis in LCC9 cells.

Perhaps the most interesting result from this work is the inhibition of regrowth of endocrine sensitive MCF-7 cells *in vivo* after cessation of treatment, suggesting that the development of resistant subpopulations of cancer cells, especially in endocrine naïve patients, may be slowed or inhibited by co-treatment. This is further supported by the results in culture after long term treatment. In both cell lines, resistant colonies formed after treatment with CEP-1347 alone, but this number was drastically reduced with the addition of ICI 182,780. While the combination was not significantly better at preventing the development of resistant colonies compared to ICI 182,780 alone in MCF-7 cells, it was impressive in LCC9 cells at reducing the number of colonies compared to either

drug alone. To more completely evaluate the development of resistance after treatment with CEP-1347 alone or in combination with ICI 182,780, it would be necessary to complete animal studies with treatment of animals followed by cessation of drug administration, and subsequent re-exposure to therapy. Data from these studies would more directly provide an answer for the question of development of drug resistance especially to the combination of CEP-1347 and ICI 182,780.

To expand this work into a more clinically relevant model, we utilized three PDX lines to test the efficacy of CEP-1347 in culture. The data from these experiments revealed that CEP-1347 continued to produce an accumulation of cells in G2/M, although the concentration required to do this was higher than that required in cell culture for two of the three PDX lines tested. Subsequent studies would further examine the phenotype of these lines after CEP-1347 treatment in culture to examine DNA condensation, mitotic spindle formation, and centrosome duplication and separation, and CEP-1347 would need to be tested against these lines *in vivo* to determine its efficacy in preventing PDX tumor growth. If these data are promising, they would further substantiate the need to continue to develop this compound as a therapeutic against ER+ breast cancer.

Finally, as briefly described in Chapter 2, lung and lymph node metastases were observed in animals with LCC9 tumors. While metastasis of ER+ breast cancer is a major clinical issue that is the major cause of patient death, ER+ models of metastasis are rare. Further exploration of the metastatic capacity of LCC9 cells would be valuable in establishing a model for ER+ metastasis in an *in vivo* system. The effects of CEP-

1347 on inhibiting this metastatic potential would additionally be an interesting and important course of study.

Determination of kinase target(s) of CEP-1347

CEP-1347 is believed to inhibit MLK3, and the majority of research on this compound has been in evaluating its effects on the MAPK pathway. I also interrogated this pathway and found that CEP-1347 leads to inhibition of JNK phosphorylation and also its downstream target, c-Jun. Upon studying the role of MLK3 in the CEP-1347 mechanism of action, I found that RNA interference to knockdown MLK3 expression did not alter cell cycle distribution, and overexpression of MLK3 had no effect on IC_{50}. With these findings, I explored the possibility that MLK3 was not the primary kinase inhibited by CEP-1347 treatment.

Further study of CEP-1347 revealed that in our models, additional kinase targets of this drug exist. The primary pathway outside of the MAPK cascade that is inhibited upon treatment with CEP-1347 is the Akt-AMPK/mTOR/p70s6k signaling pathway. Among the proteins in this pathway, phosphorylation of AMPK was the most inhibited after exposure to CEP-1347 and was thus selected to further investigate. I found that pharmaceutical inhibition of AMPK led to an accumulation of cells in G2/M, similar to the phenotype seen upon treatment with CEP-1347. However, after examining cellular and nuclear morphology of synchronized cells after AMPK inhibition, I found that the vast majority of cells to be in interphase and concluded that the cell cycle arrest caused by AMPK inhibition was in G2, unlike the mitotic arrest caused by CEP-1347 treatment.

Further work is needed to more completely elucidate the mechanism of CEP-1347 action and determine the targets whose inhibition lead to the observed phenotype. The few experiments looking at MLK3 knockdown and overexpression should be expanded. Alternate inhibitors of MLK3, such as URMC-099, could be utilized to compare the phenotype resulting from independent MLK3 inhibition to that which is achieved after CEP-1347 treatment. Furthermore, the cellular and nuclear morphology of cells treated with URMC-099 and after knockdown or MLK3 should be analyzed. Additionally, the expression and activity of all members of the MLK family should be examined. We previously explored the relative levels of mRNA expression of MLKs 1, 3, 4, LZK, and DLK in ER+ tumorigenic and non-tumorigenic breast cell lines and found that MLK3 and DLK are the only two of these five MLKs that were more highly expressed in tumorigenic cell lines. Thus, it may be warranted to study the role of DLK the context of CEP-1347 action.

Multiple kinases are involved in regulating progression into and throughout mitosis. Aurora kinases A and B play roles in centrosome duplication and separation and microtubule attachment to kinetochores at centromeres, respectively. While the phenotypes we observe upon treatment with CEP-1347 make it less likely that these two kinases are major targets of this compound, it may be prudent to further evaluate their role in CEP-1347 mediated cell cycle arrest. Additionally, polo-like kinase 1 (PLK1) is involved in multiple stages of mitotic progression. I was unable to determine the effect of CEP-1347 on modulating expression and phosphorylation of this kinase in our high-

throughput screen, but its prominent role in mitosis makes it another protein that would be desirable to further examine.

Finally, the studies completed to examine the effect of AMPK inhibition utilized pharmacologic inhibition with Compound C, a drug that is described as an AMPK inhibitor. However, a number of studies have found that this compound is not specific for AMPK and may inhibit other kinases to cause the G2 arrest observed. Rather, RNA interference mediated knockdown of AMPK should be utilized to more specifically examine the role of AMPK in cell cycle progression and cellular and nuclear phenotypes, as well as cell cycle distribution.

Final remarks

Targeting of the MLK signaling cascade to inhibit ER+ breast cancer growth has not been widely studied and this work necessitates continued investigation of the role of this pathway in ER+ tumorigenesis. Its previous validation in Phase I studies for Parkinson's Disease established the safety and tolerability of CEP-1347 in humans. Thus, clinical exploration of this compound for breast cancer could readily progress into Phase II/III trials to optimize dosing and determine efficacy in human patients. CEP-1347, especially in combination with ICI 182,780, shows promise as a novel therapy for patients with endocrine sensitive or endocrine resistant ER+ breast cancer.

APPENDIX

Appendix: Optimization of *In Vivo* Drug Dosing

CEP-1347 was provided by Teva Pharmaceuticals, along with formulation and pharmacokinetic data suggesting that plasma levels of 100-1000 ng/mL (~160-1600 nM) of CEP-1347 were achievable up to 12 hours after administration using 10 mg/kg in a 50% softigen/50% MYR-J formulation with oral dosing. Based on *in vitro* data, IC_{50} for viability of MCF-7 cells were determined to be approximately 17 nM, and 100 nM was the minimum concentration of drug that elicited a maximal response [1]. Initial treatment conditions for ICI 182,780 were determined based on the published literature [2].

A pilot study was conducted in mice containing MCF-7 tumors with 4 treatment groups: vehicle, ICI 182,780 alone, CEP-1347 alone, and the combination of CEP-1347 and ICI 182,780. CEP-1347 was administered by oral gavage (p.o.) daily at 10 mg/kg in a Softigen:MYRJ formulation, with the drug dissolved in DMSO prior to preparation. ICI 182,780 was dosed weekly by intraperitoneal (i.p.) injection at 5 mg/animal using 5% DMSO/95% peanut oil as vehicle. The results of this study showed no significant difference between the treatment groups with regard to tumor growth measured by volume and RFP fluorescence (data not shown). Blood was collected from animals after several days of treatment and upon sacrifice at the end of the study to ensure that CEP-1347 had reached therapeutic levels. Sera was isolated from whole blood by removal of red blood cells and plasma proteins to analyze concentrations of CEP-1347 using mass spectrometry with atmospheric pressure chemical ionization (APCI) and a targeted MS/MS method. These analyses showed that CEP-1347 was virtually undetectable in all samples tested.

The undetectable levels of CEP-1347 in serum explained its lack of effect, but MCF-7 tumors are known to be very sensitive to ICI 182,780 treatment. Further review of the literature revealed that many studies used subcutaneous rather than intraperitoneal dosing, with castor oil rather than peanut oil as vehicle [3]. In our remaining tumor studies, subcutaneous administration of 5 mg ICI 182,780 per week in castor oil was used and was effective.

To study the pharmacokinetics of CEP-1347, two vehicle combinations were used: (1) 1% DMSO/99% peanut oil, and (2) 25% propylene glycol/75% Gelucire 44/14. Peanut oil was administered orally with CEP-1347 concentrations of 10 mg/kg and 20 mg/kg, and propylene glycol/Gelucire was administered orally with 20 mg/kg CEP-1347. A second method of administration was subcutaneous injection in 1% DMSO/99% peanut oil, also at both 10 mg/kg and 20 mg/kg of drug. Blood was collected at a number of time points ranging from 30 minutes to 24 hours post-dosing. Rather than preparing sera, plasma was isolated from blood and analyzed for concentrations of CEP-1347. As CEP-1347 is highly hydrophobic and lipophilic, I hypothesized that it might be highly protein-bound in the blood stream, and collection of plasma rather than sera allowed us to retain these plasma proteins.

Initially, all samples tested exhibited sub-therapeutic concentrations of drug, regardless of the concentration or method of administration. After consulting with the mass spectrometry core, the analysis method was optimized and samples were re-analyzed. Using electrospray ionization (ESI) with a time-of-flight machine and an untargeted

method, I was able to detect CEP-1347 at concentrations as low as 2 nM in standards (Figure A-1A). While all of the pharmacokinetic trials using DMSO/peanut oil, both s.c. and p.o, still showed nearly undetectable levels of CEP-1347, the trial using 25% propylene glycol/75% gelucire 44/14 showed promising results, with CEP-1347 detectable, but at sub-therapeutic levels (Figure A-1B).

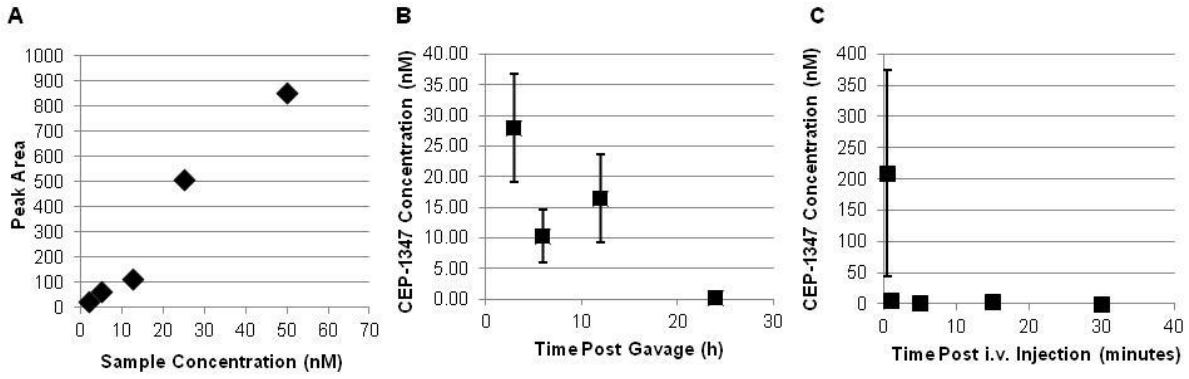

Figure A-1: Pharmacokinetic studies. A) Standard curve using ESI and untargeted analysis. B) CEP-1347 was dosed orally at 20 mg/kg in 25% propylene glycol/75% gelucire 44/14. Blood was drawn from 3 animals each at 3, 6, 12, and 24 hours post dosing and analyzed by MS. C) CEP-1347 was dosed intravenously at 2 uM in 1% DMSO/99% PBS. Blood was drawn at 30 seconds, 1, 5, and 15 minutes post injection and analyzed by mass spectrometry.

A timed intravenous (i.v.) study using 1% DMSO/99% PBS showed that CEP-1347 was readily detectable in animal plasma 30 seconds after i.v. injection. Interestingly, the level of CEP-1347 drastically dropped off within the next 30 seconds and was again virtually undetectable at 1 minute post i.v. injection. This suggested that CEP-1347 is

very rapidly absorbed across cell membranes and quickly leaves the blood stream after entry (Figure A-1C).

I posited that since 20 mg/kg led to approximately one-third of our ideal therapeutic dose, a dose of 60 mg/kg would provide therapeutic levels of drug in plasma. I conducted a trial MCF-7 tumor study administering CEP-1347 p.o. at 60 mg/kg 6 days/week in 25% propylene glycol/75% gelucire 44/14 for 5 weeks. I hypothesized that perhaps the lack of effect in our first trial may have been due to excessive estrogen levels due to the implanted estrogen pellets. Therefore, in this second pilot tumor study, they were removed prior to initiation of treatment. There was again no significant effect on tumor growth as tumors did not continue to proliferate after the removal of estrogen pellets. However, plasma samples collected after 3 and 5 weeks of 6 day/week drug administration were analyzed using the ESI mass spectrometry method. These samples indicated approximately 1000 nM of CEP-1347 detectable in all dosed animals, both at 3 weeks and at 5 weeks of dosing (Figure A-2).

This result led us to hypothesize that multiple doses of CEP-1347 are required to achieve therapeutic levels in animal plasma, and that this method of dosing, could be effective in preventing tumor growth *in vivo*. I concluded that a dosing regimen of 60 mg/kg p.o. every other day in 25% propylene glycol/75% gelucire 44/14 would allow animals to reach therapeutic concentrations of CEP-1347 in their blood while minimizing stress from daily oral gavage.

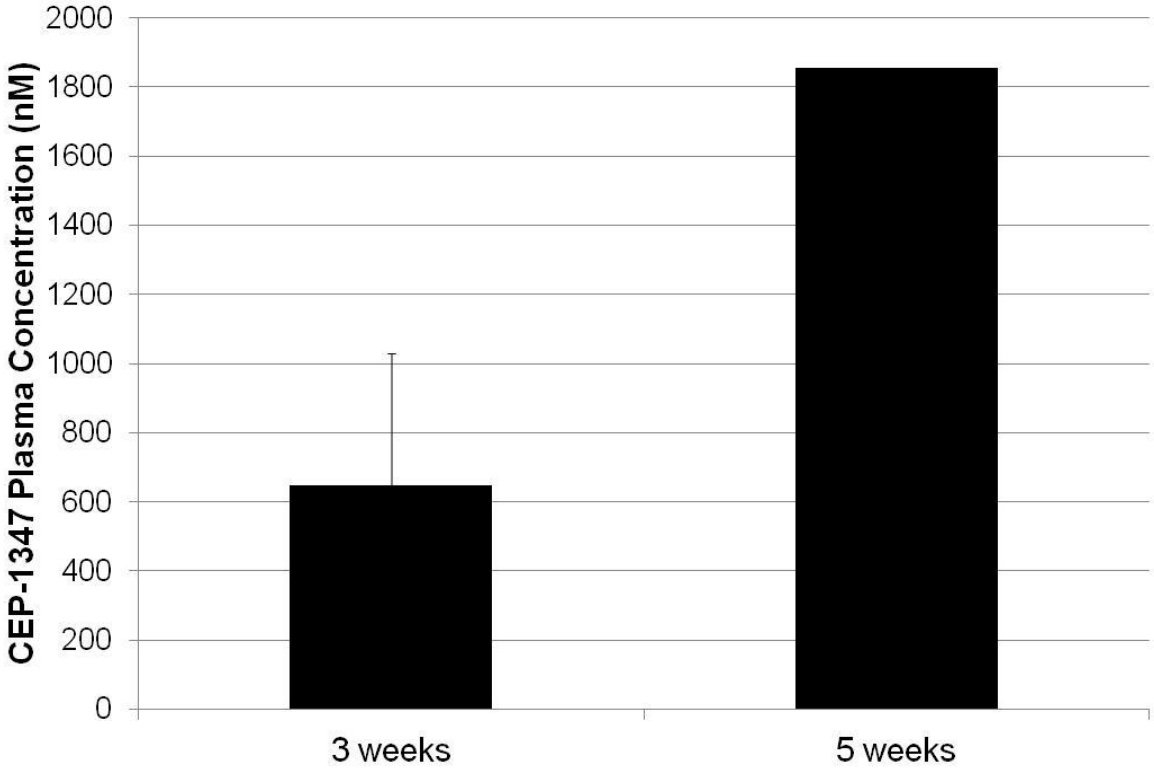

Figure A-2: CEP-1347 plasma concentrations. CEP-1347 was dosed daily at 60 mg/kg in 25% propylene glycol/75% gelucire 44/14 orally and blood was collected after 3 weeks and 5 weeks of administration. Plasma was isolated from blood and analyzed using ESI mass spectrometry. At 3 weeks, N = 4 and at 5 weeks, N = 2.

I tested this dosing regimen in a third pilot tumor study using MCF-7 cells and three treatment groupd: vehicle (25% propylene glycol/75% Gelucire 44/14 every other day

p.o.), ICI 182,780 alone (5 mg/week s.c. in castor oil), and CEP-1347 alone (60 mg/kg p.o. in 25% propylene glycol/75% Gelucire 44/14 every other day). After 3 weeks of treatment, animals treated with ICI 182,780 alone or CEP-1347 alone grew significantly smaller tumors compared to animals treated with vehicle (Figure A-3), and these were the dosing regimens used in Chapter 2.

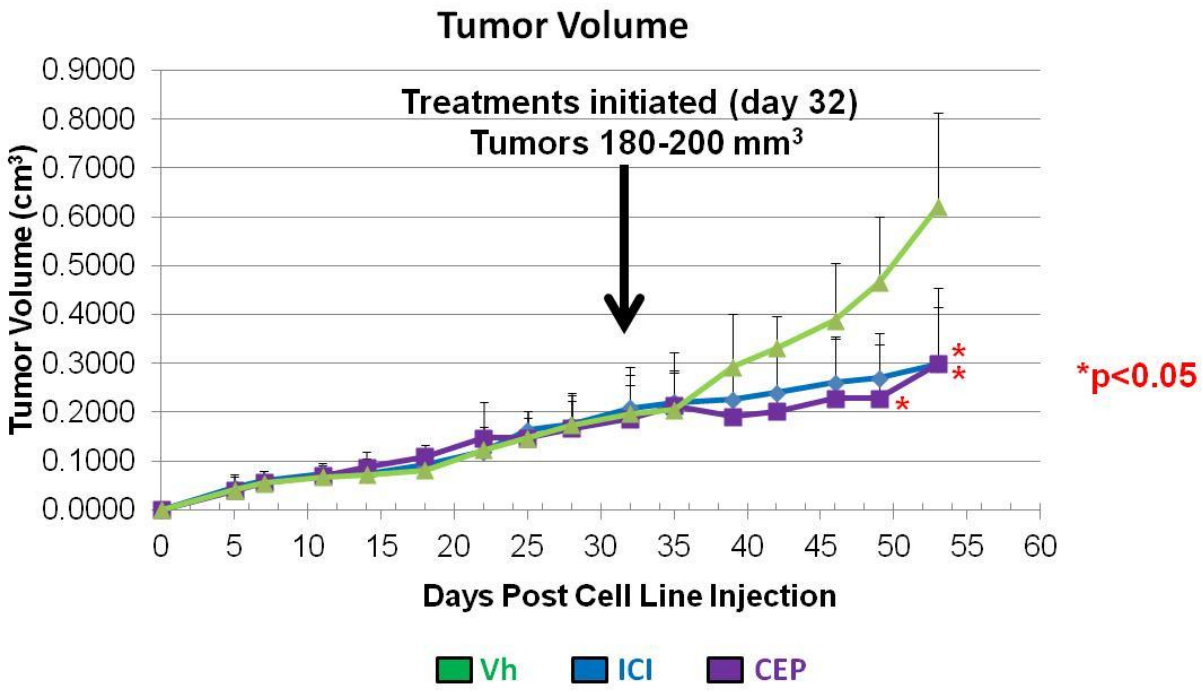

Figure A-3: Growth curves from third pilot tumor study. Animals were injected orthotopically with $5x10^6$ cells. Once tumor reached approximately 100 mm^3, 4 animals were randomized into one of three treatment groups: vehicle, ICI 182,780 alone, or CEP-1347 alone and dosed for 3 weeks.

Results from all pharmacokinetic experiments are summarized in Table A-1, and all pilot tumor studies are summarized in Table A-2.

Method of Delivery	Time Points	Method(s) of Detection	Maximally Detectable CEP-1347
10 mg/kg in 99% Peanut Oil/1% DMSO ORAL	30 min, 1 hr, 2 hr, 3 hr	APCI/targeted MS/MS	25 nM at 30 minutes
		ESI-TOF/untargeted MS	45 nM at 30 minutes
20 mg/kg in 99% Peanut Oil/1% DMSO ORAL	3 hr, 6 hr, 12 hr, 24 hr	APCI/targeted MS/MS	5 nM at 30 minutes
		ESI-TOF/untargeted MS	6 nM at 3 hours
10 mg/kg in 99% Peanut Oil/1%DMSO SUBCUTANEOUS	30 min, 1 hr, 2 hr, 3 hr	APCI/targeted MS/MS	10 nM at 6 hours
		ESI-TOF/untargeted MS	10 nM at 3 hours
20 mg/kg in 99% Peanut Oil/1% DMSO SUBCUTANEOUS	3 hr, 6 hr, 12 hr, 24 hr	APCI/targeted MS/MS	15 nM at 6 hours
		ESI-TOF/untargeted MS	11 nM at 12 hours
20 mg/kg in 75% Gelucire/25% Propylene Glycol ORAL	3 hr, 6 hr, 12 hr, 24 hr	APCI/targeted MS/MS	3 nM at 6 hours
		ESI-TOF/untargeted MS	27 nM at 3 hr
2 µM in 99% PBS/1% DMSO INTRAVENOUS	30 sec, 1 min, 5 min, 15 min, 30 min	APCI/targeted MS/MS	6 nM at 30 seconds
		ESI-TOF/untargeted MS	200 nM at 30 seconds

Table A-1: Summary of pharmacokinetic studies conducted. Mice were dosed at either 10 mg/kg or 20 mg/kg, subcutaneously or orally, in DMSO/oil or gelucire/propylene glycol. An i.v. study was also conducted using 2 µM CEP-1347 in DMSO/PBS. Data is summarized from each study.

Estrogen Pellet	ICI	CEP
0.72 mg, 60 day release (Innovative Research)	**5 mg/week DMSO/peanut oil i.p. injection**	**10 mg/kg daily Softigen/MYRJ Oral gavage Levels undetectable**
1 mg beeswax (homemade) – removed before treatment initiation	**5 mg/week DMSO/peanut oil s.c. injection**	**60 mg/kg daily Gelucire/propylene glycol Oral gavage 600 nM detectable at 3 weeks 1800 nM detectable at 5 weeks**
0.5 mg beeswax (homemade)	**5 mg/week DMSO/castor oil s.c. injection**	**60 mg/kg every other day Gelucire/propylene glycol Oral gavage**

Table A-2: Summary of trial tumor studies completed. $5x10^6$ cells were injected orthotopically into the fat pads of athymic Nu/Nu mice. Once tumors measured

Table A-2 (cont'd)

approximately 100 mm^3, animals were randomized into treatment groups and dosed as specified.

REFERENCES

REFERENCES

1. Wang, L., K.A. Gallo, and S.E. Conrad, *Targeting mixed lineage kinases in ER-positive breast cancer cells leads to G2/M cell cycle arrest and apoptosis.* Oncotarget, 2013. **4**(8): p. 1158-71.

2. Osborne, C.K., et al., *Comparison of the effects of a pure steroidal antiestrogen with those of tamoxifen in a model of human breast cancer.* J Natl Cancer Inst, 1995. **87**(10): p. 746-50.

3. Bross, P.F., et al., *FDA drug approval summaries: fulvestrant.* Oncologist, 2002. **7**(6): p. 477-80.